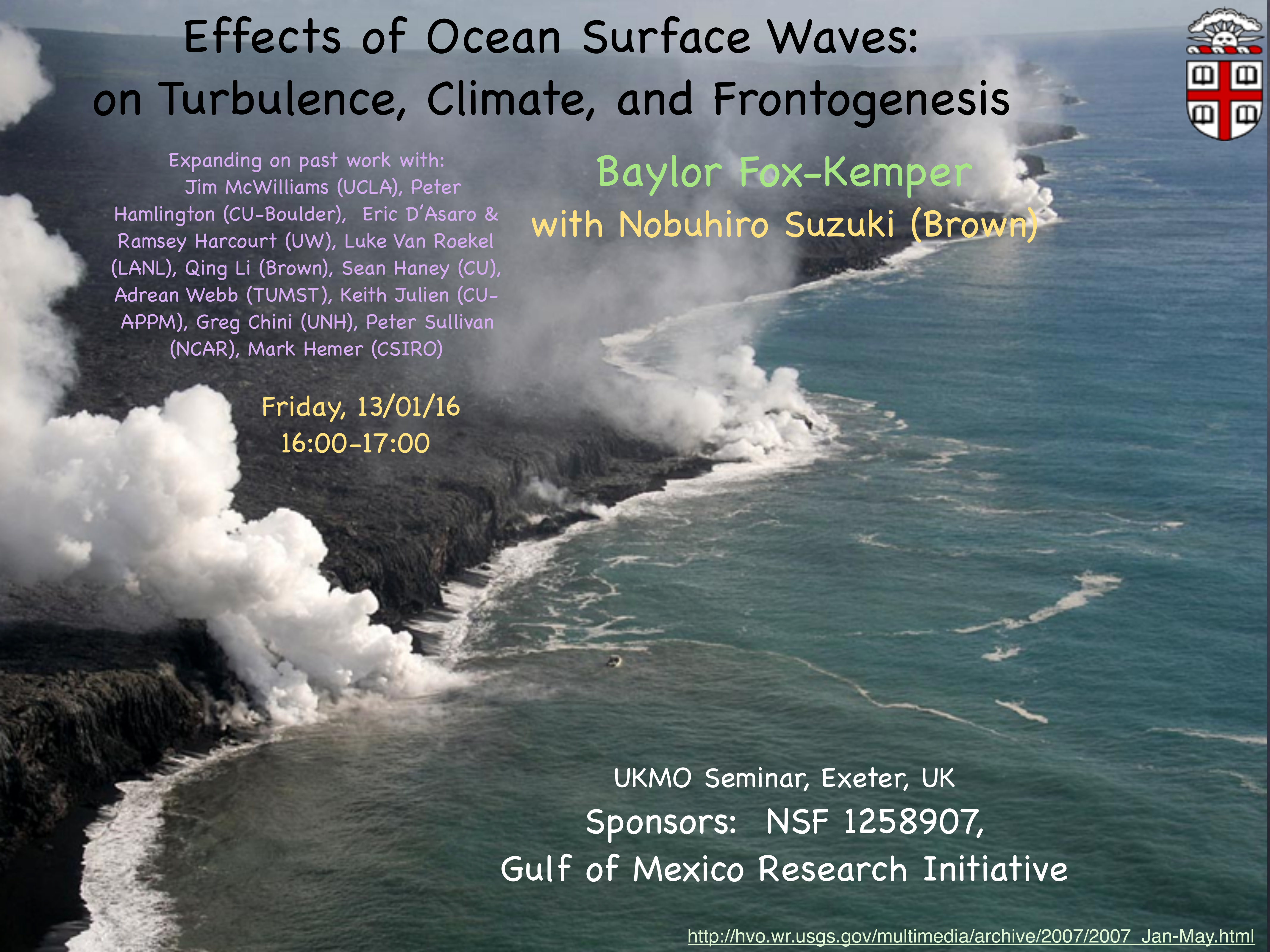

Effects of Ocean Surface Waves: on Turbulence, Climate, and Frontogenesis

Expanding on past work with: Jim McWilliams (UCLA), Peter Hamlington (CU-Boulder), Eric D'Asaro & Ramsey Harcourt (UW), Luke Van Roekel (LANL), Qing Li (Brown), Sean Haney (CU), Adrean Webb (TUMST), Keith Julien (CU-APPM), Greg Chini (UNH), Peter Sullivan (NCAR), Mark Hemer (CSIRO)

Baylor Fox-Kemper

with Nobuhiro Suzuki (Brown)

Friday, 13/01/16
16:00-17:00

UKMO Seminar, Exeter, UK

Sponsors: NSF 1258907,
Gulf of Mexico Research Initiative

http://hvo.wr.usgs.gov/multimedia/archive/2007/2007_Jan-May.html

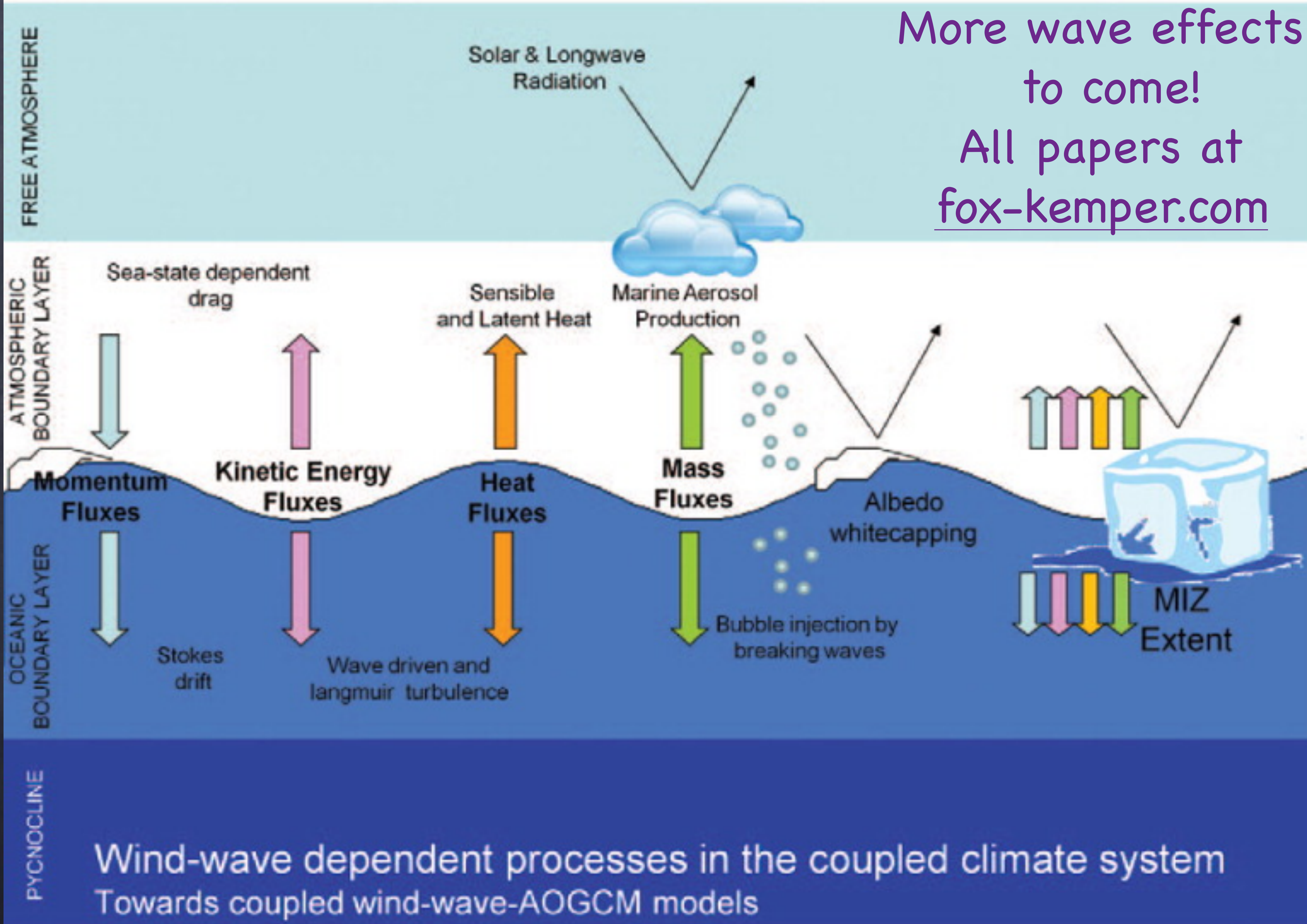

L. Cavaleri, BFK, and M. Hemer. Wind waves in the coupled climate system. Bulletin of the American Meteorological Society, 93(11):1651-1661, 2012.

Surface Waves are...

Fast, small, irrotational solutions of the Boussinesq Equations

Have a Stokes drift depending on sea state (wave age, winds)

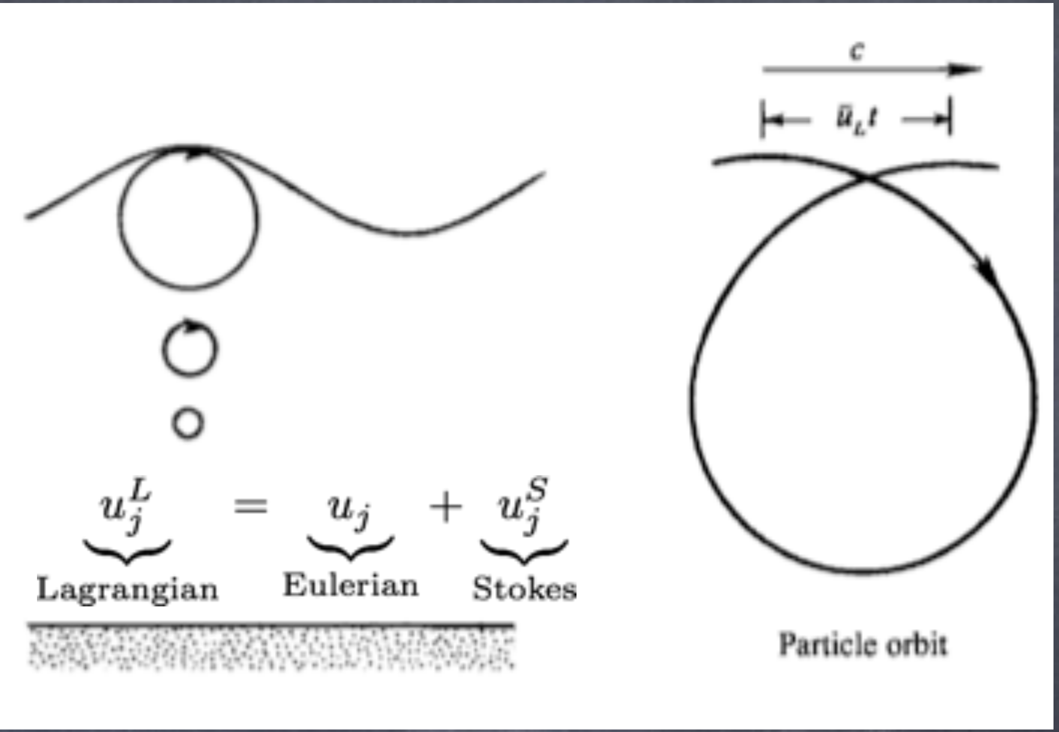

A. Webb and B. Fox-Kemper. Wave spectral moments and Stokes drift estimation. Ocean Modelling, 40(3-4):273-288, 2011.

A. Webb and B. Fox-Kemper. Impacts of wave spreading and multidirectional waves on estimating Stokes drift. Ocean Modelling, 96(1):49-64, 2015.

Surface Waves are...

Fast, small, irrotational solutions of the Boussinesq Equations

Have a Stokes drift depending on sea state (wave age, winds)

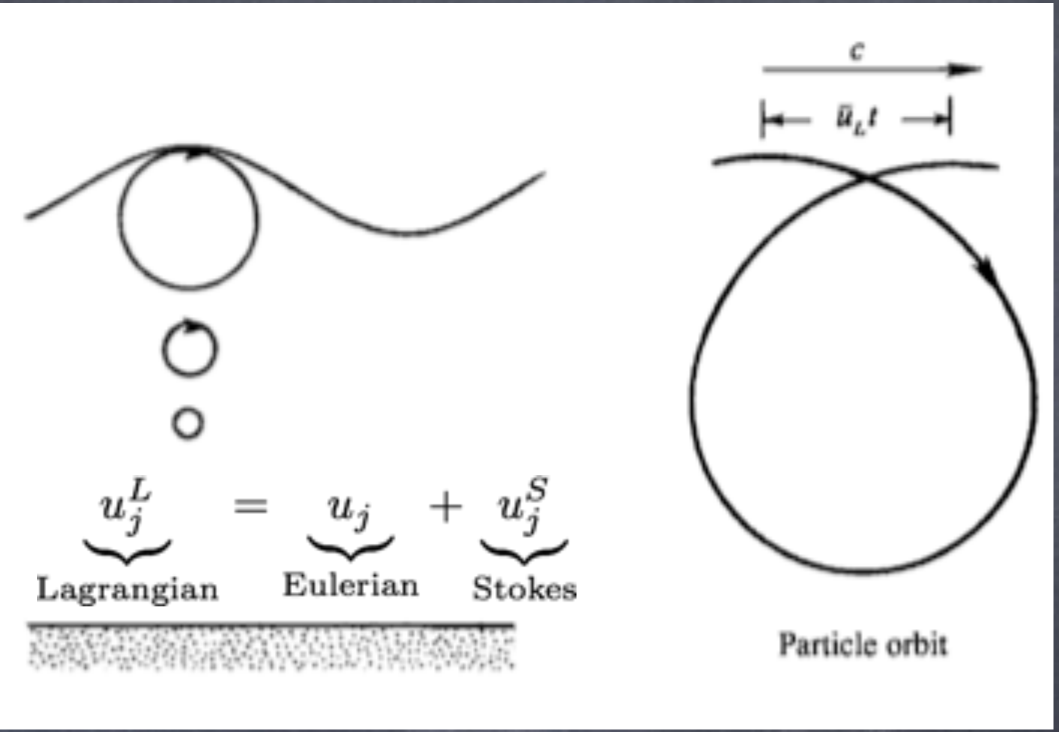

A. Webb and B. Fox-Kemper. Wave spectral moments and Stokes drift estimation. Ocean Modelling, 40(3-4):273-288, 2011.

A. Webb and B. Fox-Kemper. Impacts of wave spreading and multidirectional waves on estimating Stokes drift. Ocean Modelling, 96(1):49-64, 2015.

Surface Waves are...

Fast, small, irrotational solutions of the Boussinesq Equations

Have a Stokes drift depending on sea state (wave age, winds)

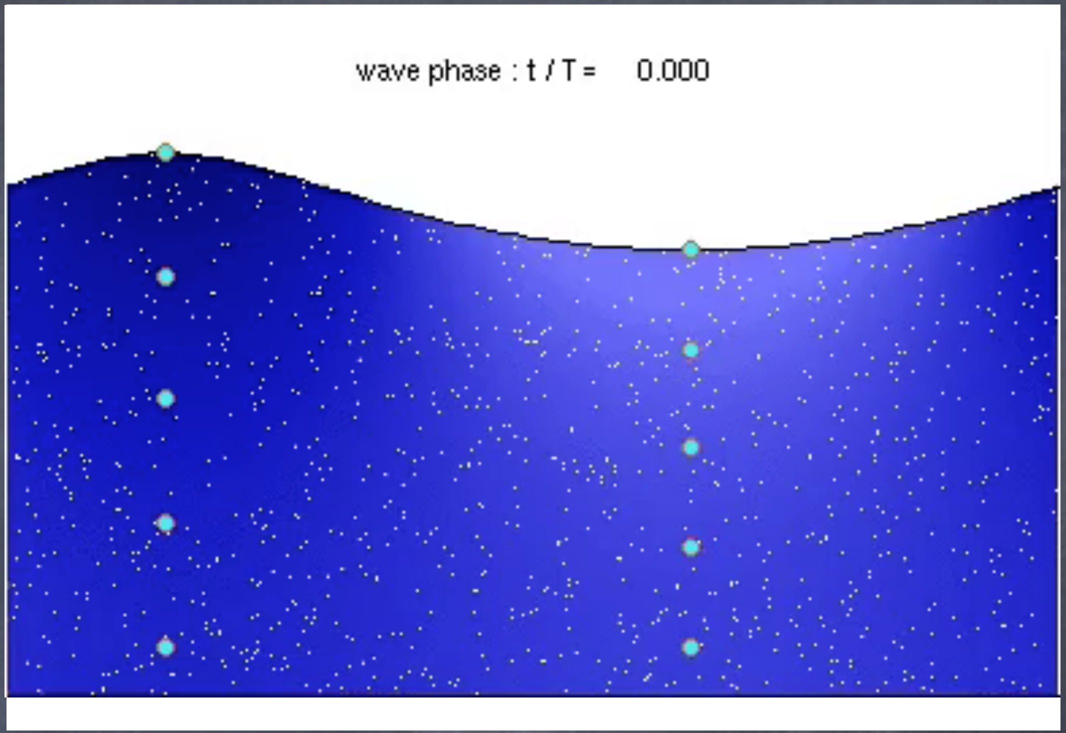

A. Webb and B. Fox-Kemper. Wave spectral moments and Stokes drift estimation. Ocean Modelling, 40(3-4):273-288, 2011.

A. Webb and B. Fox-Kemper. Impacts of wave spreading and multidirectional waves on estimating Stokes drift. Ocean Modelling, 96(1):49-64, 2015.

Wave-Averaged Equations

following Lane et al. (07), McWilliams & F-K (13) and Suzuki & F-K (16)

$$\underbrace{v_j^L}_{\text{Lagrangian}} = \underbrace{v_j}_{\text{Eulerian}} + \underbrace{v_j^S}_{\text{Stokes}}$$

Coupling Depends on Stokes drift—WAVE effects in YELLOW

Boundary conditions, plus:

(Lagrangian) geostrophic

$$Ro\left[v_{i,t} + v_j^L v_{i,j}\right] + \frac{M_{Ro}}{Ri} w v_{i,z} + \boxed{\epsilon_{izj} v_j^L = -M_{Ro}\pi_{,i}} + \frac{Ro}{Re} v_{i,jj}$$

$$\frac{\alpha^2}{Ri}\left[w_{,t} + v_j^L w_{,j} + \frac{M_{Ro}}{RoRi} w w_{,z}\right] = \boxed{-\pi_{,z} + b} - \varepsilon v_j^L v_{j,z}^s + \frac{\alpha^2}{ReRi} w_{,jj}$$

hydrostatic

$$b_t + v_j^L b_{,j} + \frac{M_{Ro}}{RoRi} w b_z = \frac{1}{Pe} b_{,jj}$$

$$v_{j,j} + \frac{M_{Ro}}{RoRi} w_z = 0$$

$$\boxed{\varepsilon = \frac{V^s H}{f L H_s}}$$

$$Re = \frac{UL}{\nu} \quad Ro = \frac{U}{fL} \quad Ri = \frac{N^2}{(U_{,z})^2} \quad \alpha = H/L \quad M_{Ro} \equiv \max(1, Ro)$$

J. C. McWilliams and BFK. Oceanic wave-balanced surface fronts and filaments. Journal of Fluid Mechanics, 730:464-490, 2013.

N. Suzuki and BFK. Understanding Stokes forces in the wave-averaged equations. JGR-Oceans, December 2015. Submitted.

3 Wave Effects, 1: Lagrangian Advection:

Particles, tracers, momentum flow with Lagrangian, not Eulerian flow

$$Ro\left[v_{i,t} + v_j^L v_{i,j}\right] + \frac{M_{Ro}}{Ri} w v_{i,z} + \epsilon_{izj} v_j^L = -M_{Ro}\pi_{,i} + \frac{Ro}{Re} v_{i,jj}$$

$$\frac{\alpha^2}{Ri}\left[w_{,t} + v_j^L w_{,j} + \frac{M_{Ro}}{RoRi} w w_{,z}\right] = -\pi_{,z} + b - \varepsilon v_j^L v_{j,z}^s + \frac{\alpha^2}{ReRi} w_{,jj}$$

$$b_t + v_j^L b_{,j} + \frac{M_{Ro}}{RoRi} w b_z = \frac{1}{Pe} b_{,jj}$$

Adding a Stokes advection term converts total to Lagrangian advection

$$\underbrace{v_j^L}_{\text{Lagrangian}} = \underbrace{v_j}_{\text{Eulerian}} + \underbrace{v_j^S}_{\text{Stokes}}$$

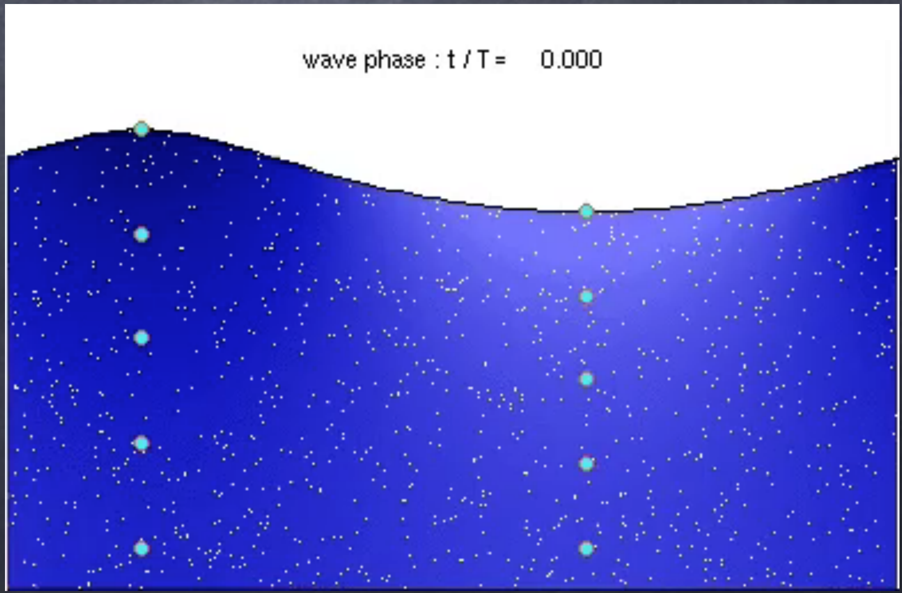

N. Suzuki and BFK. Understanding Stokes forces in the wave-averaged equations. JGR-Oceans, December 2015. Submitted.

3 Wave Effects, 1: Lagrangian Advection:

Particles, tracers, momentum flow with Lagrangian, not Eulerian flow

$$Ro\left[v_{i,t} + v_j^L v_{i,j}\right] + \frac{M_{Ro}}{Ri} w v_{i,z} + \epsilon_{izj} v_j^L = -M_{Ro}\pi_{,i} + \frac{Ro}{Re} v_{i,jj}$$

$$\frac{\alpha^2}{Ri}\left[w_{,t} + v_j^L w_{,j} + \frac{M_{Ro}}{RoRi} w w_{,z}\right] = -\pi_{,z} + b - \varepsilon v_j^L v_{j,z}^s + \frac{\alpha^2}{ReRi} w_{,jj}$$

$$b_t + v_j^L b_{,j} + \frac{M_{Ro}}{RoRi} w b_z = \frac{1}{Pe} b_{,jj}$$

Adding a Stokes advection term converts total to Lagrangian advection

$$\underbrace{v_j^L}_{\text{Lagrangian}} = \underbrace{v_j}_{\text{Eulerian}} + \underbrace{v_j^S}_{\text{Stokes}}$$

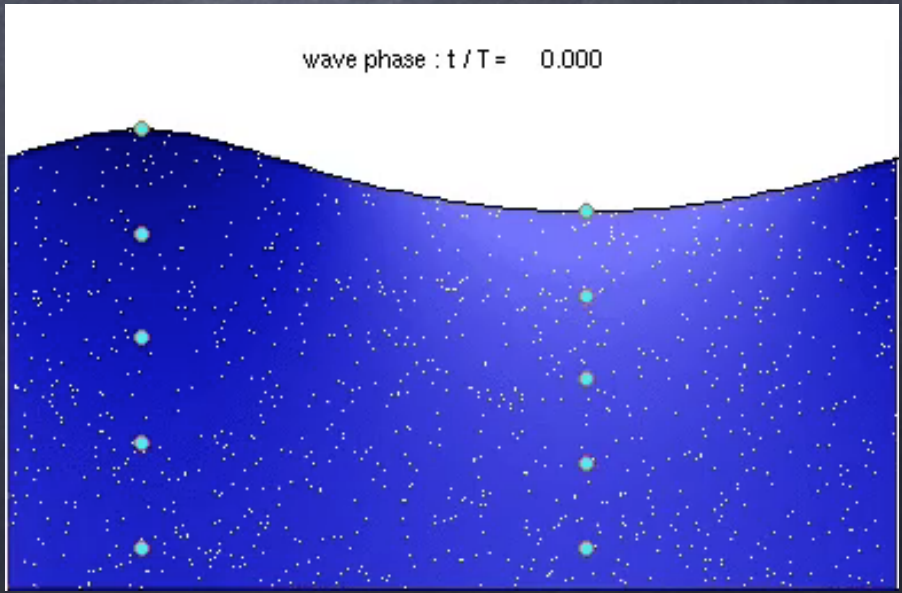

N. Suzuki and BFK. Understanding Stokes forces in the wave-averaged equations. JGR-Oceans, December 2015. Submitted.

3 Wave Effects, 2: Lagrangian Coriolis:

Particles, tracers, momentum flow with Lagrangian, not Eulerian flow—Experience Coriolis force during this motion

$$Ro\left[v_{i,t} + v_j^L v_{i,j}\right] + \frac{M_{Ro}}{Ri} w v_{i,z} + \epsilon_{izj} v_j^L = -M_{Ro}\pi_{,i} + \frac{Ro}{Re} v_{i,jj}$$

$$\frac{\alpha^2}{Ri}\left[w_{,t} + v_j^L w_{,j} + \frac{M_{Ro}}{RoRi} w w_{,z}\right] = -\pi_{,z} + b - \varepsilon v_j^L v_{j,z}^s + \frac{\alpha^2}{ReRi} w_{,jj}$$

$$b_t + v_j^L b_{,j} + \frac{M_{Ro}}{RoRi} w b_z = \frac{1}{Pe} b_{,jj}$$

Adding a Stokes Coriolis term converts total to Lagrangian

$$\underbrace{v_j^L}_{\text{Lagrangian}} = \underbrace{v_j}_{\text{Eulerian}} + \underbrace{v_j^S}_{\text{Stokes}}$$

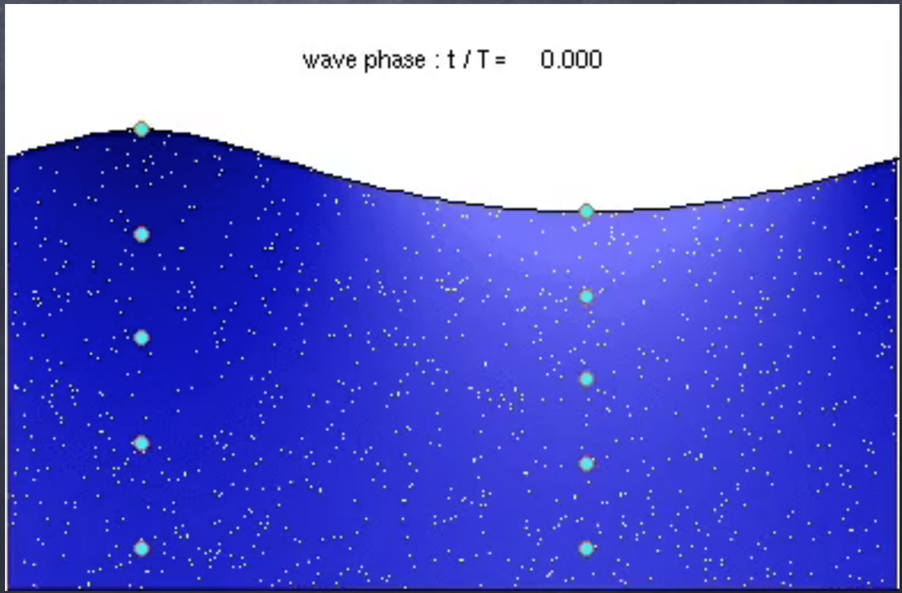

N. Suzuki and BFK. Understanding Stokes forces in the wave-averaged equations. JGR-Oceans, December 2015. Submitted.

3 Wave Effects, 2: Lagrangian Coriolis:

Particles, tracers, momentum flow with Lagrangian, not Eulerian flow—Experience Coriolis force during this motion

$$Ro\left[v_{i,t} + v_j^L v_{i,j}\right] + \frac{M_{Ro}}{Ri} w v_{i,z} + \epsilon_{izj} v_j^L = -M_{Ro}\pi_{,i} + \frac{Ro}{Re} v_{i,jj}$$

$$\frac{\alpha^2}{Ri}\left[w_{,t} + v_j^L w_{,j} + \frac{M_{Ro}}{RoRi} w w_{,z}\right] = -\pi_{,z} + b - \varepsilon v_j^L v_{j,z}^s + \frac{\alpha^2}{ReRi} w_{,jj}$$

$$b_t + v_j^L b_{,j} + \frac{M_{Ro}}{RoRi} w b_z = \frac{1}{Pe} b_{,jj}$$

Adding a Stokes Coriolis term converts total to Lagrangian

$$\underbrace{v_j^L}_{\text{Lagrangian}} = \underbrace{v_j}_{\text{Eulerian}} + \underbrace{v_j^S}_{\text{Stokes}}$$

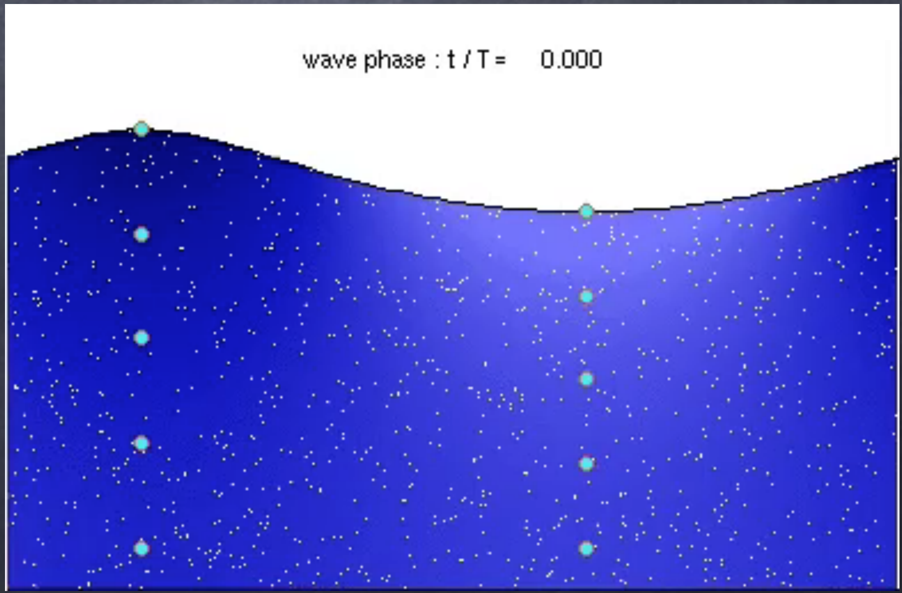

N. Suzuki and BFK. Understanding Stokes forces in the wave-averaged equations. JGR-Oceans, December 2015. Submitted.

3 Wave Effects, 3: Stokes Shear Force

and the CL2 mechanism for Langmuir circulations

Flow directed along Stokes shear=downward force

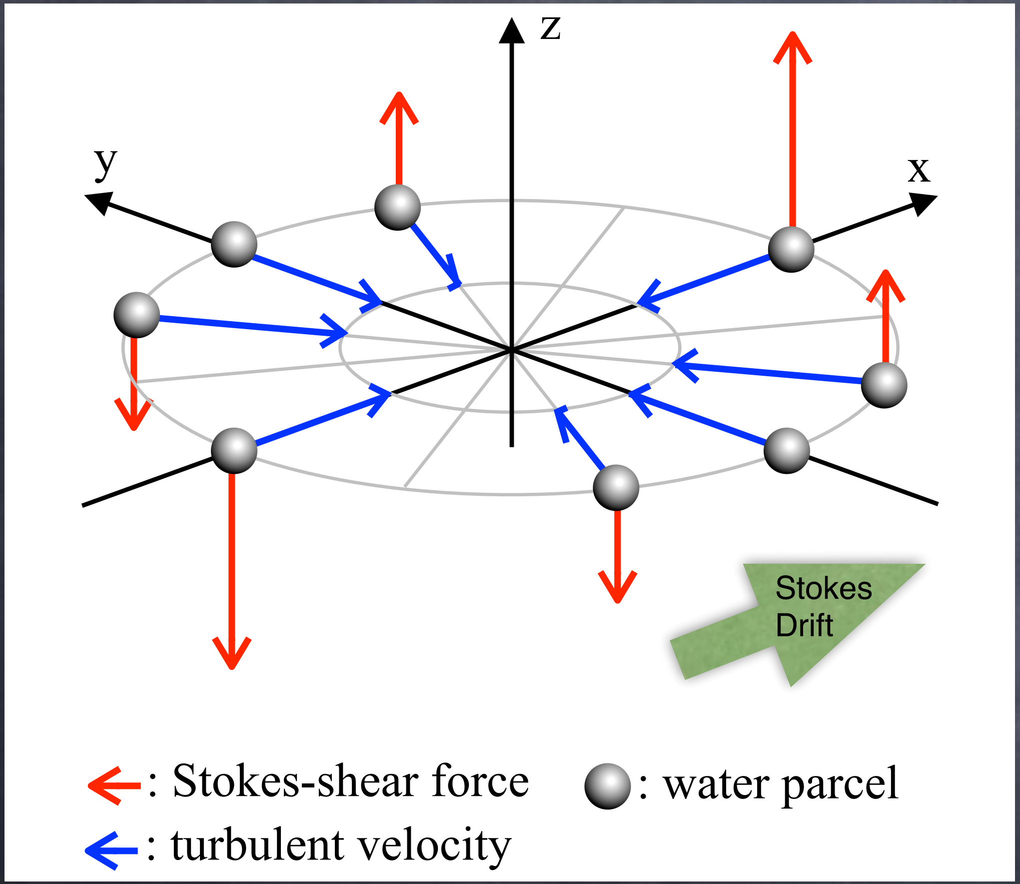

$$\varepsilon = \frac{V^s H}{f L H_s}$$

hydrostatic

$$\frac{\alpha^2}{Ri}\left[w_{,t} + v_j^L w_{,j} + \frac{M_{Ro}}{RoRi} w w_{,z}\right] = \boxed{-\pi_{,z} + b} - \varepsilon v_j^L v_{j,z}^s + \frac{\alpha^2}{ReRi} w_{,jj}$$

N. Suzuki and BFK. Understanding Stokes forces in the wave-averaged equations. JGR-Oceans, December 2015. Submitted.

3 Wave Effects, 3: Stokes Shear Force

and the CL2 mechanism for Langmuir circulations

Flow directed along Stokes shear=downward force

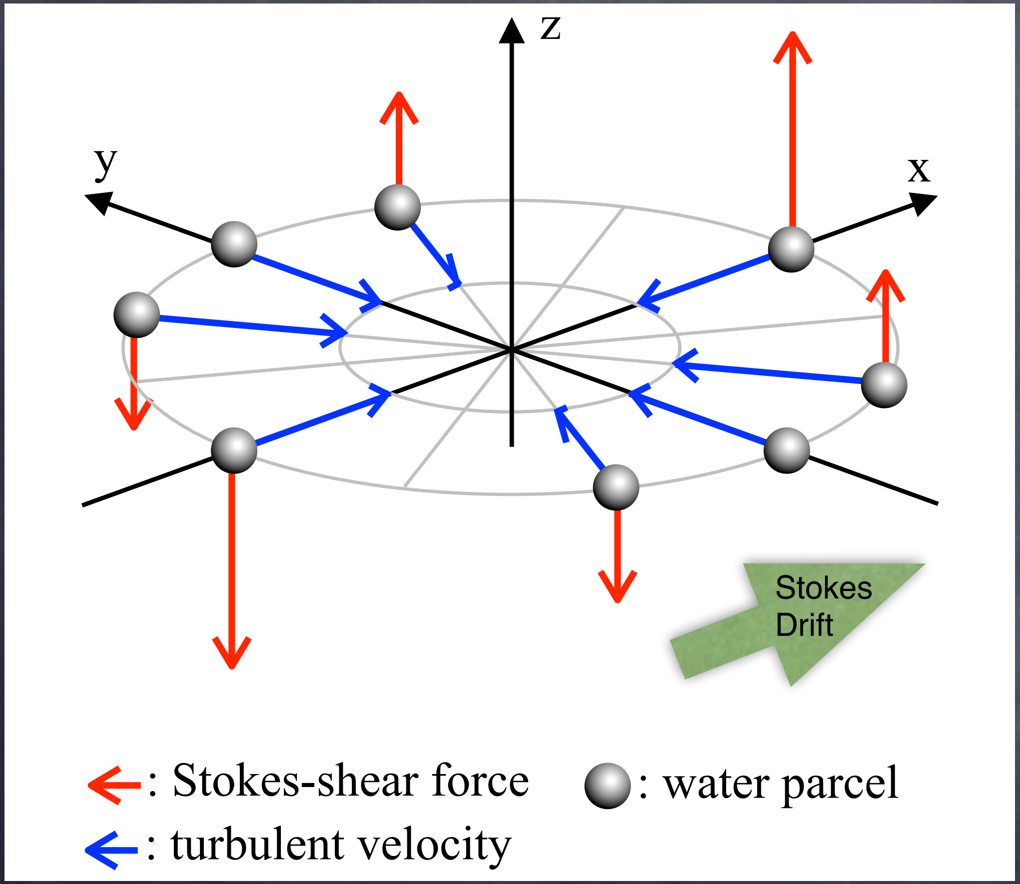

$$\varepsilon = \frac{V^s H}{f L H_s}$$

$$\frac{\alpha^2}{Ri}\left[w_{,t} + v_j^L w_{,j} + \frac{M_{Ro}}{RoRi} w w_{,z}\right] = -\pi_{,z} + b - \varepsilon v_j^L v_{j,z}^s + \frac{\alpha^2}{ReRi} w_{,jj}$$

N. Suzuki and BFK. Understanding Stokes forces in the wave-averaged equations. JGR-Oceans, December 2015. Submitted.

3 Wave Effects, 3: Stokes Shear Force

and the CL2 mechanism for Langmuir circulations

Flow directed along Stokes shear=downward force

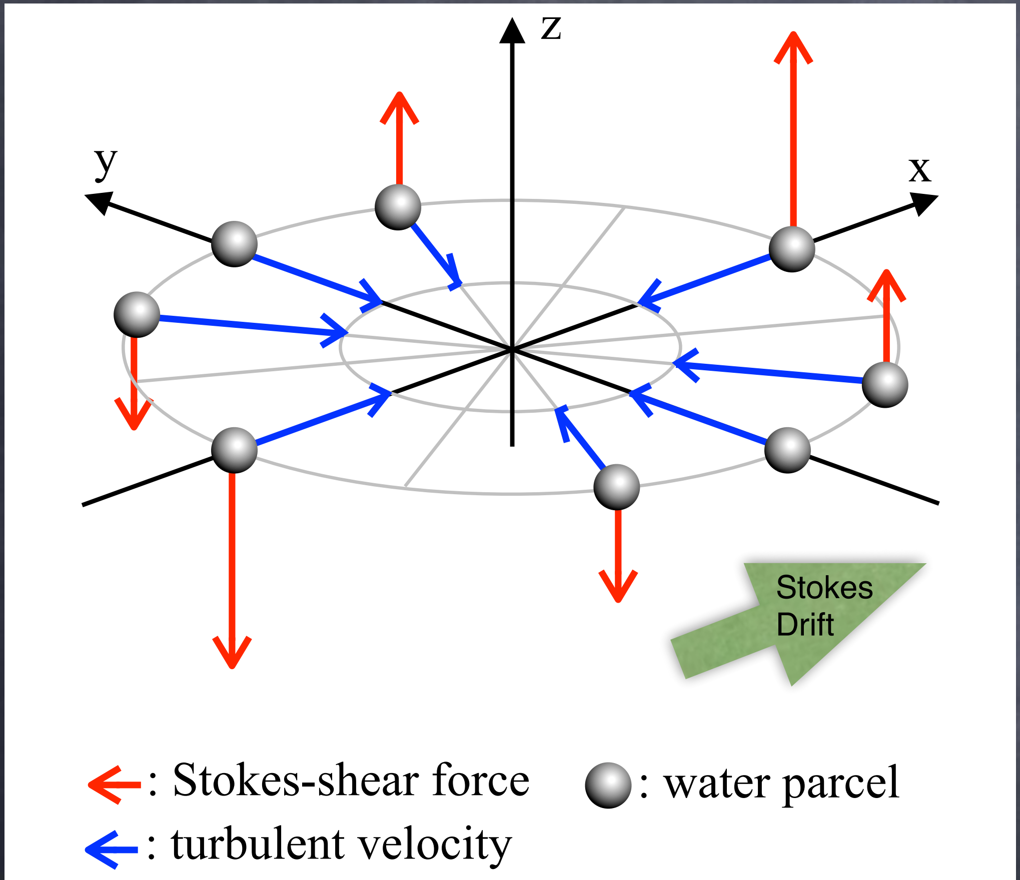

$$\varepsilon = \frac{V^s H}{f L H_s}$$

"wavy hydrostatic" if

$$\epsilon \gg 1$$

$$\frac{\alpha^2}{Ri}\left[w_{,t} + v_j^L w_{,j} + \frac{M_{Ro}}{RoRi} w w_{,z}\right] = \boxed{-\pi_{,z} + b - \varepsilon v_j^L v_{j,z}^s} + \frac{\alpha^2}{ReRi} w_{,jj}$$

N. Suzuki and BFK. Understanding Stokes forces in the wave-averaged equations. JGR-Oceans, December 2015. Submitted.

Stokes force directly affects larger scales?

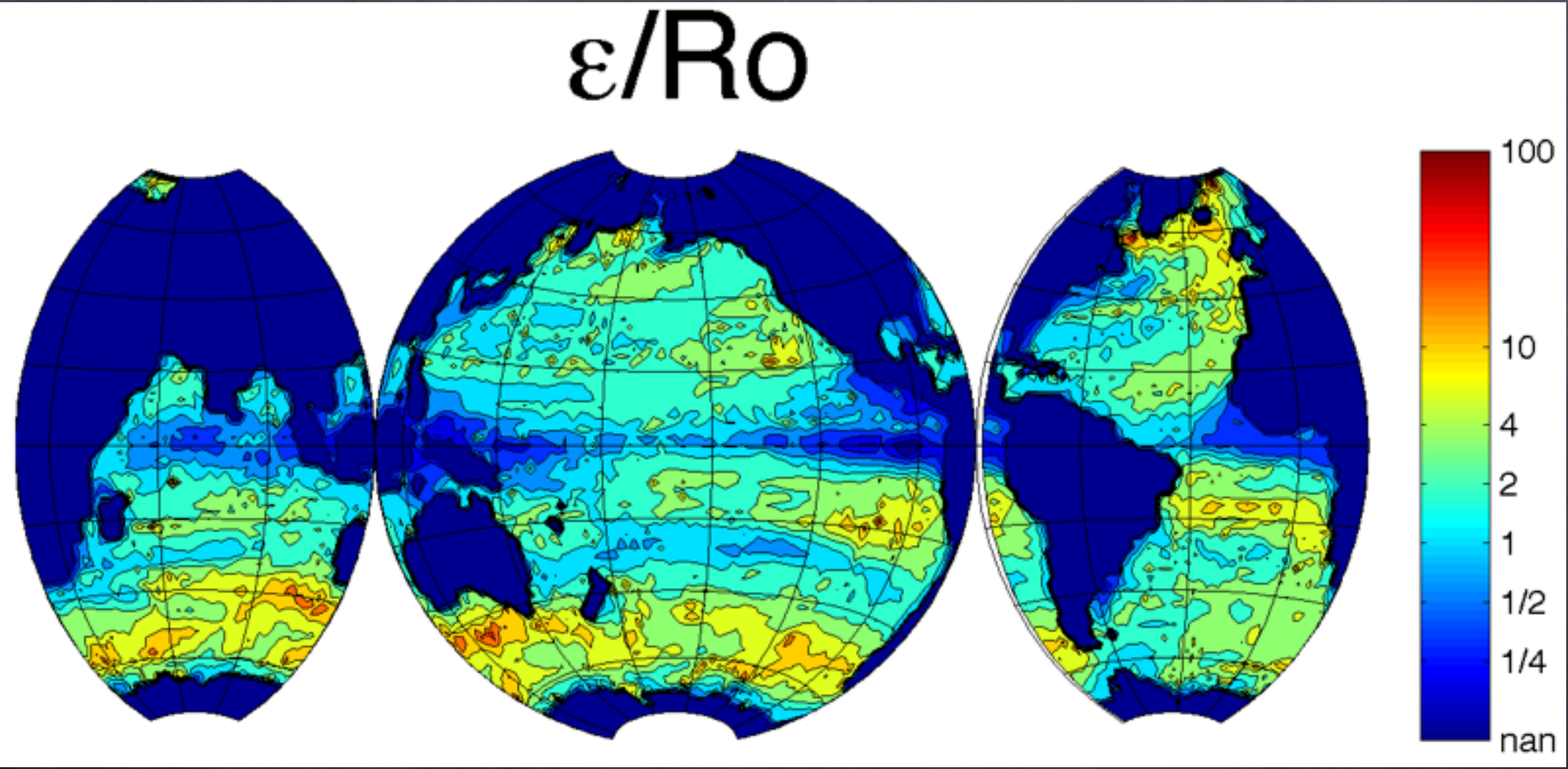

$$\frac{\varepsilon}{Ro} = \frac{V_s}{fL}\frac{H}{H_s}\frac{fL}{V} = \frac{V_s}{V}\frac{H}{H_s}$$

$$\varepsilon = \frac{V^s H}{f L H_s} \qquad Ro = \frac{U}{fL}$$

J. C. McWilliams and BFK. Oceanic wave-balanced surface fronts and filaments. Journal of Fluid Mechanics, 730:464-490, 2013.

The Character of Langmuir Turbulence

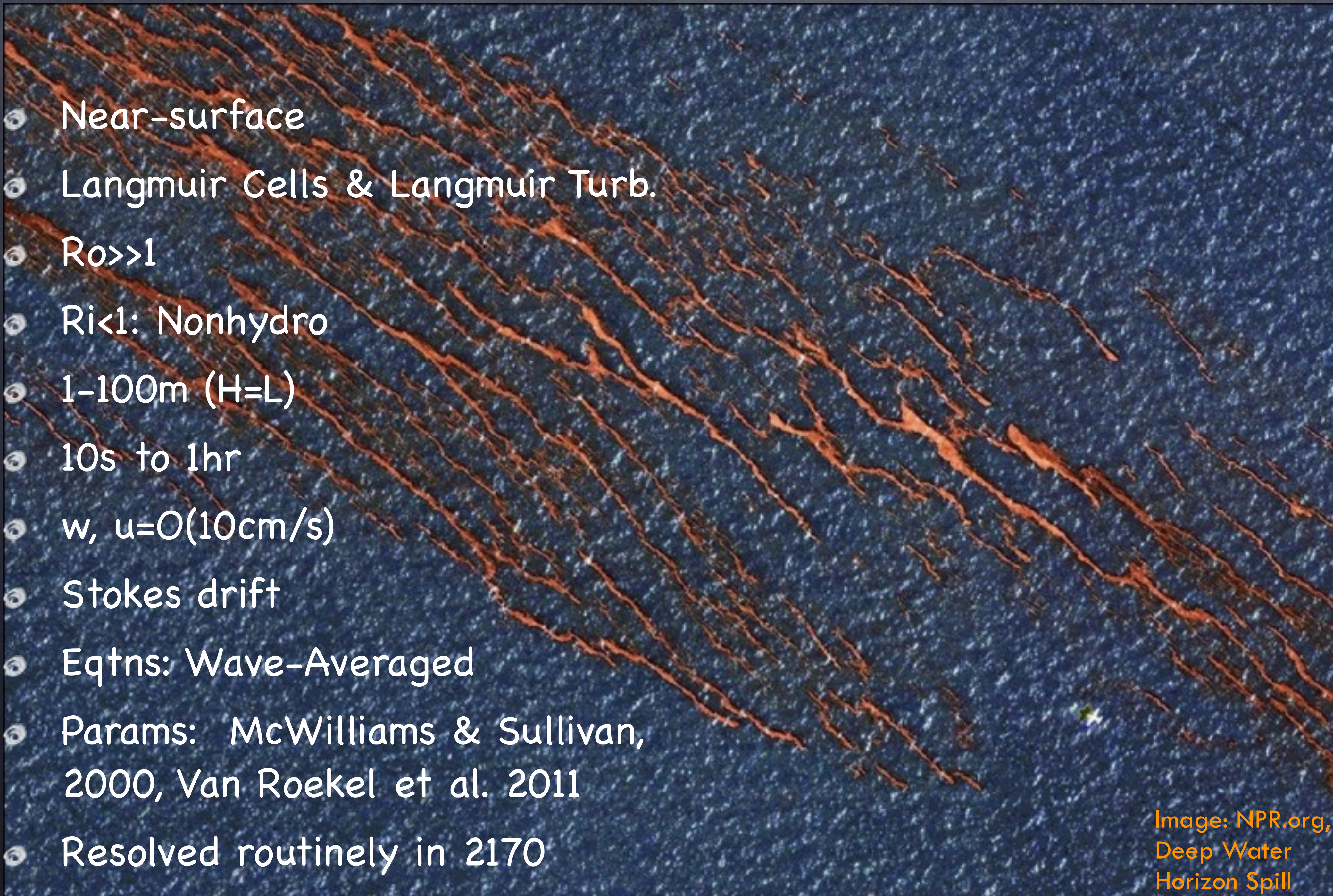

- Near-surface
- Langmuir Cells & Langmuir Turb.
- Ro>>1
- Ri<1: Nonhydro
- 1-100m (H=L)
- 10s to 1hr
- w, u=O(10cm/s)
- Stokes drift
- Eqtns: Wave-Averaged
- Params: McWilliams & Sullivan, 2000, Van Roekel et al. 2011
- Resolved routinely in 2170

Image: NPR.org, Deep Water Horizon Spill

image:
Thorpe, 04

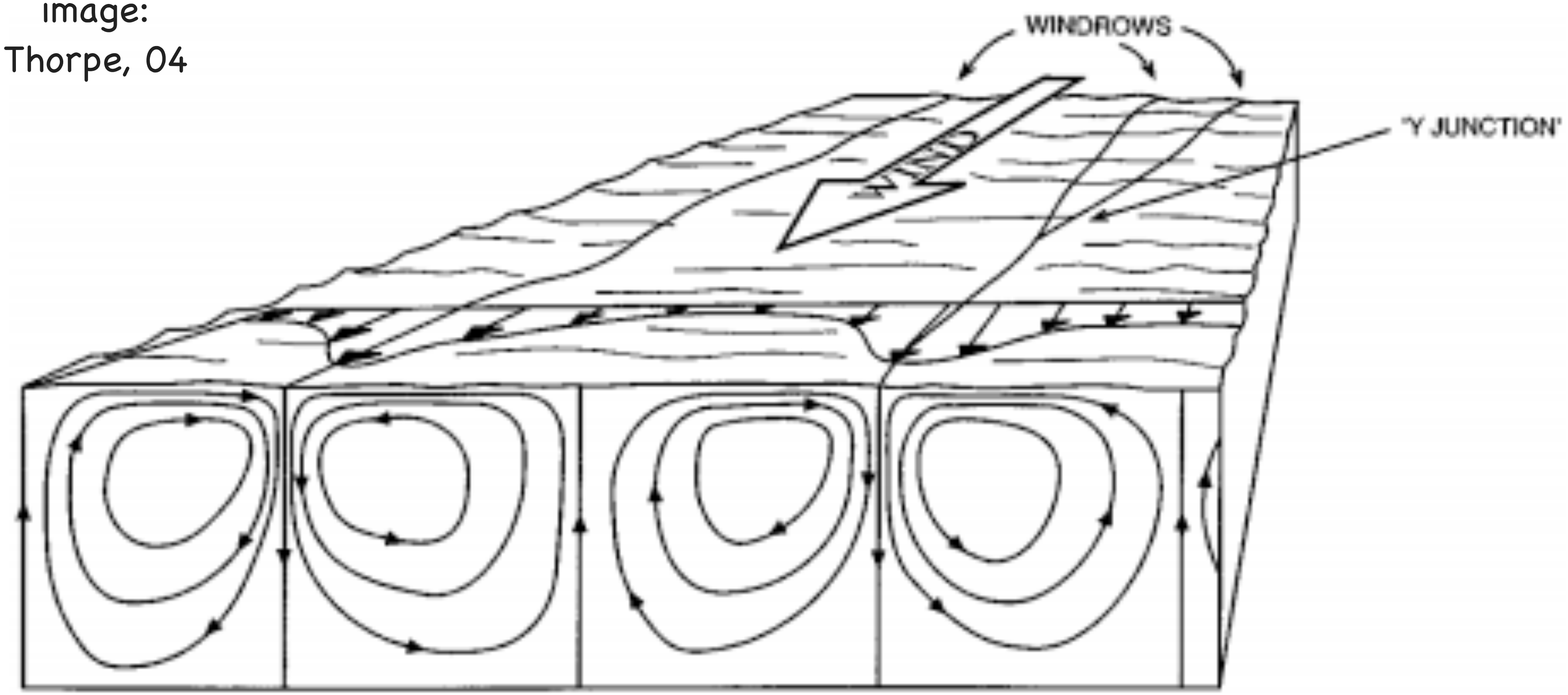

Figure 1 Sketch showing the pattern of mean flow in idealized Langmuir circulation. The windrows may be 2 m to 300 m apart, and the cell form is roughly square (as shown). In practice the flow is turbulent, especially near the water surface, and the windrows (Figure 2) amalgamate and meander in space and time. Bands of bubbles or buoyant algae may form within the downward-going (or downwelling) flow (see Figure 3).

$$\frac{\alpha^2}{Ri}\left[w_{,t} + v_j^L w_{,j} + \frac{M_{Ro}}{RoRi} w w_{,z}\right] = -\pi_{,z} + b - \varepsilon v_j^L v_{j,z}^s + \frac{\alpha^2}{ReRi} w_{,jj}$$

N. Suzuki and BFK. Understanding Stokes forces in the wave-averaged equations. JGR-Oceans, December 2015. Submitted.

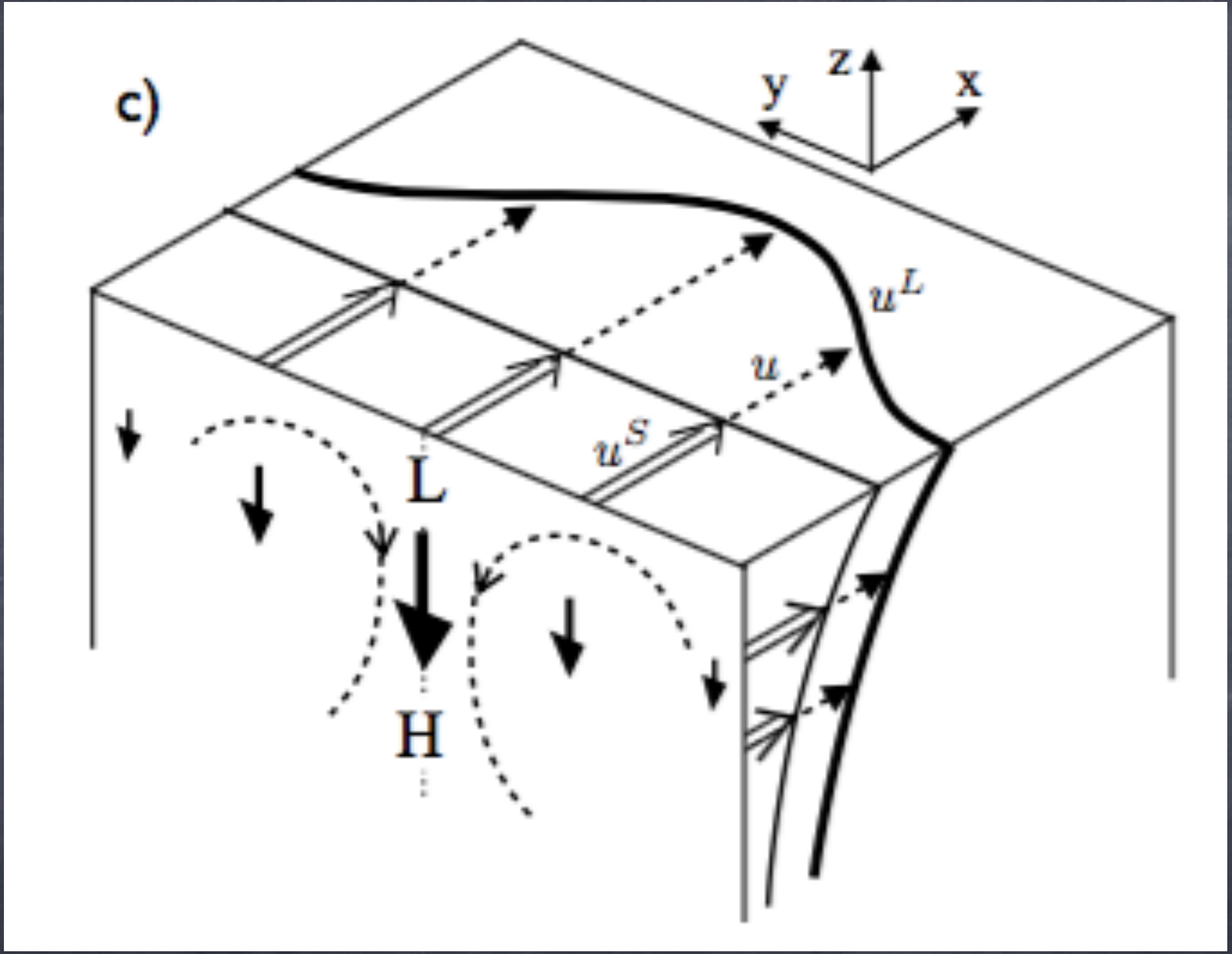

$$\frac{\alpha^2}{Ri}\left[w_{,t} + v_j^L w_{,j} + \frac{M_{Ro}}{RoRi} w w_{,z}\right] = -\pi_{,z} + b - \varepsilon v_j^L v_{j,z}^s + \frac{\alpha^2}{ReRi} w_{,jj}$$

N. Suzuki and BFK. Understanding Stokes forces in the wave-averaged equations. JGR-Oceans, December 2015. Submitted.

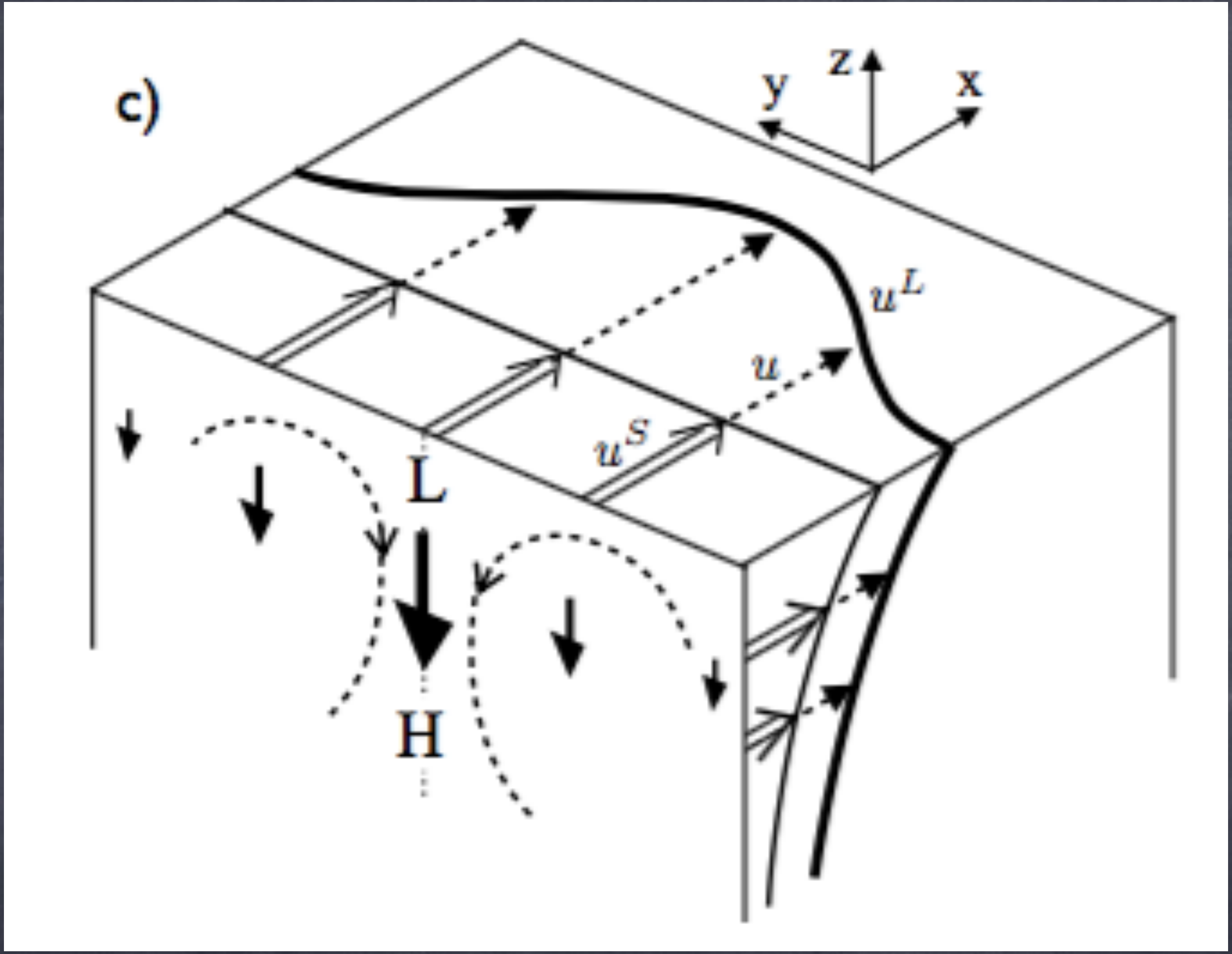

Typical effect: Downward Force for down-Flow Stokes Drift

$$\frac{\alpha^2}{Ri}\left[w_{,t} + v_j^L w_{,j} + \frac{M_{Ro}}{RoRi} w w_{,z}\right] = -\pi_{,z} + b - \varepsilon v_j^L v_{j,z}^s + \frac{\alpha^2}{ReRi} w_{,jj}$$

N. Suzuki and BFK. Understanding Stokes forces in the wave-averaged equations. JGR-Oceans, December 2015. Submitted.

To quantify Langmuir Turb. effects on climate: 3 WAYS

- 1) From OBSERVATIONS, estimate wave effects on key parameters ($\langle w^2 \rangle$, sources of energy) using scalings from Large Eddy Simulations. MODEL INDEPENDENT

- 2) OFFLINE 1d mixing with waves parameterized, mixing into observed Argo profiles, reanalysis winds, waves, cooling. ROBUST TO MODEL ERRORS

- 3) In a climate model, *add in a wave forecast model as a new component in addition to atmosphere, ocean, ice, etc.*, use this to drive parameterizations of wave mixing in ocean component. FEEDBACKS PRESENT

No Retuning! All coefficents from LES

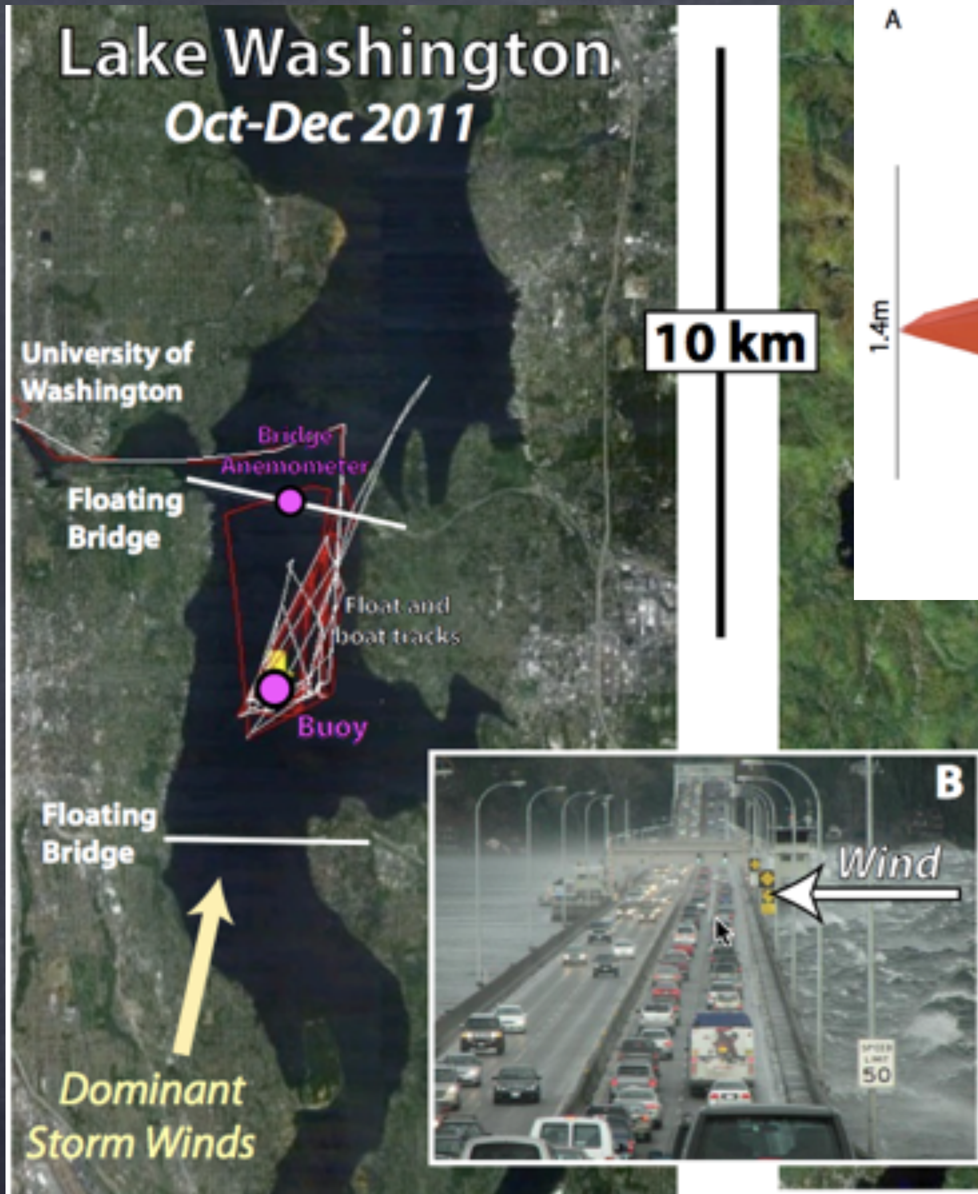

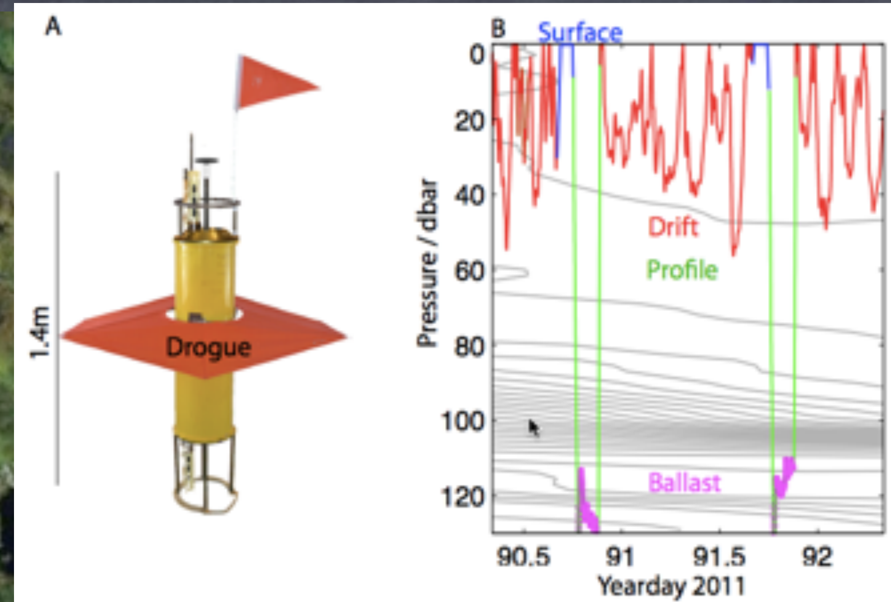

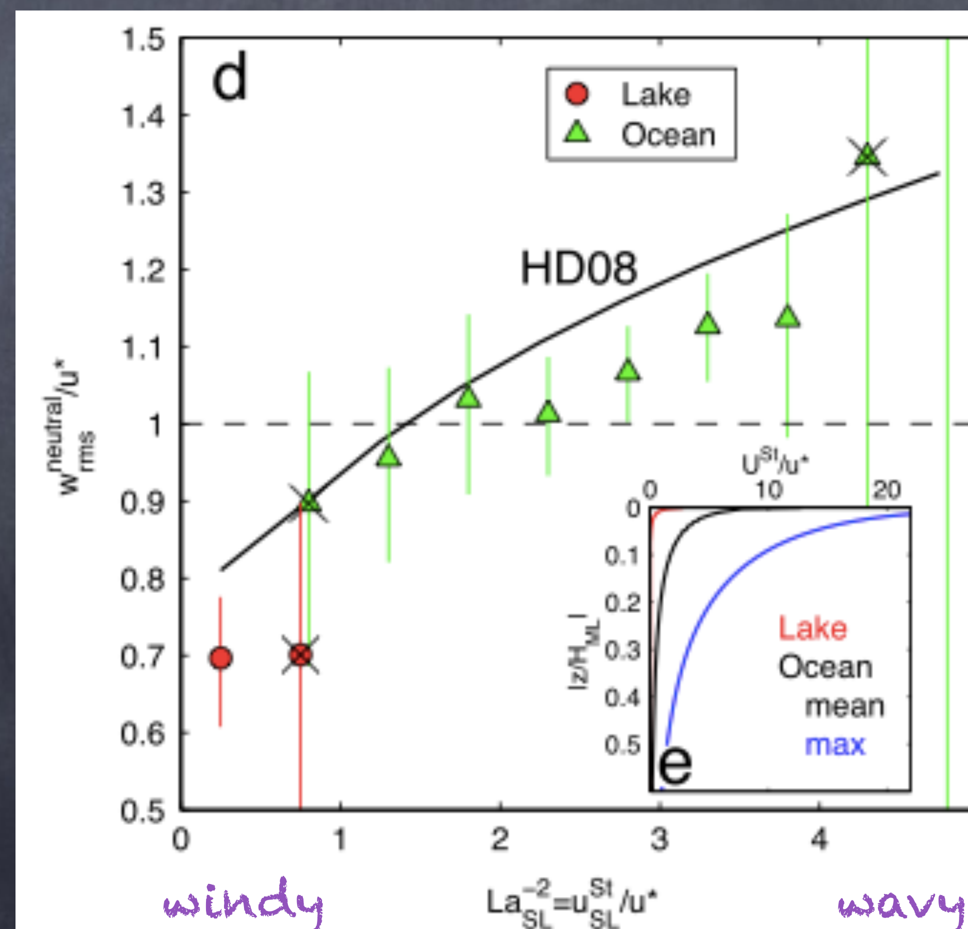

E. A. D'Asaro, J. Thomson, A. Y. Shcherbina, R. R. Harcourt, M. F. Cronin, M. A. Hemer, and BFK. Quantifying upper ocean turbulence driven by surface waves. Geophysical Research Letters, 41(1):102-107, January 2014.

1) Observations obey a particular scaling for $\langle w^2 \rangle$!

To quantify Langmuir Turb. effects on climate: 3 WAYS

- 1) From OBSERVATIONS, estimate wave effects on key parameters ($\langle w^2 \rangle$, sources of energy) using scalings from Large Eddy Simulations. MODEL INDEPENDENT

Langmuir important ✓

E. A. D'Asaro, J. Thomson, A. Y. Shcherbina, R. R. Harcourt, M. F. Cronin, M. A. Hemer, and BFK. Quantifying upper ocean turbulence driven by surface waves. Geophysical Research Letters, 41(1):102-107, January 2014.

- 2) OFFLINE 1d mixing with waves parameterized, mixing into observed Argo profiles, reanalysis winds, waves, cooling. ROBUST TO MODEL ERRORS

- 3) In a climate model, *add in a wave forecast model as a new component in addition to atmosphere, ocean, ice, etc.*, use this to drive parameterizations of wave mixing in ocean component. FEEDBACKS PRESENT

No Retuning! All coefficents from LES

Data + Large Eddy Simulation for scaling laws, Southern Ocean data to determine available mixing energy

So, waves are likely to drive mixing via Stokes drift (combines with cooling & winds)

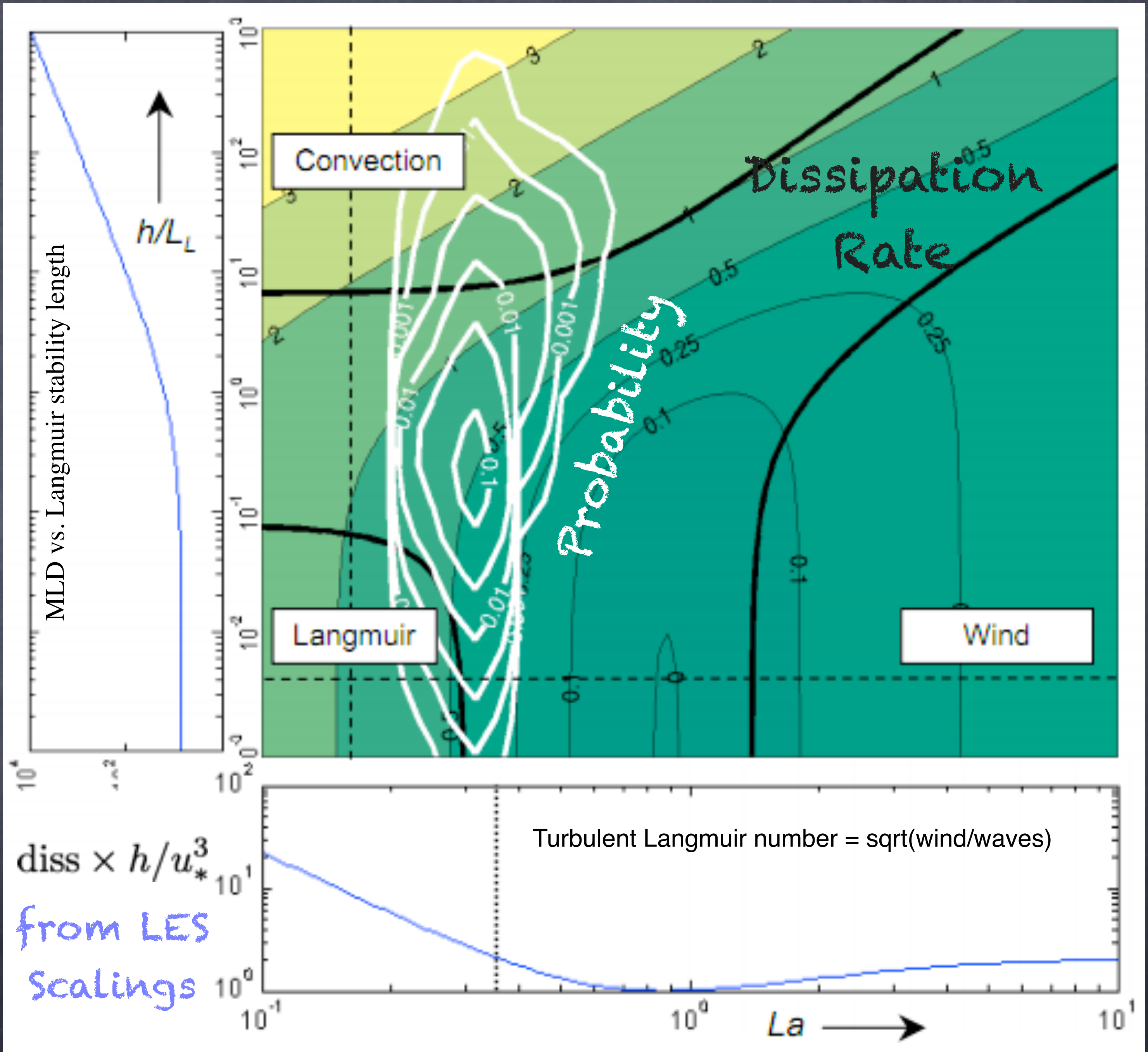

S. E. Belcher, A. A. L. M. Grant, K. E. Hanley, BFK, L. Van Roekel, P. P. Sullivan, W. G. Large, A. Brown, A. Hines, D. Calvert, A. Rutgersson, H. Petterson, J. Bidlot, P. A. E. M. Janssen, and J. A. Polton. A global perspective on Langmuir turbulence in the ocean surface boundary layer. Geophysical Research Letters, 39(18):L18605, 9pp, 2012.

Including Stokes-driven Mixing should deepen the Mixed Layer!

E. A. D'Asaro, J. Thomson, A. Y. Shcherbina, R. R. Harcourt, M. F. Cronin, M. A. Hemer, and BFK. Quantifying upper ocean turbulence driven by surface waves. Geophysical Research Letters, 41(1):102-107, January 2014.

As estimated with:
Argo-observed stratification,
modeled waves,
an LES-validated mixing parameterization,
and observed winds, solar, latent, etc.

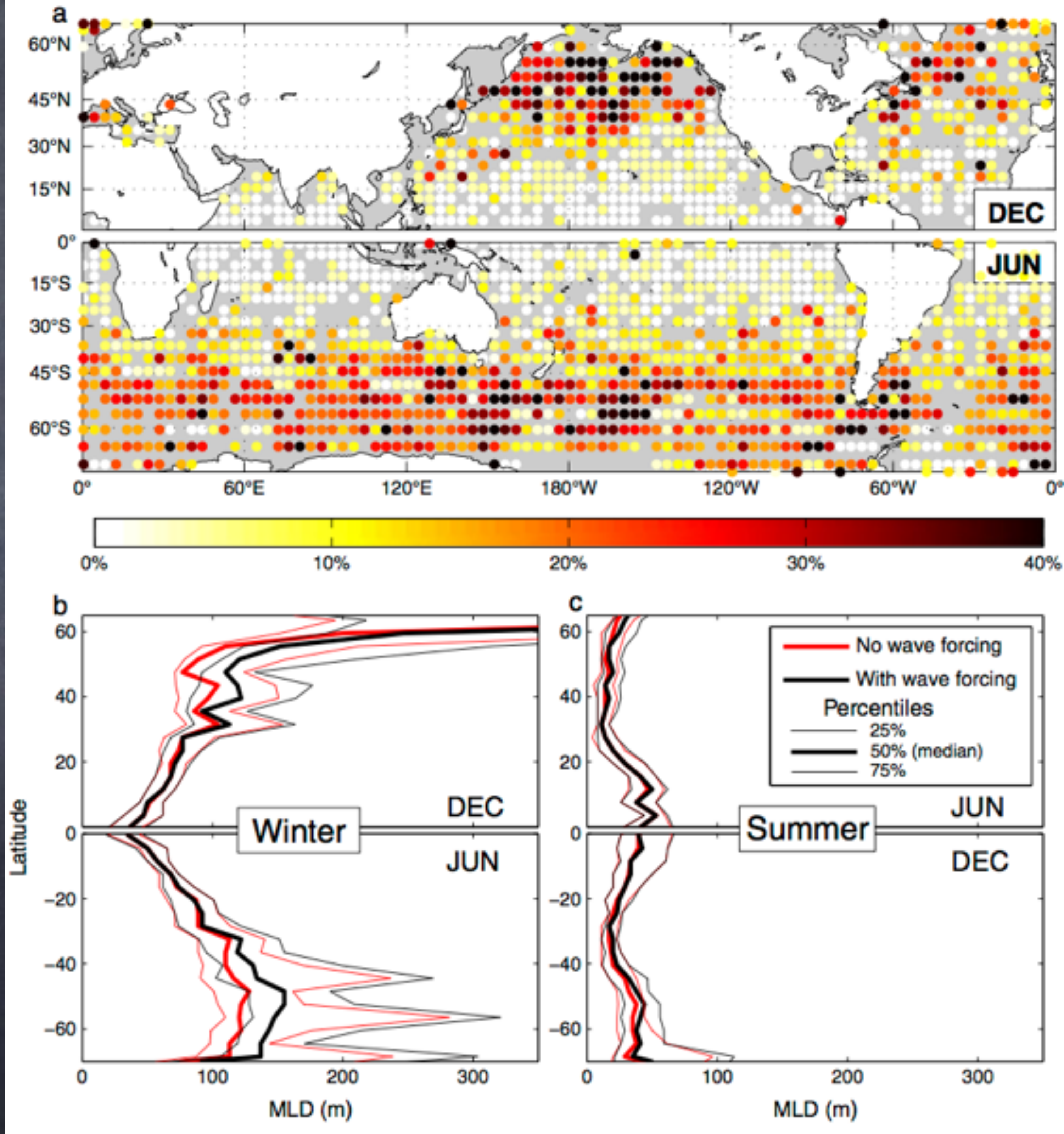

To quantify Langmuir Turb. effects on climate: 3 WAYS

- 1) From OBSERVATIONS, estimate wave effects on key parameters ($\langle w^2 \rangle$, sources of energy) using scalings from Large Eddy Simulations. MODEL INDEPENDENT

Langmuir important

E. A. D'Asaro, J. Thomson, A. Y. Shcherbina, R. R. Harcourt, M. F. Cronin, M. A. Hemer, and BFK. Quantifying upper ocean turbulence driven by surface waves. Geophysical Research Letters, 41(1):102-107, January 2014.

- 2) OFFLINE 1d mixing with waves parameterized, mixing into observed Argo profiles, reanalysis winds, waves, cooling. ROBUST TO MODEL ERRORS

Langmuir important

S. E. Belcher, A. A. L. M. Grant, K. E. Hanley, BFK, L. Van Roekel, P. P. Sullivan, W. G. Large, A. Brown, A. Hines, D. Calvert, A. Rutgersson, H. Petterson, J. Bidlot, P. A. E. M. Janssen, and J. A. Polton. A global perspective on Langmuir turbulence in the ocean surface boundary layer. Geophysical Research Letters, 39(18):L18605, 9pp, September 2012.

- 3) In a climate model, *add in a wave forecast model as a new component in addition to atmosphere, ocean, ice, etc.*, use this to drive parameterizations of wave mixing in ocean component. FEEDBACKS PRESENT

No Retuning! All coefficents from LES

U. S. Department of Commerce
National Oceanic and Atmospheric Administration
National Weather Service
National Centers for Environmental Prediction
5200 Auth Road
Camp Springs, MD 20746

Technical Note

User manual and system documentation of WAVEWATCH III [TM] version 3.14 [†]

Hendrik L. Tolman [‡]

Environmental Modeling Center
Marine Modeling and Analysis Branch

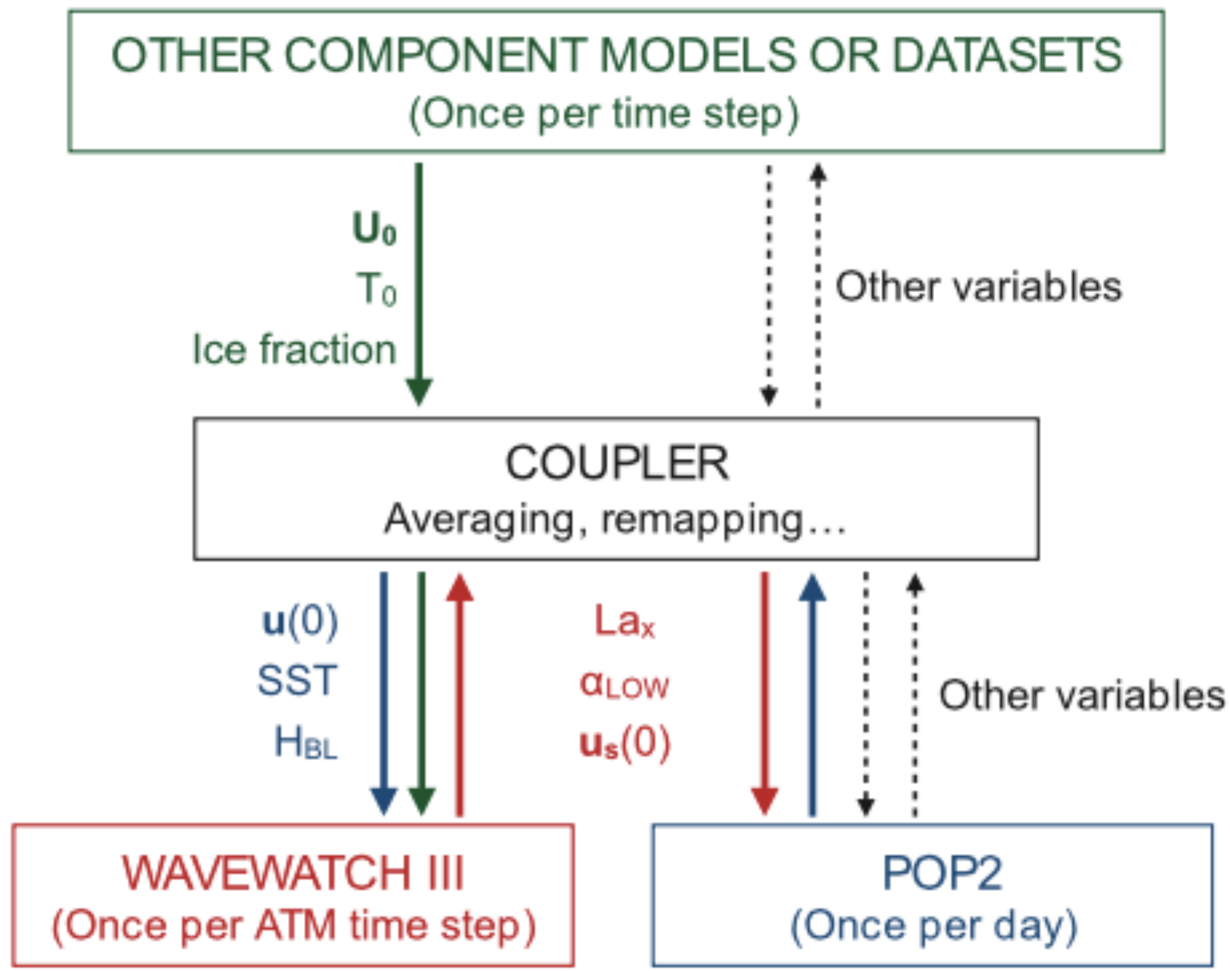

Q. Li, A. Webb, BFK, A. Craig, G. Danabasoglu, W. G. Large, and M. Vertenstein. Langmuir mixing effects on global climate: WAVEWATCH III in CESM. Ocean Modelling, August 2015. in press.

Something that happens often with waves:
Tricky: Misaligned Wind & Waves

A. Webb and BFK. Impacts of wave spreading and multidirectional waves on estimating Stokes drift. Ocean Modelling, 96(1): 49-64, December 2015.

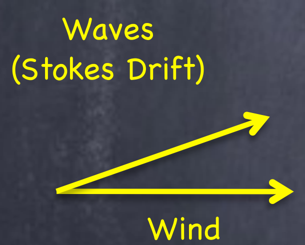

L. P. Van Roekel, BFK, P. P. Sullivan, P. E. Hamlington, and S. R. Haney. The form and orientation of Langmuir cells for misaligned winds and waves. Journal of Geophysical Research-Oceans, 117:C05001, 22pp, May 2012.

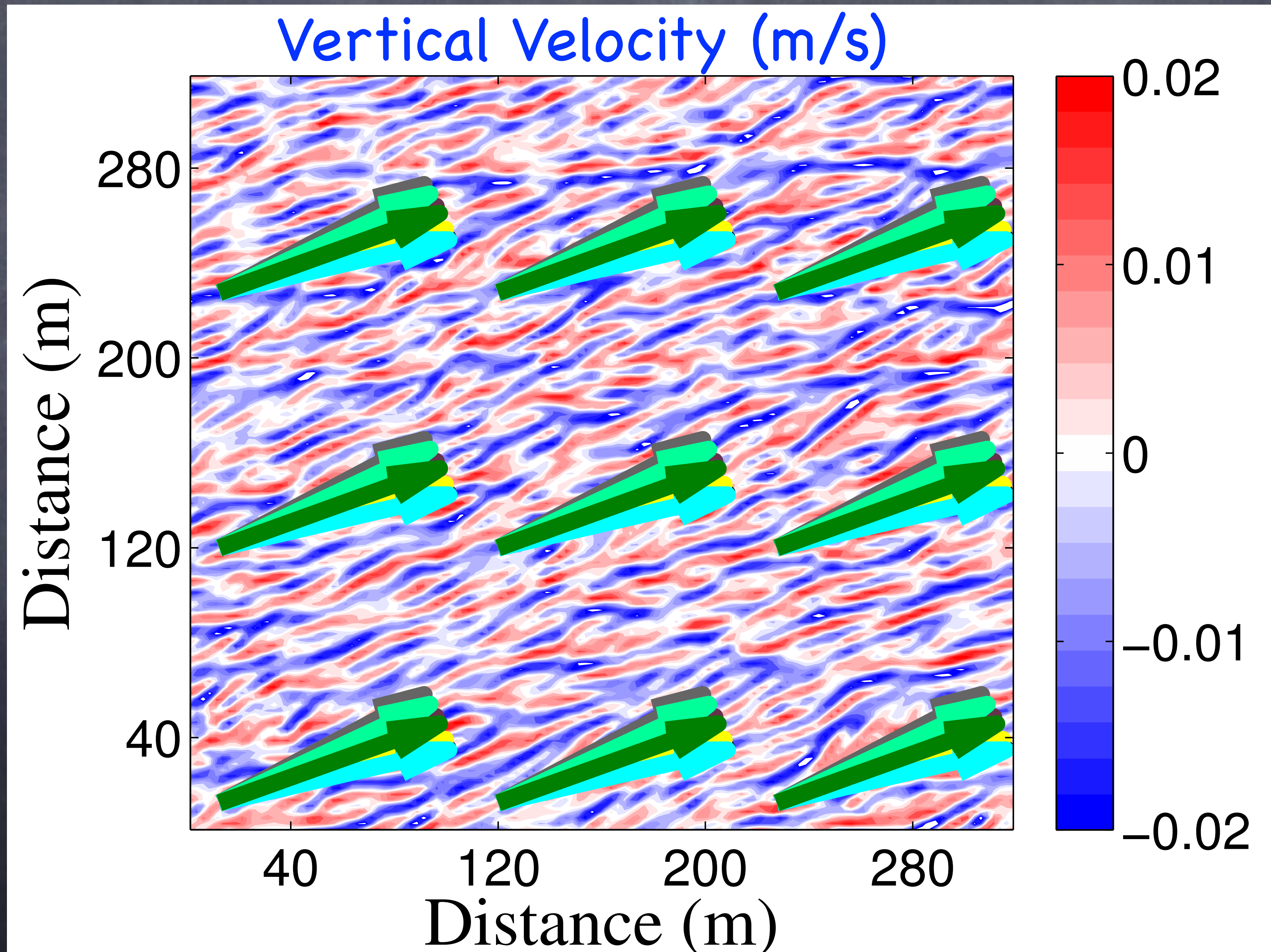

Tricky: Misaligned Wind & Waves

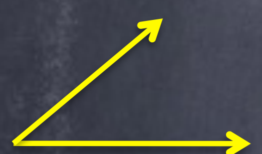

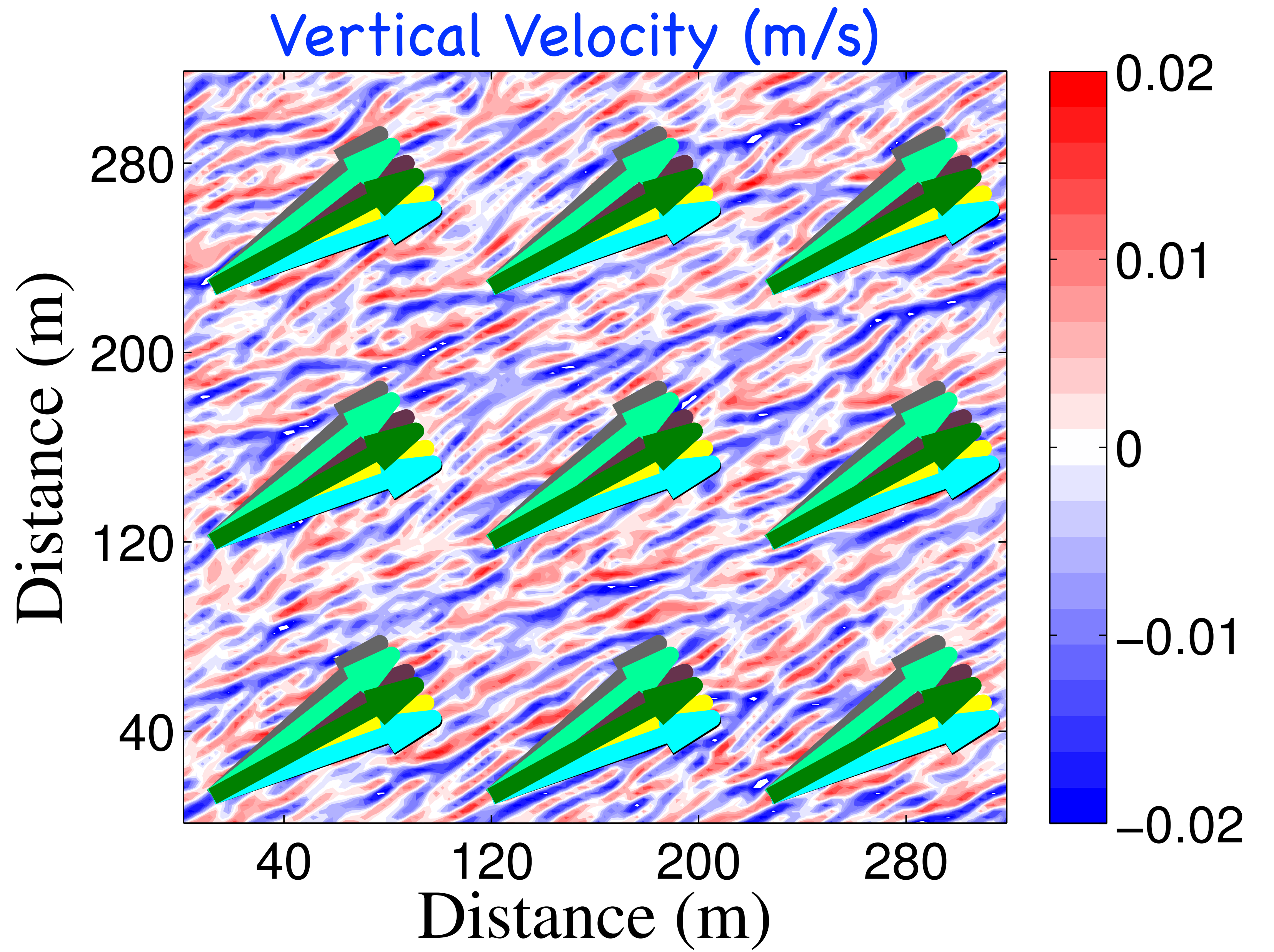

L. P. Van Roekel, BFK, P. P. Sullivan, P. E. Hamlington, and S. R. Haney. The form and orientation of Langmuir cells for misaligned winds and waves. Journal of Geophysical Research-Oceans, 117:C05001, 22pp, May 2012.

Tricky: Misaligned Wind & Waves

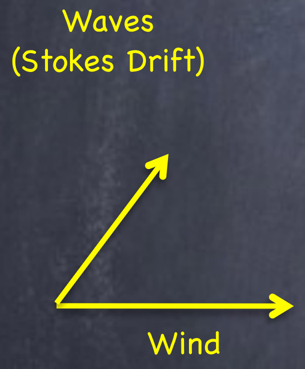

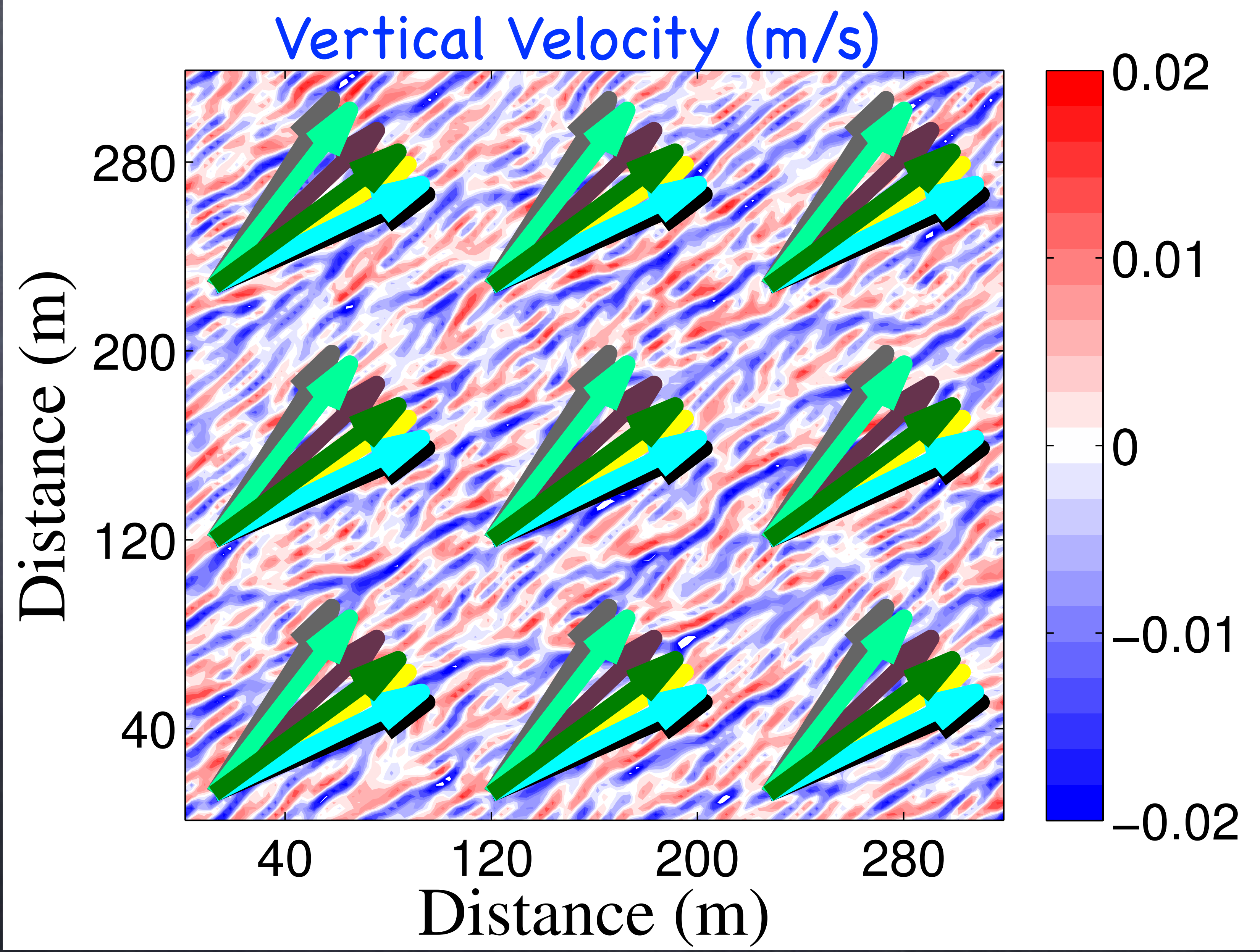

L. P. Van Roekel, BFK, P. P. Sullivan, P. E. Hamlington, and S. R. Haney. The form and orientation of Langmuir cells for misaligned winds and waves. Journal of Geophysical Research-Oceans, 117:C05001, 22pp, May 2012.

Tricky: Misaligned Wind & Waves

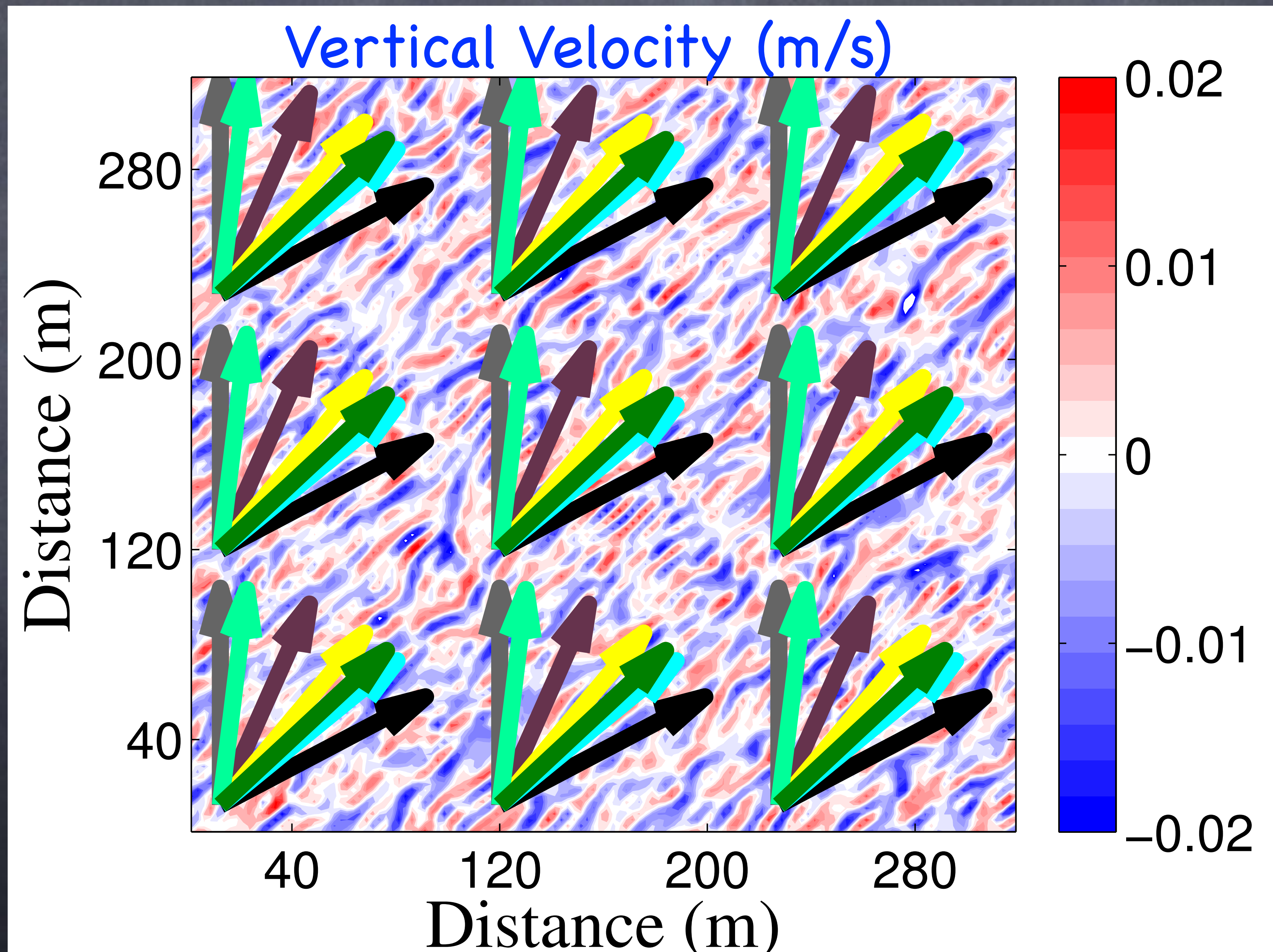

L. P. Van Roekel, BFK, P. P. Sullivan, P. E. Hamlington, and S. R. Haney. The form and orientation of Langmuir cells for misaligned winds and waves. Journal of Geophysical Research-Oceans, 117:C05001, 22pp, May 2012.

Langmuir Mixing in KPP for use in CESM1.2

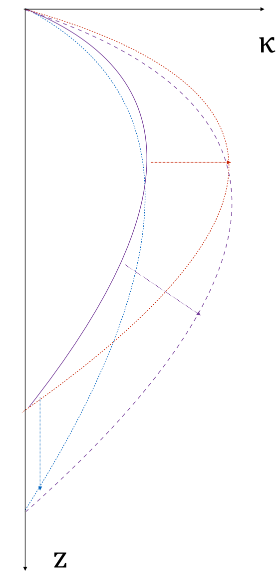

Q. Li, A. Webb, B. Fox-Kemper, A. Craig, G. Danabasoglu, W. G. Large, and M. Vertenstein. Langmuir mixing effects on global climate: WAVEWATCH III in CESM. Ocean Modelling, 2015. In press.

- WaveWatch-III (Stokes drift) <-> POP2 (U, T, H_{BL})
- CORE2 interannual forcing (Large and Yeager,2009), or fully coupled
- 4 IAF cycles; average over last 50 years for climatology (over 200 years total)
- Or fully coupled climate model—active atmosphere.

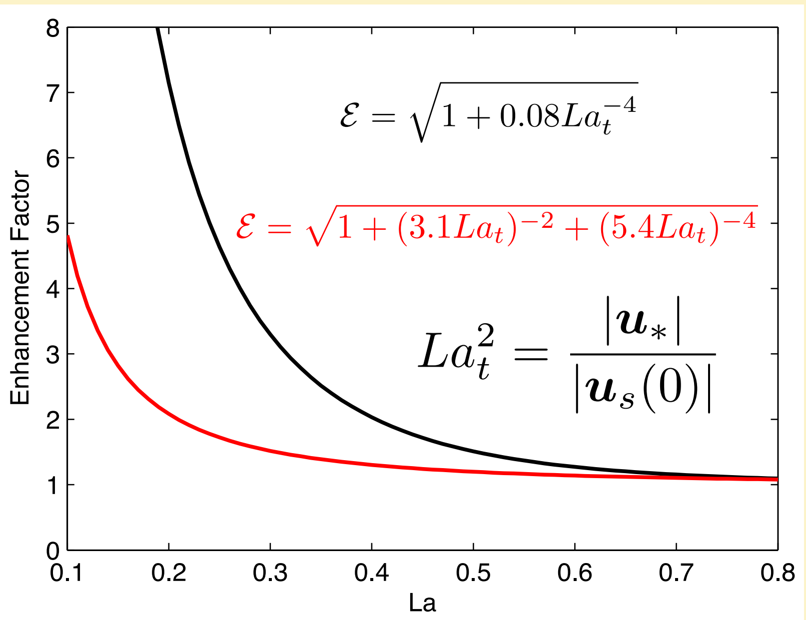

MS2K

VR12-AL

Revise Enhancement factor to vertical velocity scale W

Aligned wind and waves

VR12-MA

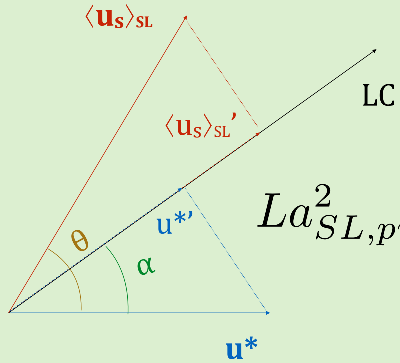

$$La^2_{SL,proj} = \frac{|\boldsymbol{u}_*| cos(\alpha)}{|\langle \boldsymbol{u}_s \rangle_{SL}| cos(\theta - \alpha)}$$

Account for Misaligned wind and waves

VR12-EN

$$Ri_b = \frac{d\,[b_r - b(d)]}{|\langle \boldsymbol{u}_r \rangle - \langle \boldsymbol{u}(d) \rangle|^2 + U_t^2 + |\boldsymbol{u}_s(0)|^2}$$

Entrain by also Including Stokes shear in mixing depth

McWilliams and Sullivan, 2000; L. P. Van Roekel, BFK, P. P. Sullivan, P. E. Hamlington, and S. R. Haney. The form and orientation of Langmuir cells for misaligned winds and waves. Journal of Geophysical Research-Oceans, 117:C05001, 22pp, 2012.

Langmuir Mixing in Climate: Boundary layer Depth Improved

Control

Competition

3 versions of Van Roekel et al

Case	Summer			Winter		
	Global	South of 30°S	30°S-30°N	Global	South of 30°S	30°S-30°N
CTRL	10.62±0.27[a]	17.24±0.48	5.38±0.14	43.85±0.38	57.19±0.76	12.57±0.28
	(13.40±0.19)[b]	(21.73±0.32)	(6.71±0.09)	(45.50±0.40)	(56.53±0.59)	(16.16±0.29)
MS2K	15.37	15.47	17.03	119.91	171.92	40.31
SS02	36.79	63.83	7.54	99.32	164.34	17.39
VR12-AL	9.06	13.47	6.49	40.45	50.33	14.52
VR12-MA	8.73±0.30	12.65±0.47	6.61±0.22	40.99±0.37	51.78±0.65	14.23±0.30
	(11.83±0.29)	(18.13±0.62)	(7.52±0.16)	(42.02±0.39)	(50.78±0.67)	(15.67±0.35)
VR12-EN	8.95	10.52	8.91	41.94	52.98	19.58

dotted when statistically significant

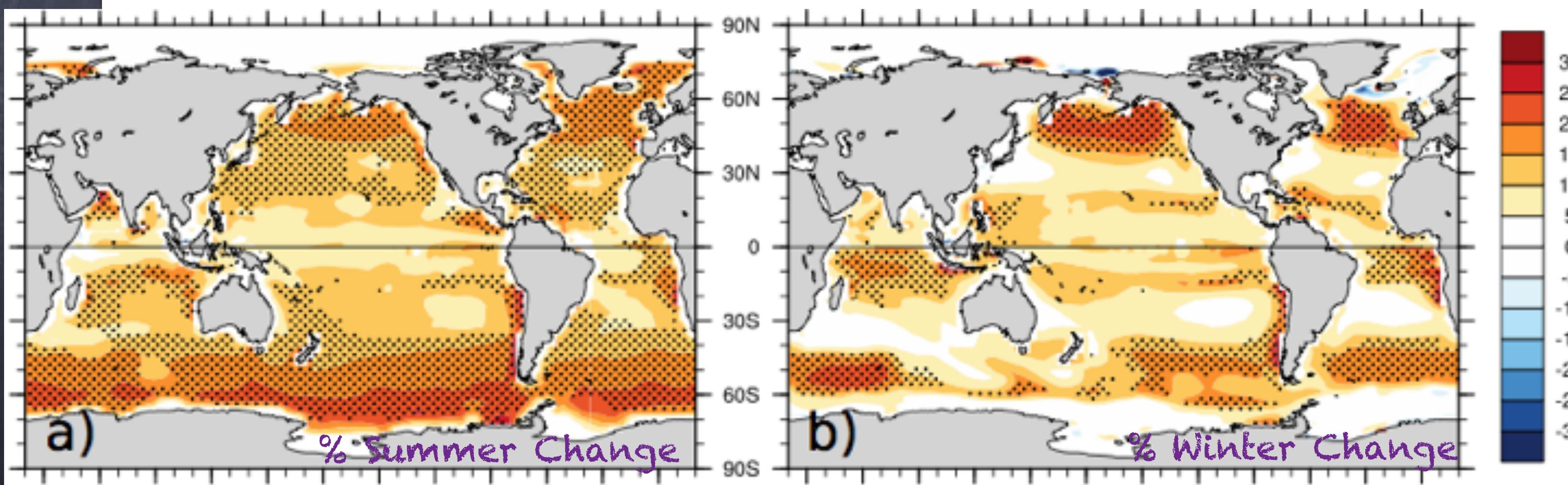

L. P. Van Roekel, BFK, P. P. Sullivan, P. E. Hamlington, and S. R. Haney. The form and orientation of Langmuir cells for misaligned winds and waves. Journal of Geophysical Research-Oceans, 117:C05001, 22pp, May 2012.

Q. Li, A. Webb, BFK, A. Craig, G. Danabasoglu, W. G. Large, and M. Vertenstein. Langmuir mixing effects on global climate: WAVEWATCH III in CESM. Ocean Modelling, August 2015. in press.

Langmuir Mixing in Climate: Boundary layer Depth Improved

Case	Summer Global	Summer South of 30°S	Summer 30°S-30°N	Winter Global	Winter South of 30°S	Winter 30°S-30°N
CTRL	10.62±0.27[a]	17.24±0.48	5.38±0.14	43.85±0.38	57.19±0.76	12.57±0.28
	(13.40±0.19)[b]	(21.73±0.32)	(6.71±0.09)	(45.50±0.40)	(56.53±0.59)	(16.16±0.29)
MS2K	15.37	15.47	17.03	119.91	171.92	40.31
SS02	36.79	63.83	7.54	99.32	164.34	17.39
VR12-AL	9.06	13.47	6.49	40.45	50.33	14.52
VR12-MA	8.73±0.30	12.65±0.47	6.61±0.22	40.99±0.37	51.78±0.65	14.23±0.30
	(11.83±0.29)	(18.13±0.62)	(7.52±0.16)	(42.02±0.39)	(50.78±0.67)	(15.67±0.35)
VR12-EN	8.95	10.52	8.91	41.94	52.98	19.58

Control

Competition

3 versions of Van Roekel et al

dotted when statistically significant

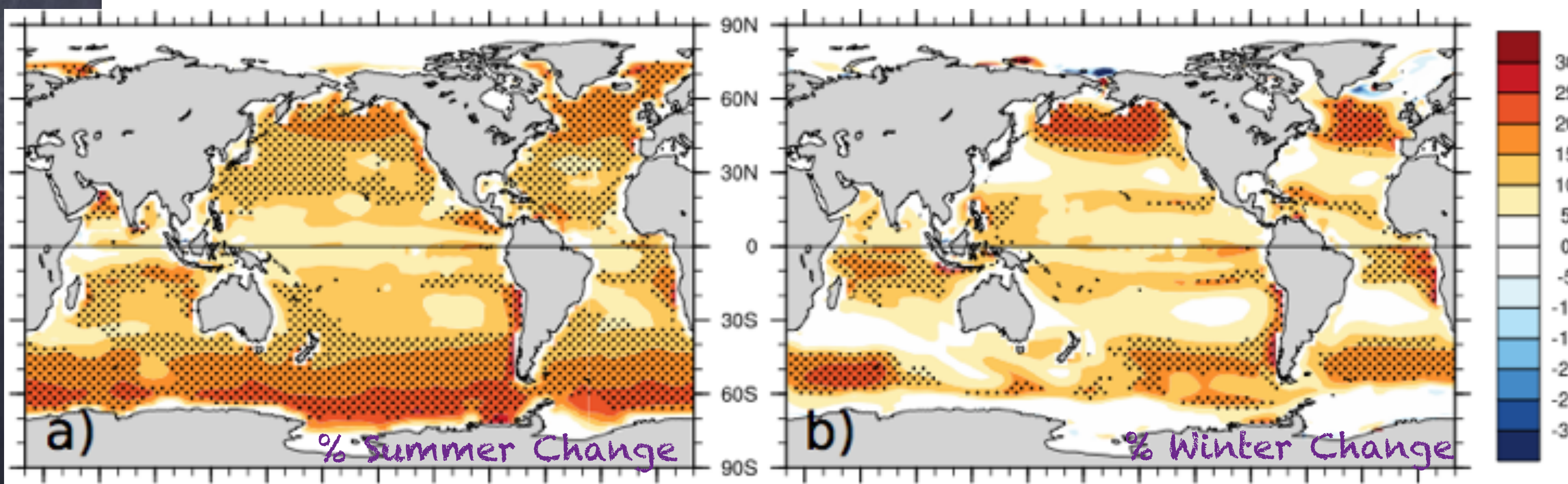

L. P. Van Roekel, BFK, P. P. Sullivan, P. E. Hamlington, and S. R. Haney. The form and orientation of Langmuir cells for misaligned winds and waves. Journal of Geophysical Research-Oceans, 117:C05001, 22pp, May 2012.

Q. Li, A. Webb, BFK, A. Craig, G. Danabasoglu, W. G. Large, and M. Vertenstein. Langmuir mixing effects on global climate: WAVEWATCH III in CESM. Ocean Modelling, August 2015. in press.

Langmuir Mixing in Climate: Boundary layer Depth Improved

Case	Summer			Winter		
	Global	South of 30°S	30°S-30°N	Global	South of 30°S	30°S-30°N
CTRL	10.62±0.27[a]	17.24±0.48	5.38±0.14	43.85±0.38	57.19±0.76	12.57±0.28
	(13.40±0.19)[b]	(21.73±0.32)	(6.71±0.09)	(45.50±0.40)	(56.53±0.59)	(16.16±0.29)
MS2K	15.37	15.47	17.03	119.91	171.92	40.31
SS02	36.79	63.83	7.54	99.32	164.34	17.39
VR12-AL	9.06	13.47	6.49	40.45	50.33	14.52
VR12-MA	8.73±0.30	12.65±0.47	6.61±0.22	40.99±0.37	51.78±0.65	14.23±0.30
	(11.83±0.29)	(18.13±0.62)	(7.52±0.16)	(42.02±0.39)	(50.78±0.67)	(15.67±0.35)
VR12-EN	8.95	10.52	8.91	41.94	52.98	19.58

Control

Competition

3 versions of Van Roekel et al

dotted when statistically significant

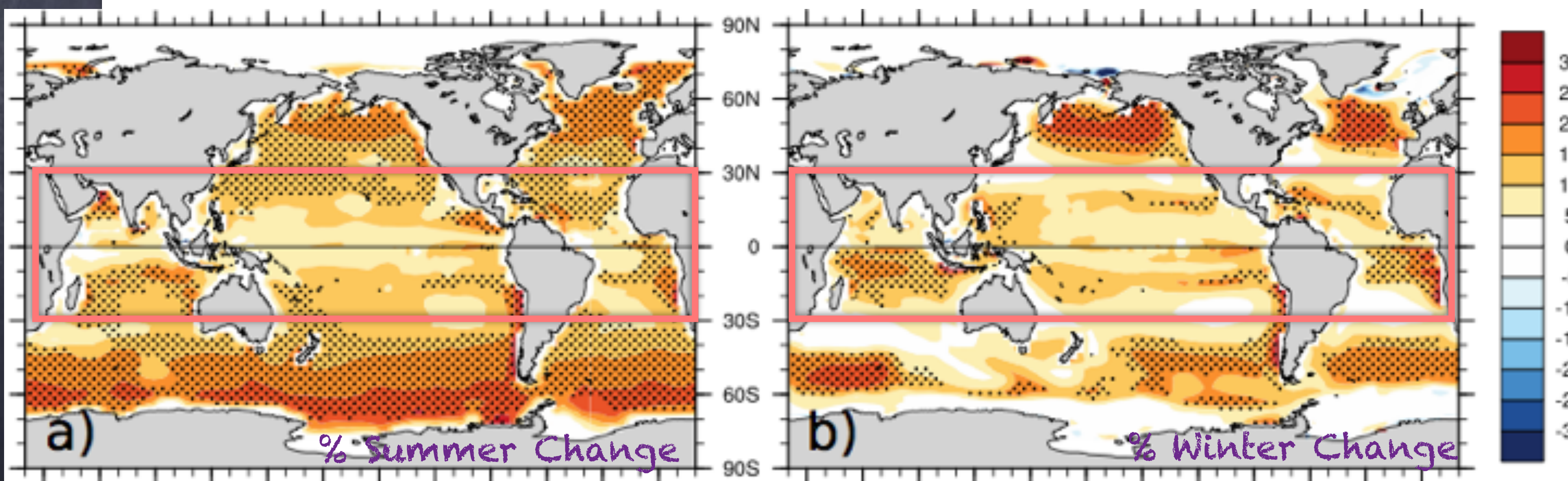

L. P. Van Roekel, BFK, P. P. Sullivan, P. E. Hamlington, and S. R. Haney. The form and orientation of Langmuir cells for misaligned winds and waves. Journal of Geophysical Research-Oceans, 117:C05001, 22pp, May 2012.

Q. Li, A. Webb, BFK, A. Craig, G. Danabasoglu, W. G. Large, and M. Vertenstein. Langmuir mixing effects on global climate: WAVEWATCH III in CESM. Ocean Modelling, August 2015. in press.

Langmuir Mixing in Climate: Boundary layer Depth Improved

	Case	Summer			Winter		
		Global	South of 30°S	30°S-30°N	Global	South of 30°S	30°S-30°N
Control	CTRL	10.62±0.27[a]	17.24±0.48	5.38±0.14	43.85±0.38	57.19±0.76	12.57±0.28
		(13.40±0.19)[b]	(21.73±0.32)	(6.71±0.09)	(45.50±0.40)	(56.53±0.59)	(16.16±0.29)
Competition	MS2K	15.37	15.47	17.03	119.91	171.92	40.31
	SS02	36.79	63.83	7.54	99.32	164.34	17.39
3 versions of Van Roekel et al	VR12-AL	9.06	13.47	6.49	40.45	50.33	14.52
	VR12-MA	8.73±0.30	12.65±0.47	6.61±0.22	40.99±0.37	51.78±0.65	14.23±0.30
		(11.83±0.29)	(18.13±0.62)	(7.52±0.16)	(42.02±0.39)	(50.78±0.67)	(15.67±0.35)
	VR12-EN	8.95	10.52	8.91	41.94	52.98	19.58

dotted when statistically significant

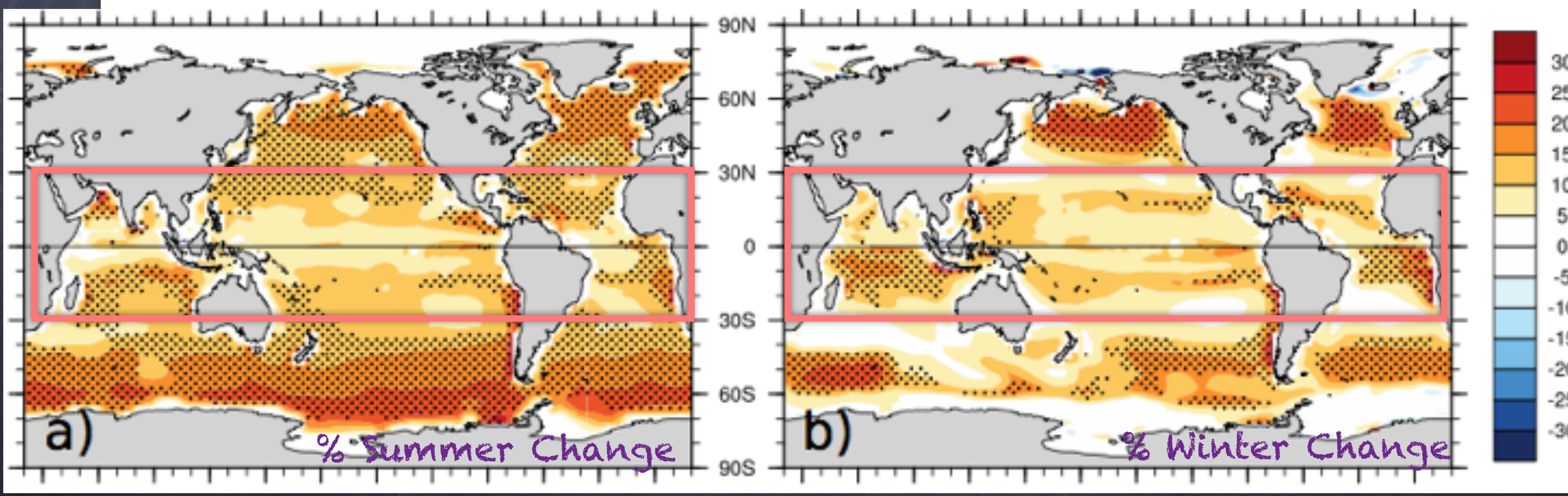

L. P. Van Roekel, BFK, P. P. Sullivan, P. E. Hamlington, and S. R. Haney. The form and orientation of Langmuir cells for misaligned winds and waves. Journal of Geophysical Research-Oceans, 117:C05001, 22pp, May 2012.

Q. Li, A. Webb, BFK, A. Craig, G. Danabasoglu, W. G. Large, and M. Vertenstein. Langmuir mixing effects on global climate: WAVEWATCH III in CESM. Ocean Modelling, August 2015. in press.

Langmuir Mixing in Climate: Boundary layer Depth Improved

Case	Summer Global	Summer South of 30°S	Summer 30°S-30°N	Winter Global	Winter South of 30°S	Winter 30°S-30°N
CTRL	10.62±0.27[a]	17.24±0.48	5.38±0.14	43.85±0.38	57.19±0.76	12.57±0.28
	(13.40±0.19)[b]	(21.73±0.32)	(6.71±0.09)	(45.50±0.40)	(56.53±0.59)	(16.16±0.29)
MS2K	15.37	15.47	17.03	119.91	171.92	40.31
SS02	36.79	63.83	7.54	99.32	164.34	17.39
VR12-AL	9.06	13.47	6.49	40.45	50.33	14.52
VR12-MA	8.73±0.30	12.65±0.47	6.61±0.22	40.99±0.37	51.78±0.65	14.23±0.30
	(11.83±0.29)	(18.13±0.62)	(7.52±0.16)	(42.02±0.39)	(50.78±0.67)	(15.67±0.35)
VR12-EN	8.95	10.52	8.91	41.94	52.98	19.58

Control

Competition

3 versions of Van Roekel et al

dotted when statistically significant

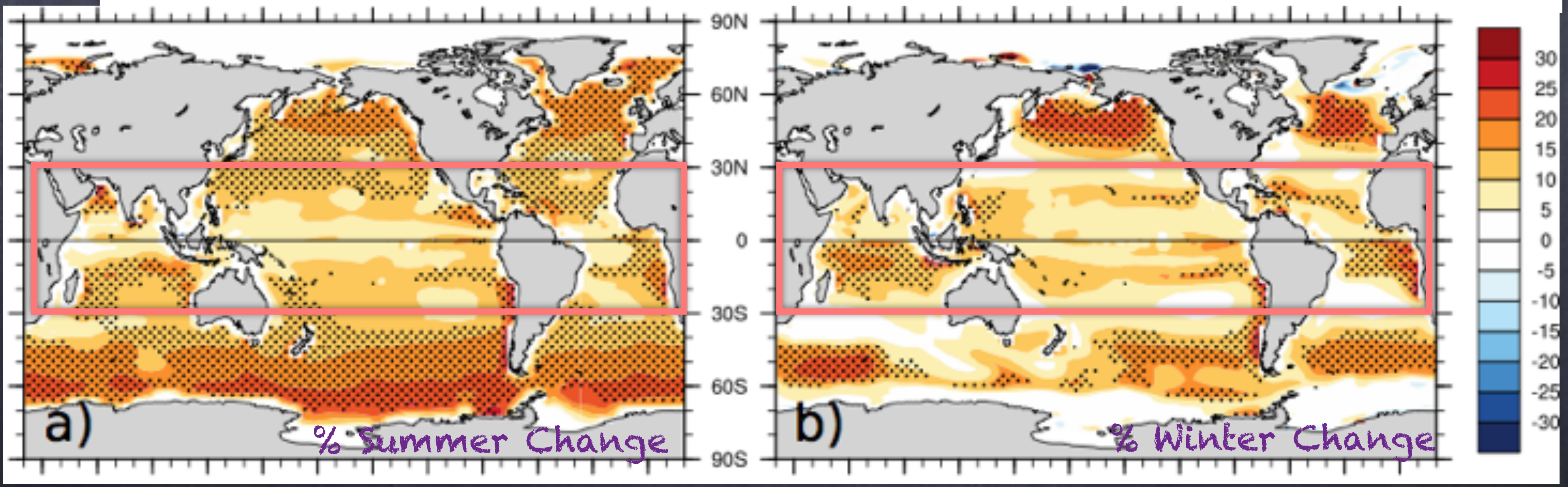

L. P. Van Roekel, BFK, P. P. Sullivan, P. E. Hamlington, and S. R. Haney. The form and orientation of Langmuir cells for misaligned winds and waves. Journal of Geophysical Research-Oceans, 117:C05001, 22pp, May 2012.

Q. Li, A. Webb, BFK, A. Craig, G. Danabasoglu, W. G. Large, and M. Vertenstein. Langmuir mixing effects on global climate: WAVEWATCH III in CESM. Ocean Modelling, August 2015. in press.

Subsurface Temperature:
Improved vs. Observations with Langmuir

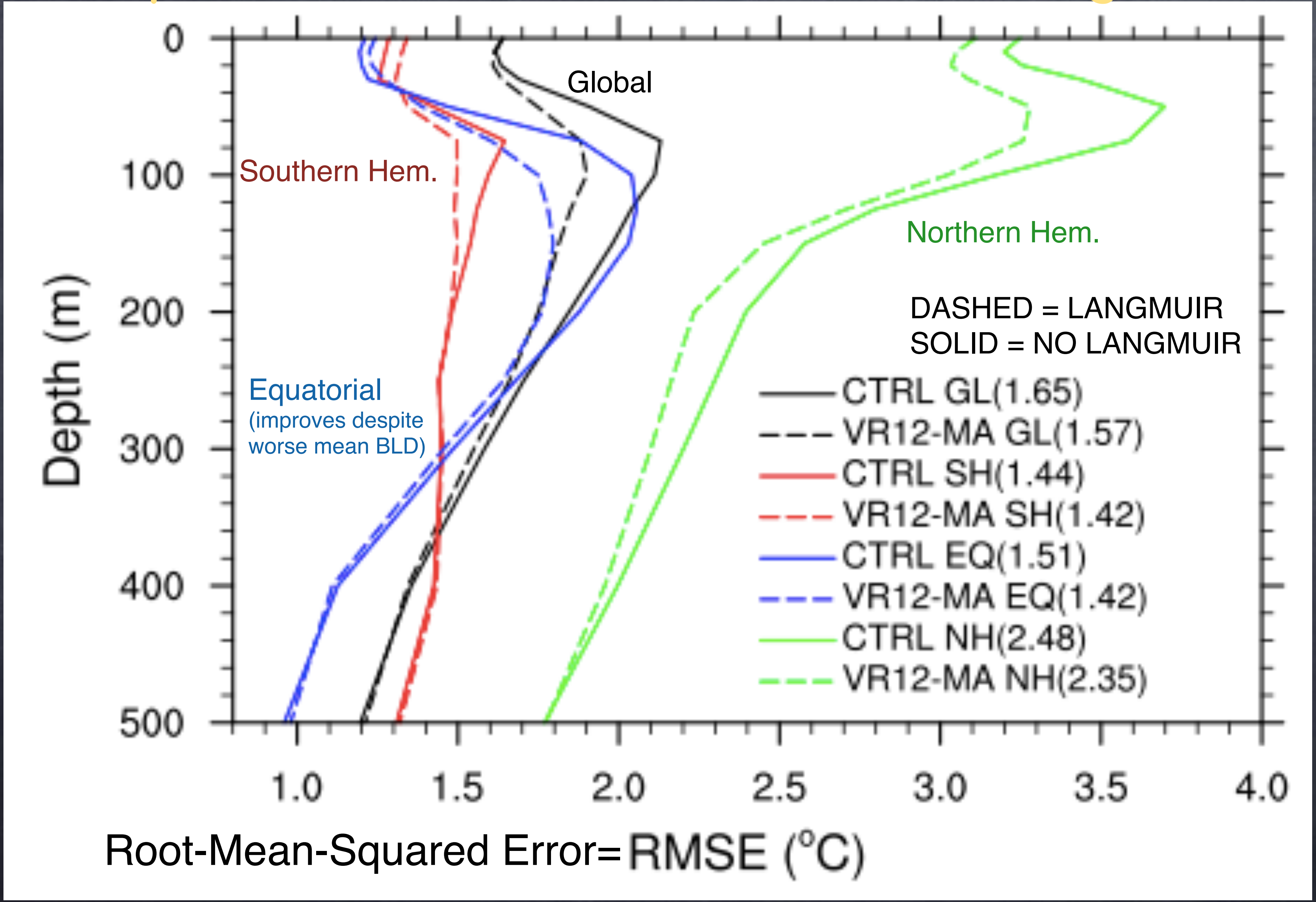

Q. Li, A. Webb, BFK, A. Craig, G. Danabasoglu, W. G. Large, and M. Vertenstein. Langmuir mixing effects on global climate: WAVEWATCH III in CESM. Ocean Modelling, August 2015. in press.

Enhancing ocean ventilation

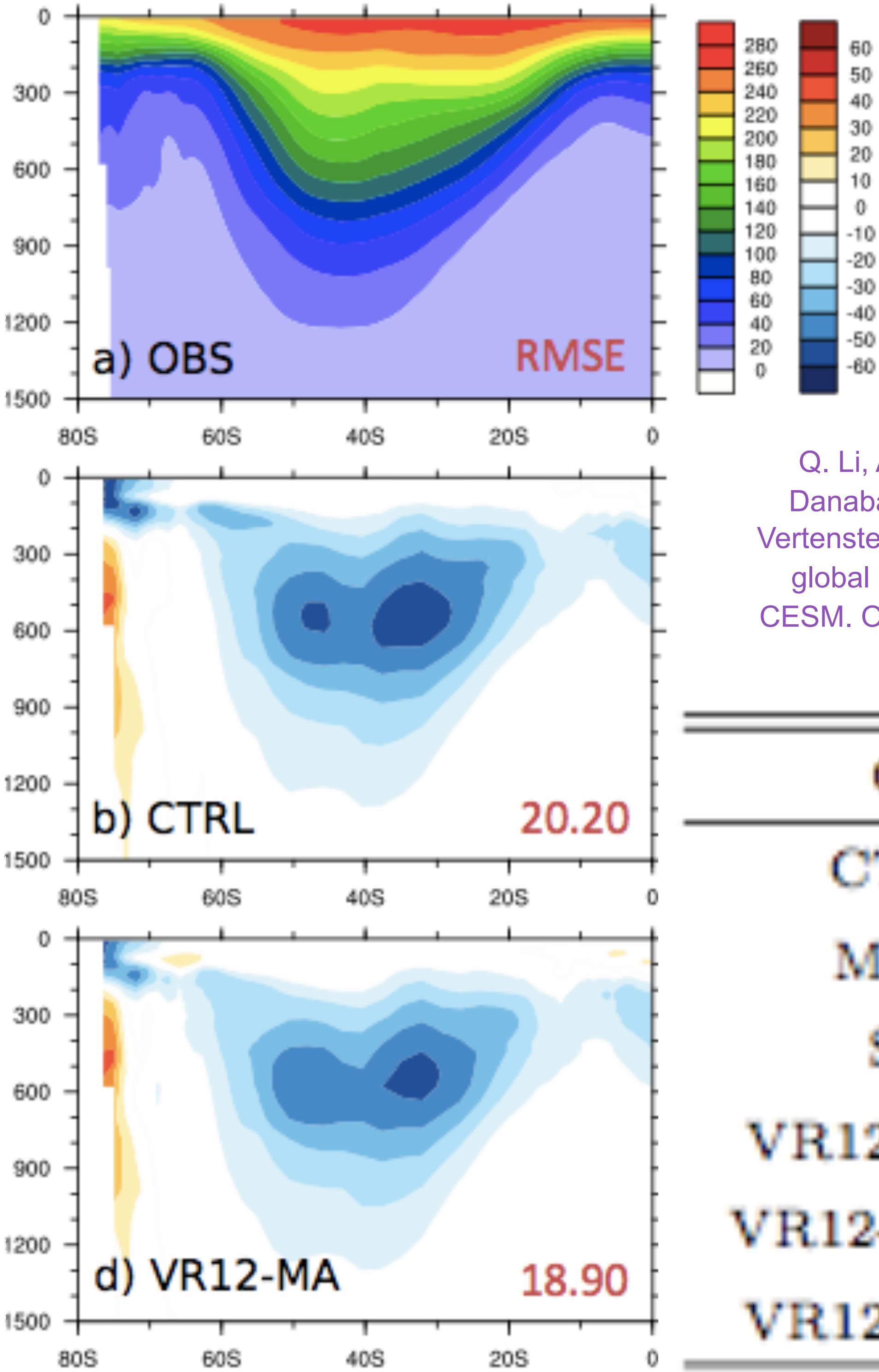

Fig. 3. Impact on the zonal mean pCFC-11 (patm) in the Southern Hemisphere. (a) Observation[6] (GLODAP); (b) Biases in the control test without Langmuir mixing; (c) - (e) Biases in tests with Langmuir mixing.

Q. Li, A. Webb, BFK, A. Craig, G. Danabasoglu, W. G. Large, and M. Vertenstein. Langmuir mixing effects on global climate: WAVEWATCH III in CESM. Ocean Modelling, August 2015. in press.

Ocean Uptake:

Chlorofluorocarbons (manmade pollutant, detectable & known source)

Improved vs. Observations with Langmuir Mixing

Case	Global	Southern Hemisphere
CTRL	23.90	20.20
MS2K	29.89	30.99
SS02	34.16	41.90
VR12-AL	22.14	18.53
VR12-MA	23.23	18.90
VR12-EN	20.67	16.44

Enhancing ocean ventilation

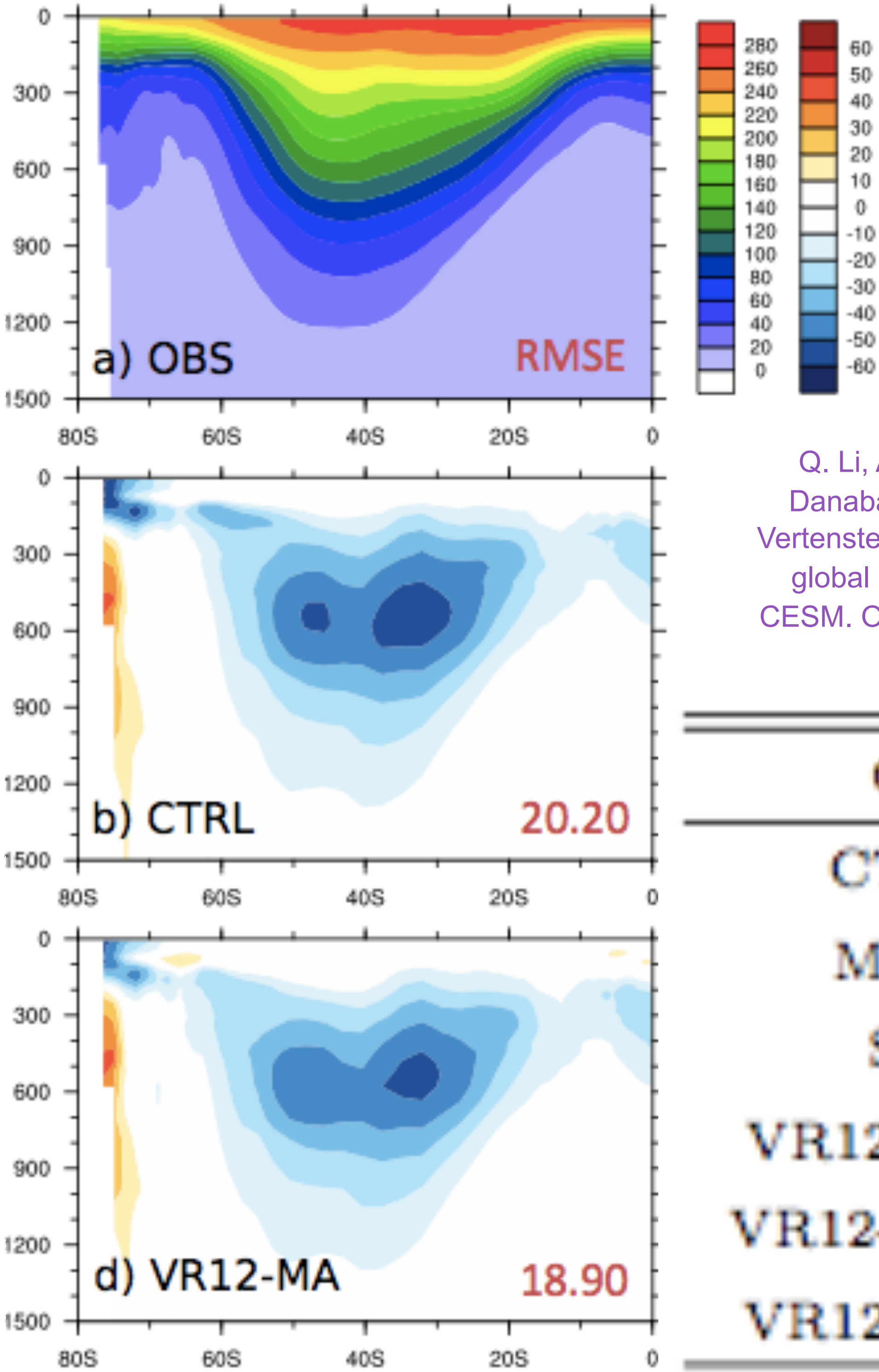

Fig. 3. Impact on the zonal mean pCFC-11 (patm) in the Southern Hemisphere. (a) Observation[6] (GLODAP); (b) Biases in the control test without Langmuir mixing; (c) - (e) Biases in tests with Langmuir mixing.

Q. Li, A. Webb, BFK, A. Craig, G. Danabasoglu, W. G. Large, and M. Vertenstein. Langmuir mixing effects on global climate: WAVEWATCH III in CESM. Ocean Modelling, August 2015. in press.

Ocean Uptake:

Chlorofluorocarbons

(manmade pollutant, detectable & known source)

Improved vs. Observations with Langmuir Mixing

Case	Global	Southern Hemisphere
CTRL	23.90	20.20
MS2K	29.89	30.99
SS02	34.16	41.90
VR12-AL	22.14	18.53
VR12-MA	23.23	18.90
VR12-EN	20.67	16.44

Enhancing ocean ventilation

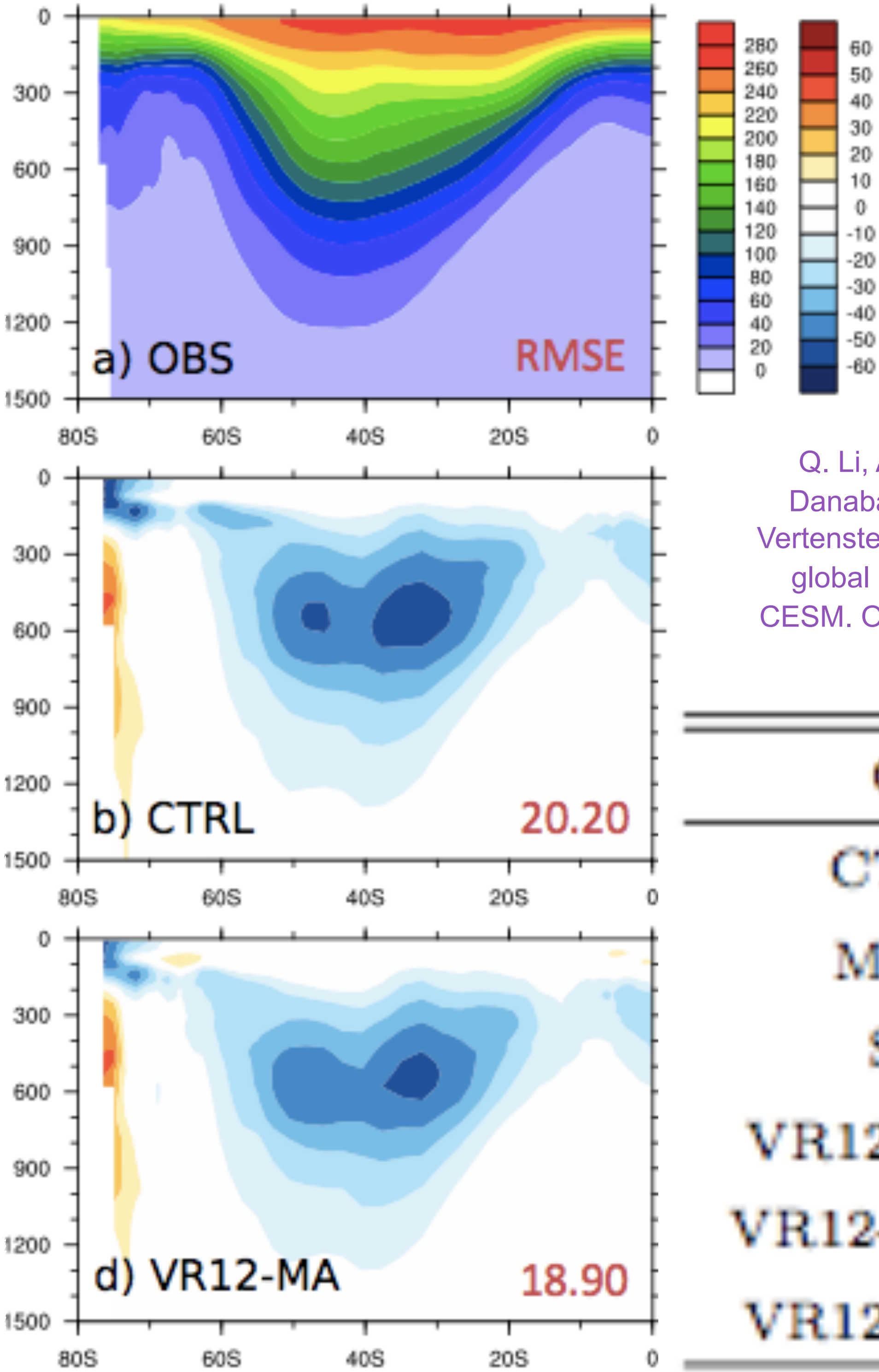

Fig. 3. Impact on the zonal mean pCFC-11 (patm) in the Southern Hemisphere. (a) Observation[6] (GLODAP); (b) Biases in the control test without Langmuir mixing; (c) - (e) Biases in tests with Langmuir mixing.

Q. Li, A. Webb, BFK, A. Craig, G. Danabasoglu, W. G. Large, and M. Vertenstein. Langmuir mixing effects on global climate: WAVEWATCH III in CESM. Ocean Modelling, August 2015. in press.

Ocean Uptake:

Chlorofluorocarbons (manmade pollutant, detectable & known source)

Improved vs. Observations with Langmuir Mixing

Case	Global	Southern Hemisphere
CTRL	23.90	20.20
MS2K	29.89	30.99
SS02	34.16	41.90
VR12-AL	22.14	18.53
VR12-MA	23.23	18.90
VR12-EN	20.67	16.44

So, we'll quantify Langmuir effects on climate

- 1) From OBSERVATIONS, estimate wave effects on key parameters ($\langle w^2 \rangle$, sources of energy) using scalings from Large Eddy Simulations. MODEL INDEPENDENT

Langmuir important ✓

- 2) OFFLINE 1d mixing with waves parameterized, mixing into observed Argo profiles, reanalysis winds, waves, cooling. ROBUST TO MODEL ERRORS

Langmuir important ✓

- 3) In a climate model, *add in a wave forecast model as a new component in addition to atmosphere, ocean, ice, etc.*, use this to drive parameterizations of wave mixing in ocean component. FEEDBACKS PRESENT

Langmuir important ✓

No Retuning! All coefficents from LES

Mid-way Conclusions

- Stokes forces may accelerate upper ocean mixing, leading to a wind-wave-convective turbulence driven partly by Stokes forces: Langmuir turbulence
- Three effects of Stokes drift are important: Stokes Advection, Stokes Coriolis, and Stokes Shear Force
- The Stokes Shear Force enhances downward and upward velocities in boundary layer turbulence.
- Including Langmuir mixing in climate models improves the climate model MLD, T, and uptake of CFCs.
- All papers at: fox-kemper.com/pubs

The Character of the Submesoscale

← 10 km

(NASA GSFC Gallery)

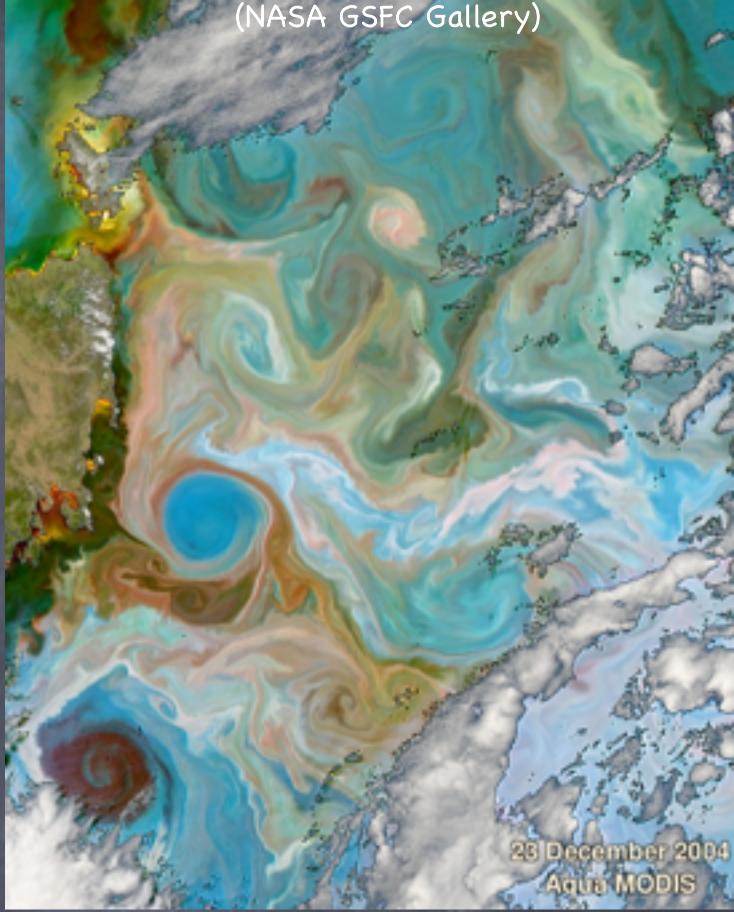

(Capet et al., 2008)

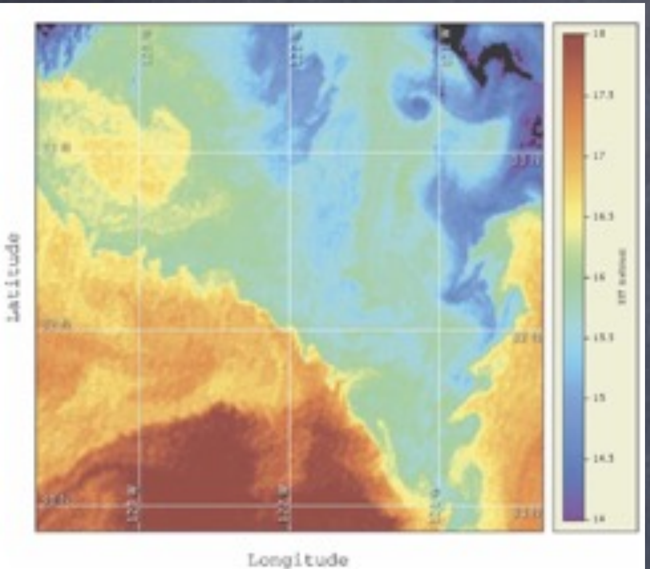

FIG. 16. Sea surface temperature measured at 1832 UTC 3 Jan 2006 off Point Conception in the California Current from CoastWatch (http://coastwatch.pfeg.noaa.gov). The fronts between recently

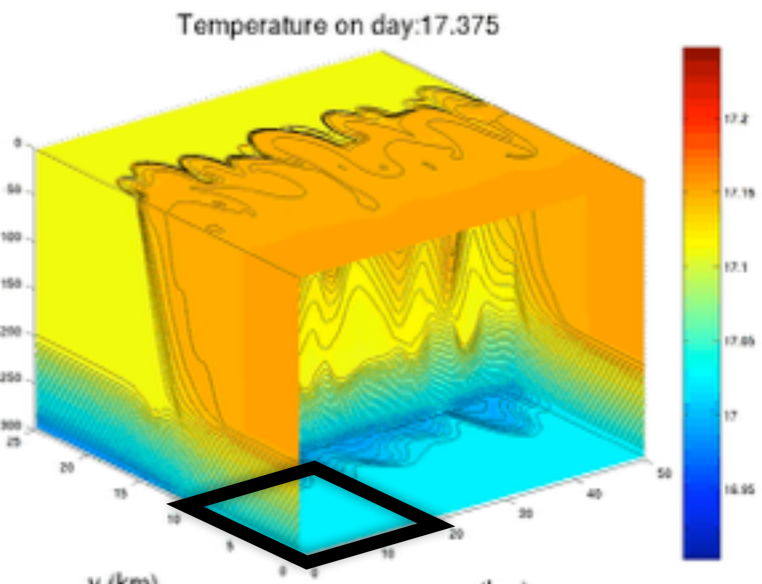

- Fronts
- Eddies
- Ro=O(1)
- Ri=O(1)
- near-surface (H=100m)
- 1-10km, days

Eddy processes often baroclinic instability

Parameterizations = BFK et al (08-11).

G. Boccaletti, R. Ferrari, and BFK. Mixed layer instabilities and restratification. Journal of Physical Oceanography, 37(9):2228-2250, 2007

BFK, R. Ferrari, and R. W. Hallberg. Parameterization of mixed layer eddies. Part I: Theory and diagnosis. Journal of Physical Oceanography, 38(6):1145-1165, 2008.

BFK, G. Danabasoglu, R. Ferrari, S. M. Griffies, R. W. Hallberg, M. M. Holland, M. E. Maltrud, S. Peacock, and B. L. Samuels. Parameterization of mixed layer eddies. III: Implementation and impact in global ocean climate simulations. Ocean Modelling, 39:61-78, 2011

The Character of the Submesoscale

← 10 km

(Capet et al., 2008)

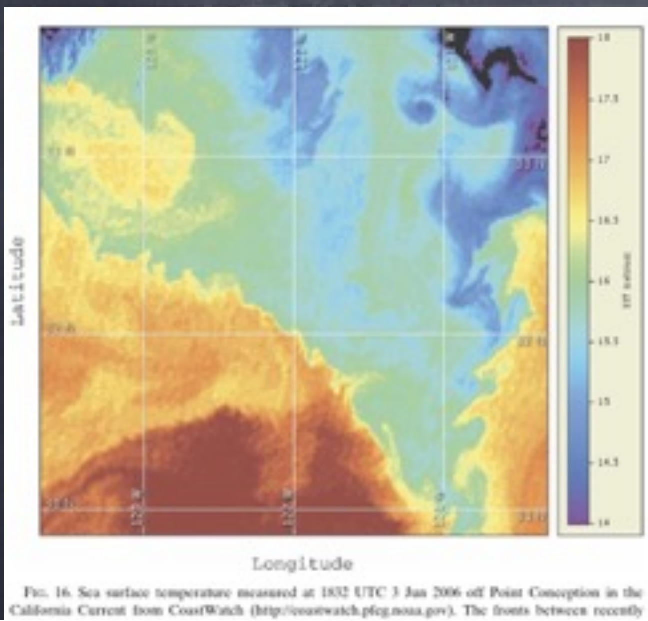

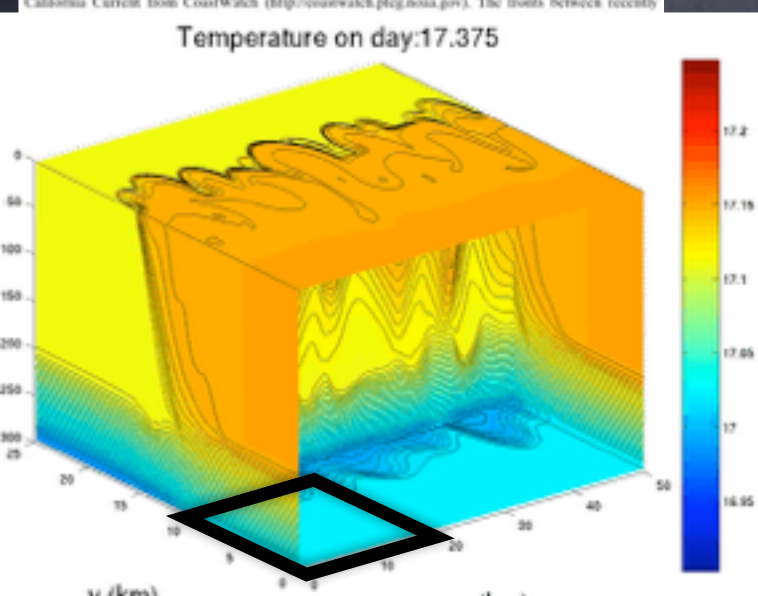

- Fronts
- Eddies
- Ro=O(1)
- Ri=O(1)
- near-surface (H=100m)
- 1-10km, days

Eddy processes often baroclinic instability

Parameterizations = BFK et al (08-11).

(NASA GSFC Gallery)

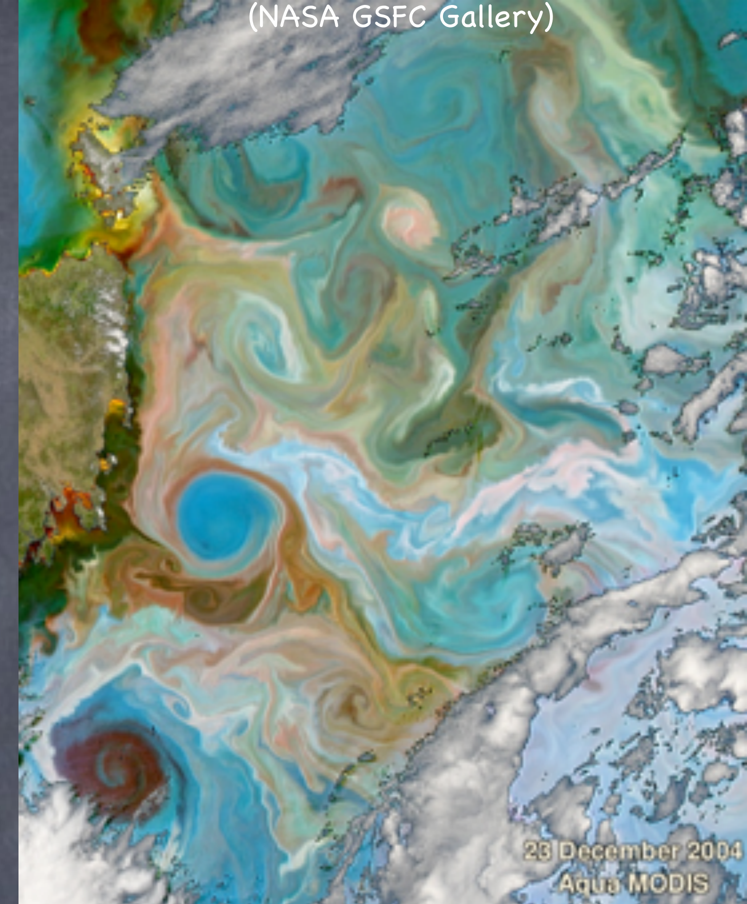

G. Boccaletti, R. Ferrari, and BFK. Mixed layer instabilities and restratification. Journal of Physical Oceanography, 37(9):2228-2250, 2007

BFK, R. Ferrari, and R. W. Hallberg. Parameterization of mixed layer eddies. Part I: Theory and diagnosis. Journal of Physical Oceanography, 38(6):1145-1165, 2008.

BFK, G. Danabasoglu, R. Ferrari, S. M. Griffies, R. W. Hallberg, M. M. Holland, M. E. Maltrud, S. Peacock, and B. L. Samuels. Parameterization of mixed layer eddies. III: Implementation and impact in global ocean climate simulations. Ocean Modelling, 39:61-78, 2011

LES of Langmuir-Front Interactions?

LES of Langmuir turbulence with a submesoscale temperature front

Use NCAR LES model to solve Wave-Averaged Eqtns.

2 Versions: 1 With Waves & Winds
1 With only Winds

Computational parameters:
Domain size: 20km x 20km x -160m
Grid points: 4096 x 4096 x 128
Resolution: 5m x 5m x -1.25m

Movie: P. Hamlington

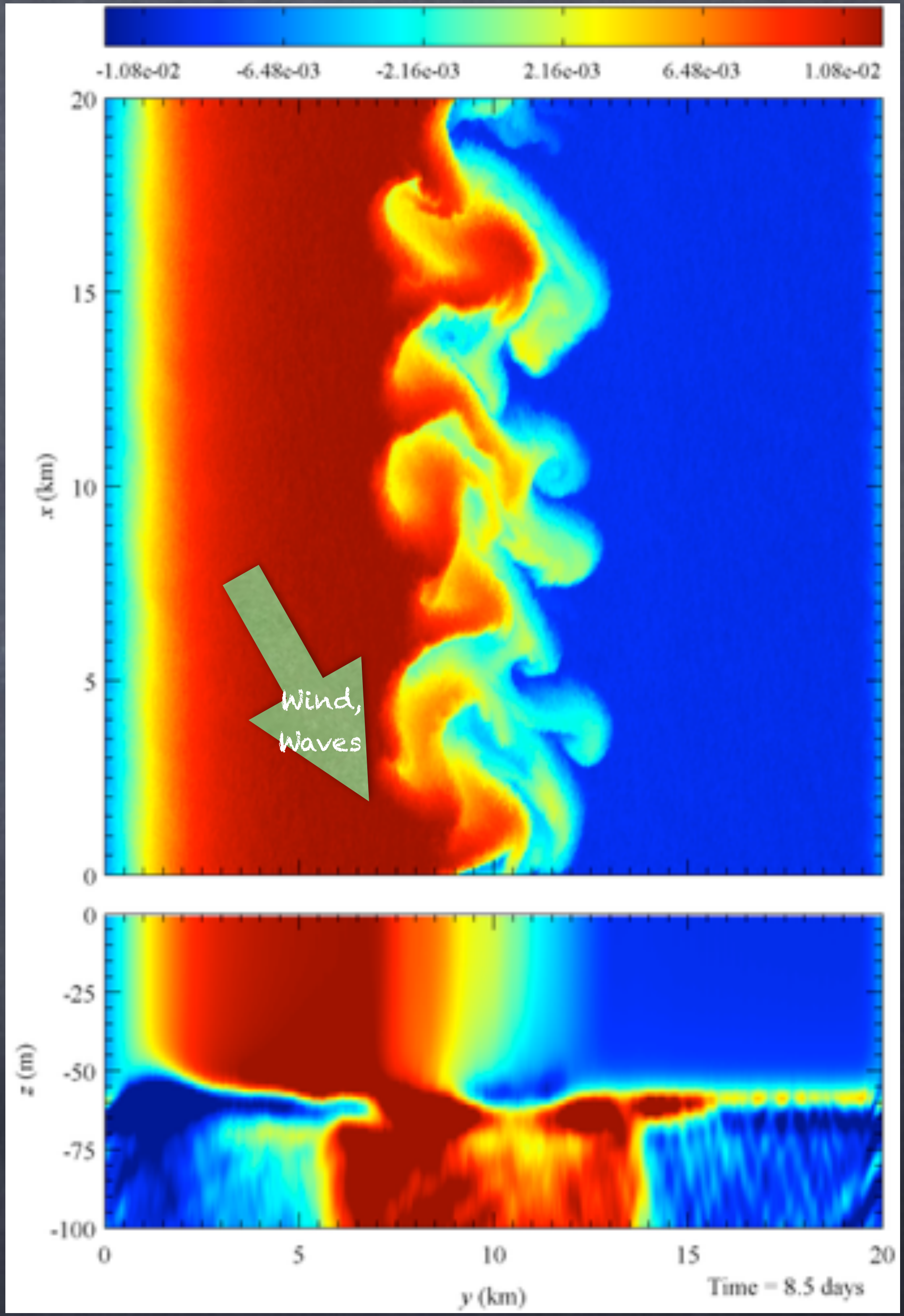

P. E. Hamlington, L. P. Van Roekel, BFK, K. Julien, and G. P. Chini. Langmuir-submesoscale interactions: Descriptive analysis of multiscale frontal spin-down simulations. Journal of Physical Oceanography, 44(9):2249-2272, September 2014.

LES of Langmuir-Front Interactions?

LES of Langmuir turbulence with a submesoscale temperature front

Use NCAR LES model to solve Wave-Averaged Eqtns.

2 Versions: 1 With Waves & Winds
1 With only Winds

Computational parameters:
Domain size: 20km x 20km x -160m
Grid points: 4096 x 4096 x 128
Resolution: 5m x 5m x -1.25m

Movie: P. Hamlington

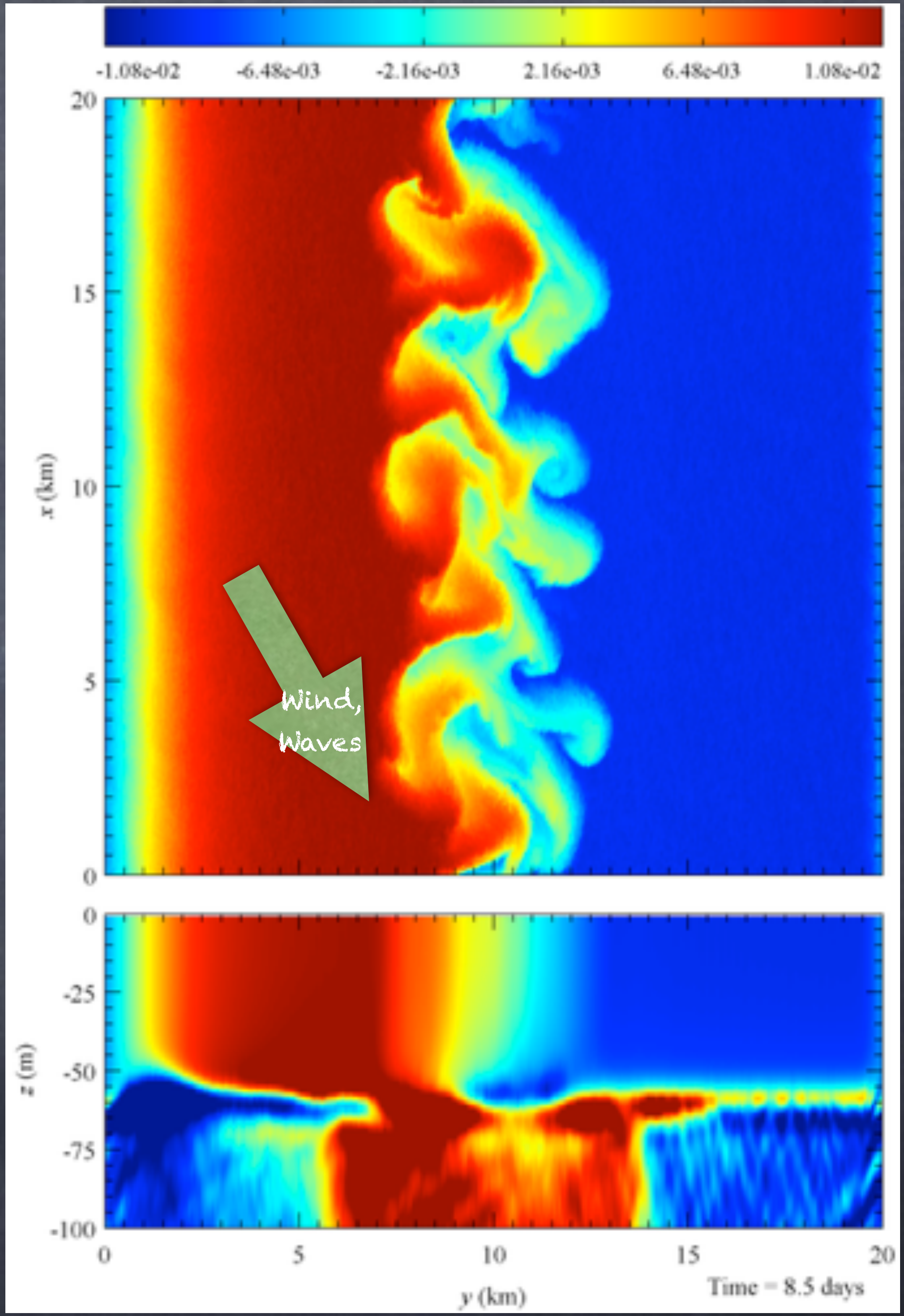

P. E. Hamlington, L. P. Van Roekel, BFK, K. Julien, and G. P. Chini. Langmuir-submesoscale interactions: Descriptive analysis of multiscale frontal spin-down simulations. Journal of Physical Oceanography, 44(9):2249-2272, September 2014.

Diverse types of interaction

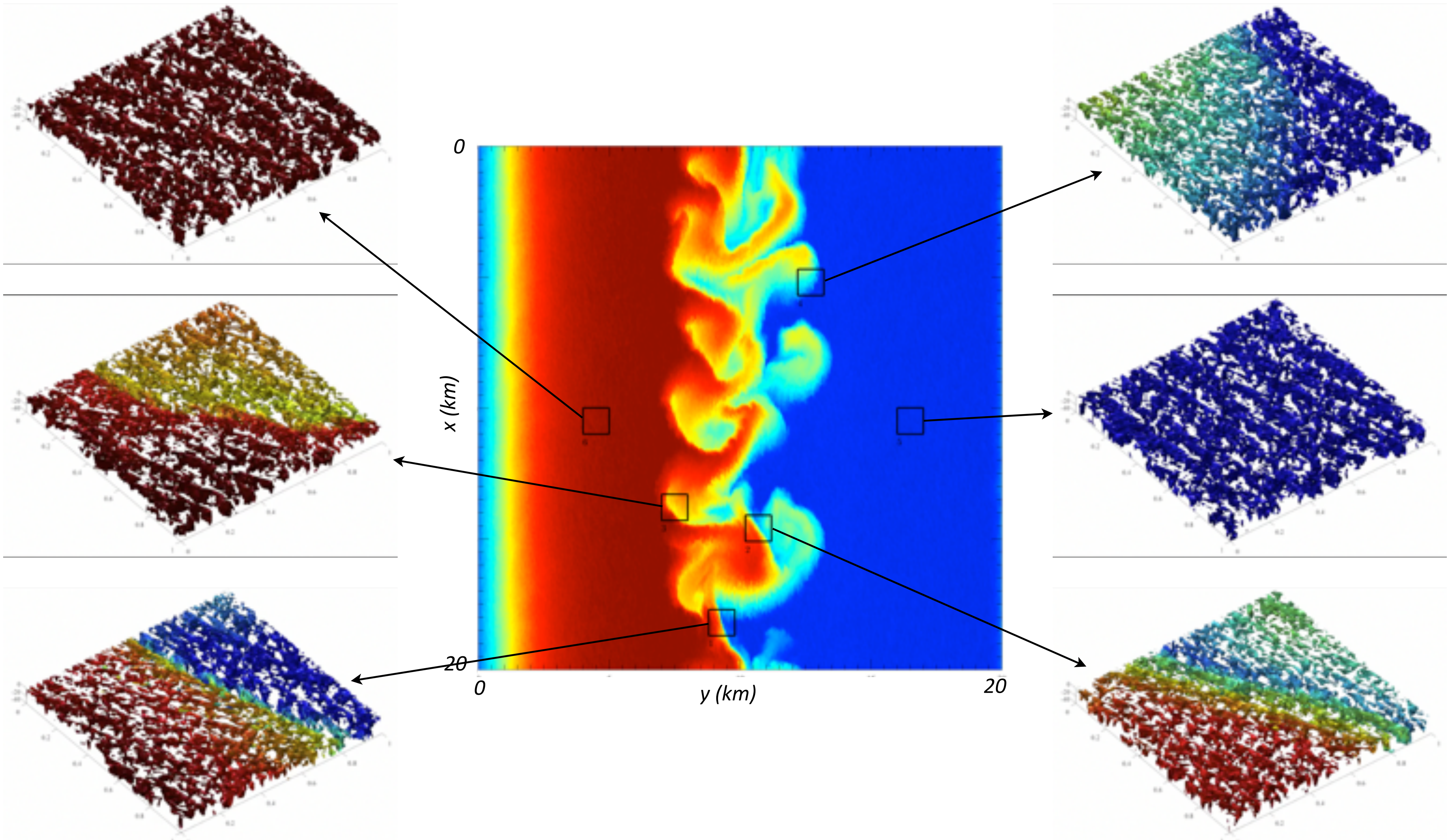

P. E. Hamlington, L. P. Van Roekel, BFK, K. Julien, and G. P. Chini. Langmuir-submesoscale interactions: Descriptive analysis of multiscale frontal spin-down simulations. Journal of Physical Oceanography, 44(9): 2249-2272, September 2014.

Diverse types of interaction

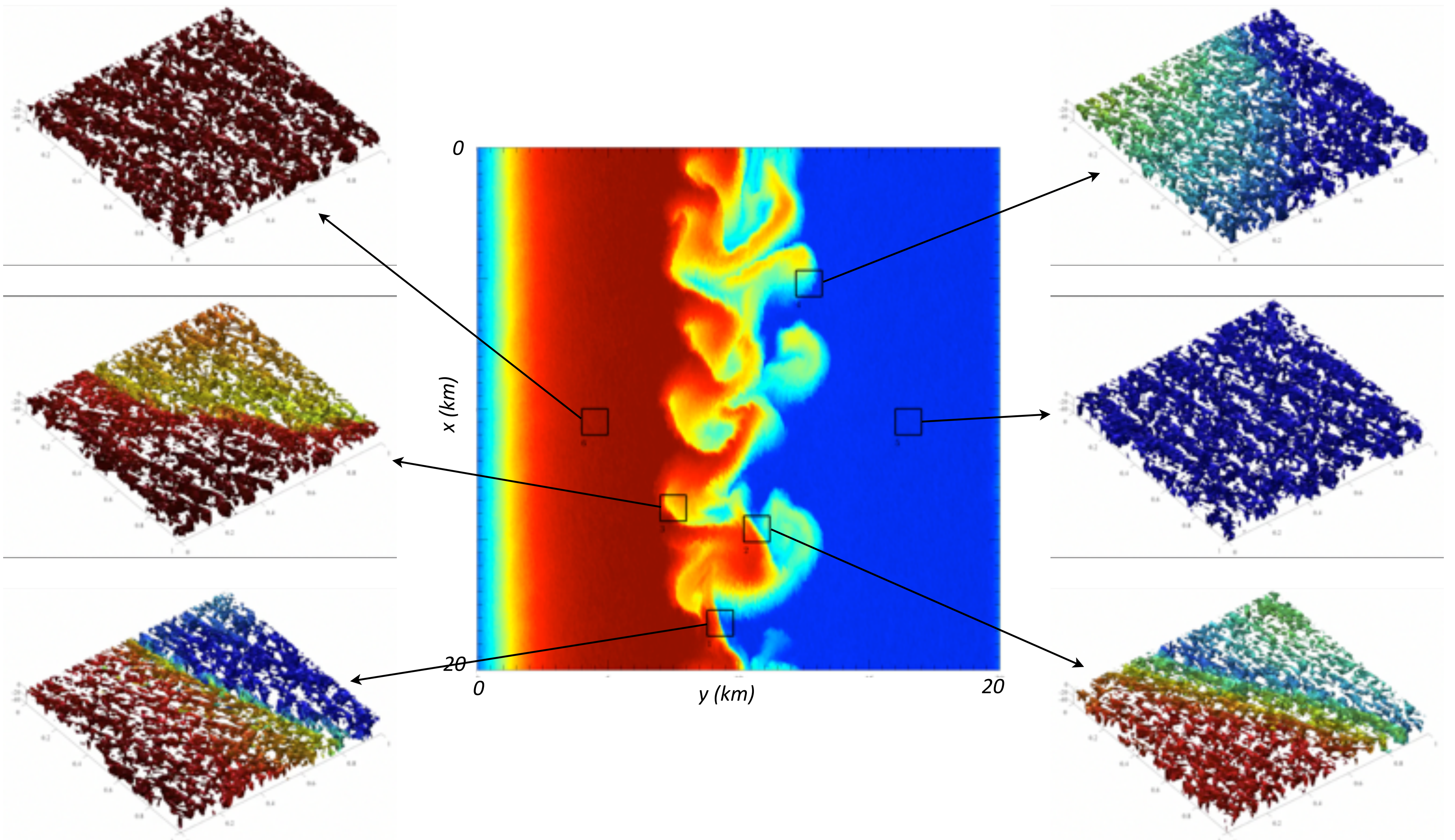

P. E. Hamlington, L. P. Van Roekel, BFK, K. Julien, and G. P. Chini. Langmuir-submesoscale interactions: Descriptive analysis of multiscale frontal spin-down simulations. Journal of Physical Oceanography, 44(9): 2249-2272, September 2014.

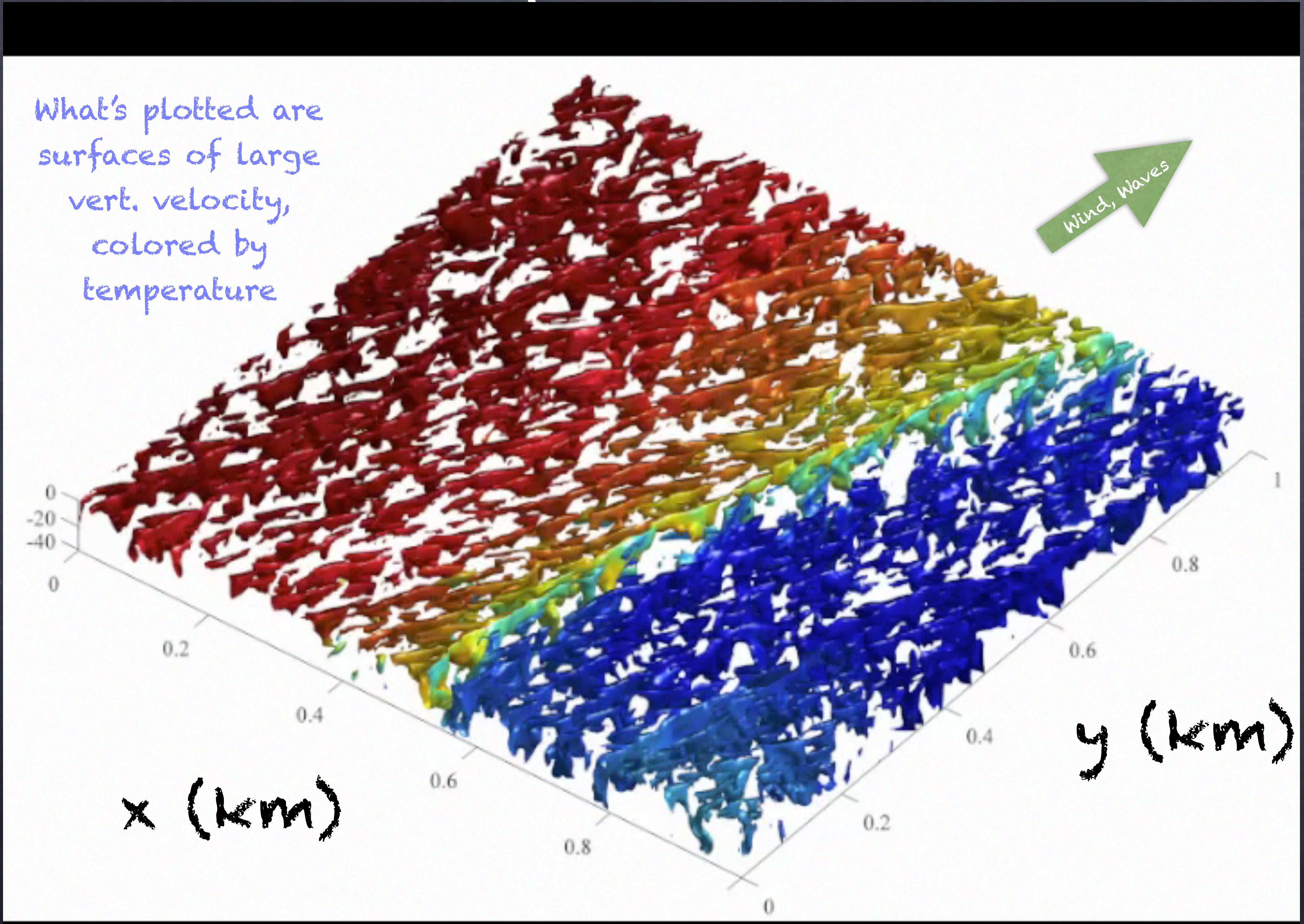

P. E. Hamlington, L. P. Van Roekel, BFK, K. Julien, and G. P. Chini. Langmuir-submesoscale interactions: Descriptive analysis of multiscale frontal spin-down simulations. Journal of Physical Oceanography, 44(9):2249-2272, September 2014.

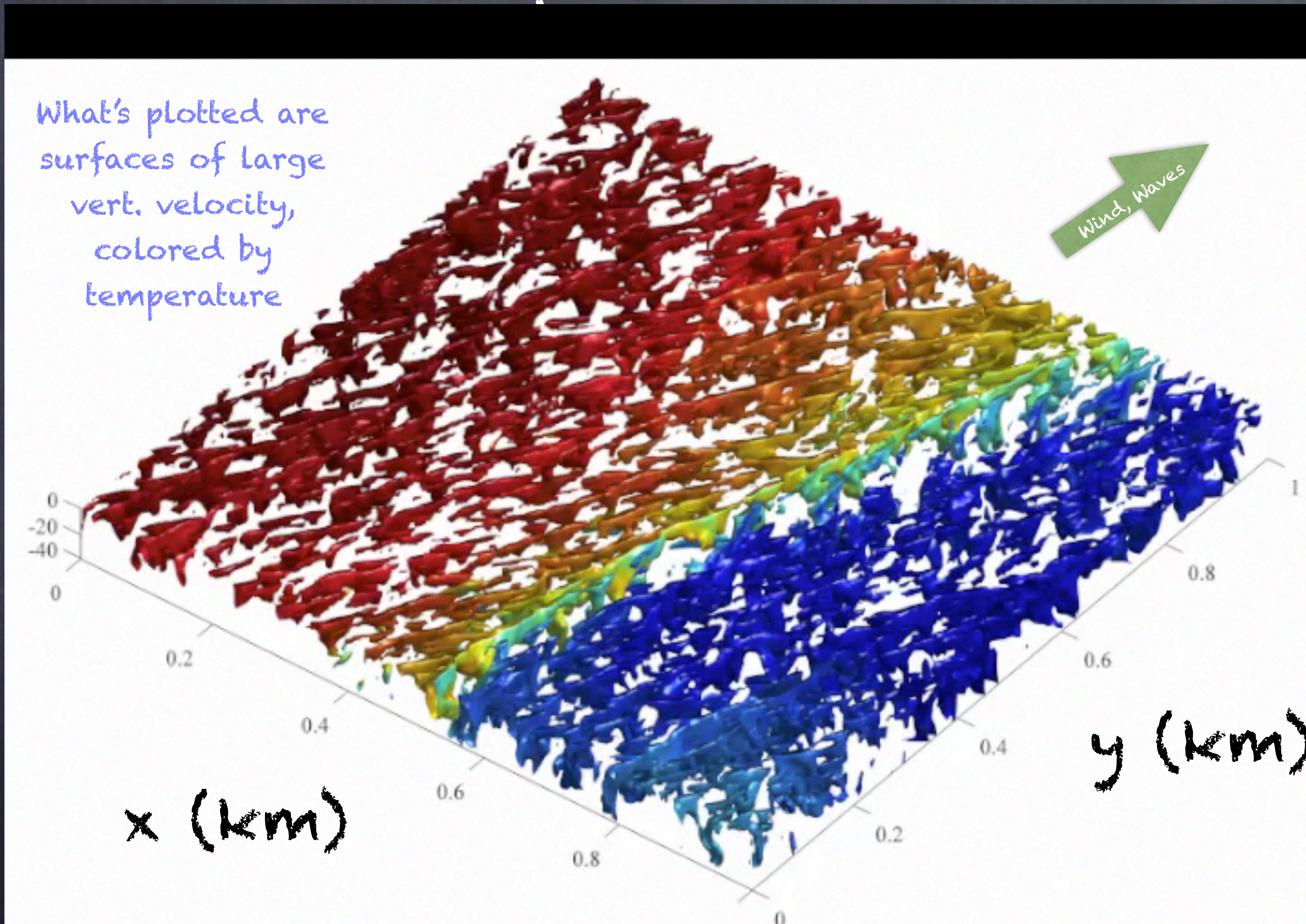

P. E. Hamlington, L. P. Van Roekel, BFK, K. Julien, and G. P. Chini. Langmuir-submesoscale interactions: Descriptive analysis of multiscale frontal spin-down simulations. Journal of Physical Oceanography, 44(9):2249-2272, September 2014.

Stokes force makes small-scale Turbulence stronger

With Stokes Forcing

Without Stokes Forcing

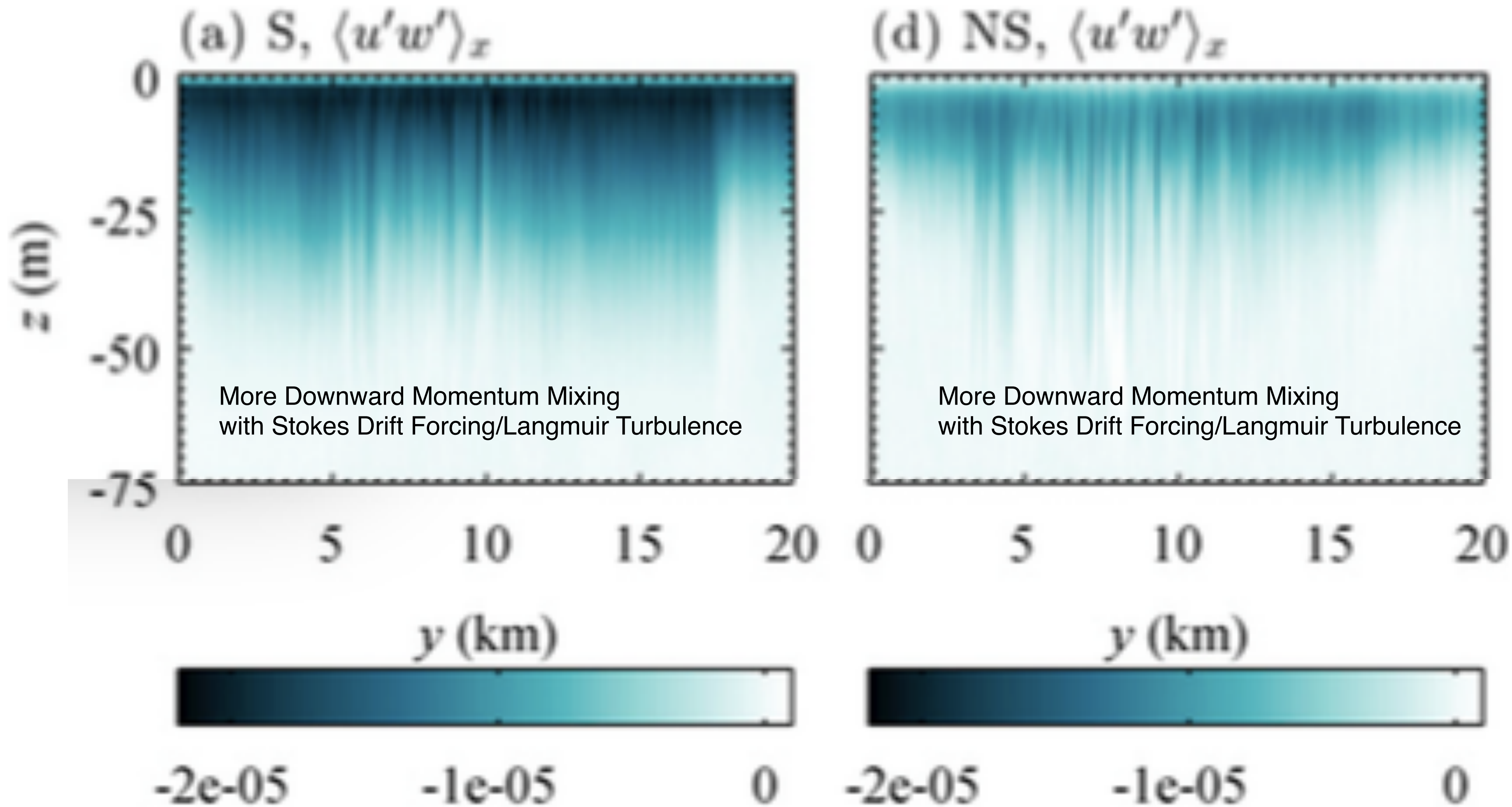

As we've seen, waves can drive turbulence that affect larger scales indirectly. This is expected.

What about direct effects of waves on larger scales?

$$\mathbf{f} \times \frac{\partial \mathbf{v}}{\partial z} = -\nabla b$$

Becomes Lagrangian Thermal Wind Balance

$$\mathbf{f} \times \frac{\partial}{\partial z}(\mathbf{v} + \mathbf{v}_s) = \mathbf{f} \times \frac{\partial \mathbf{v}_L}{\partial z} = -\nabla b$$

Now the temperature gradients govern the Lagrangian flow, not the not the Eulerian!

The Eulerian response to Stokes is often to cancel it out!

(Anti-Stokes flow, Lab: Monismith et al., Obs: Lentz et al.)

J. C. McWilliams and BFK. Oceanic wave-balanced surface fronts and filaments. Journal of Fluid Mechanics, 730:464-490, 2013.

Lagrangian Thermal Wind Linear Stability

Like Eady, but with Lagrangian Thermal Wind Background State

$$U + U^S = -\Psi^L_y, \quad \text{such that} \quad U = -\Psi_y, \quad \text{and}$$

$$V + V^S = \Psi^L_x = 0.$$

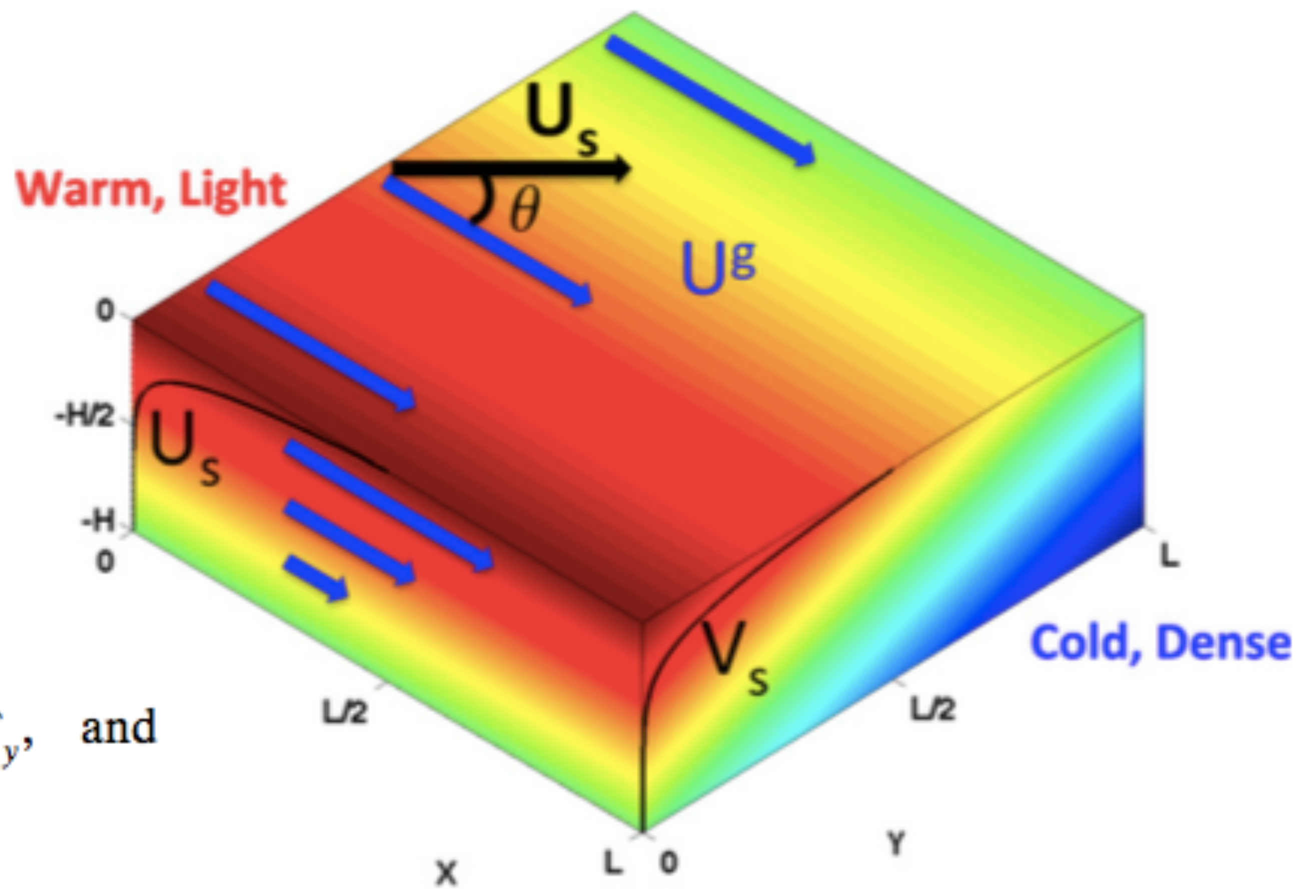

FIG. 2. The background flow with arbitrary θ (the angle between the Stokes drift and the geostrophic flow) and a prescribed exponential Stokes drift U^S, V^S profile. The geostrophic flow U^G, corresponding to the imposed buoyancy gradient, is shown with blue arrows.

S. Haney, BFK, K. Julien, and A. Webb. Symmetric and geostrophic instabilities in the wave-forced ocean mixed layer. JPO 45:3033-3056, 2015.

Analytic & Numerical Wavy Submesoscale Stability:

Geostrophic (Mixed Layer) Instabilities

Charney, Stern, Pedlosky criteria (appropriately generalized) apply:

- Instability allowed if:

1) Q_Y^L changes sign in the interior of the domain;
2) Q_Y^L is the opposite sign as U_z^L at $z = 0$;
3) Q_Y^L is the same sign as U_z^L at $z = -H$;
4) U_z^L has the same sign at $z = -H$ and $z = 0$.

$$Q^L = \nabla_H^2 \Psi + \beta Y + \partial_z \left(\frac{f_0^2}{N^2} \frac{\Psi_z^L}{B_z} \right)$$

Streamfunctions with and w/o Stokes

$U + U^S = -\Psi_y^L$, such that $U = -\Psi_y$, and

$V + V^S = \Psi_x^L = 0.$

S. Haney, BFK, K. Julien, and A. Webb. Symmetric and geostrophic instabilities in the wave-forced ocean mixed layer. JPO 45:3033-3056, 2015.

Analytic & Numerical Wavy Submesoscale Stability:
Geostrophic Instabilities

- For typical conditions, the Stokes effect amounts to a small change in geostrophic instability (mixed layer eddy) growth rates.

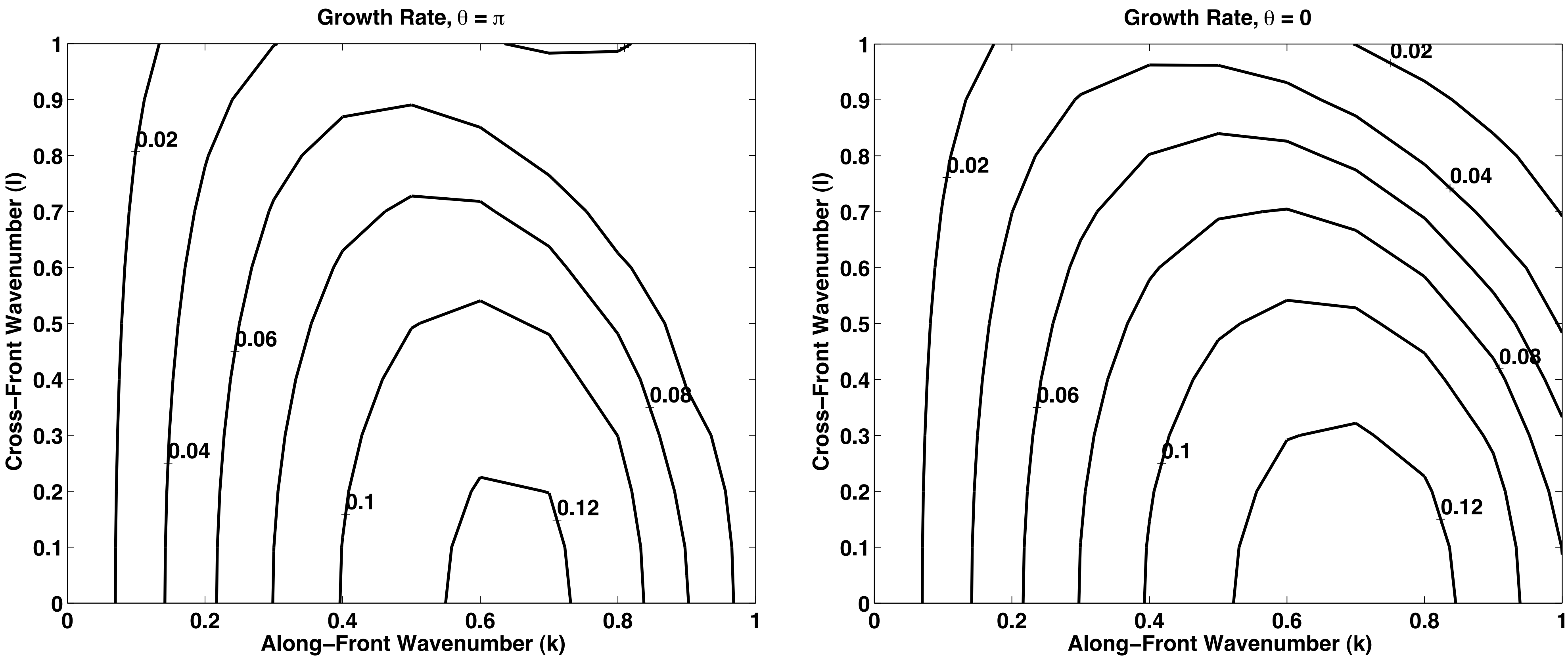

S. Haney, BFK, K. Julien, and A. Webb. Symmetric and geostrophic instabilities in the wave-forced ocean mixed layer. JPO 45:3033-3056, 2015.

Analytic & Numerical Wavy Submesoscale Stability:
Symmetric Instabilities

- Hoskins (1974) showed that if a front in thermal wind balance is symmetrically unstable, the PV must be anticyclonic.
- Haney et al extend Hoskins' analysis to flows in Lagrangian thermal wind balance in the special case that the Stokes shear is constant.

Vert. Density Gradient — Horiz. Density Gradient — Anti-Stokes Shear

$$fQ = \underbrace{f^2N^2 - M^4}_{\text{geostrophic } fQ} - \underbrace{fM^2U_z^S}_{\text{Stokes-modified } fQ} < 0.$$

- In the absence of Stokes drift, this is equivalent to the familiar criteria on Richardson Number, with Stokes drift is distinct.

S. Haney, BFK, K. Julien, and A. Webb. Symmetric and geostrophic instabilities in the wave-forced ocean mixed layer. JPO 45:3033-3056, 2015.

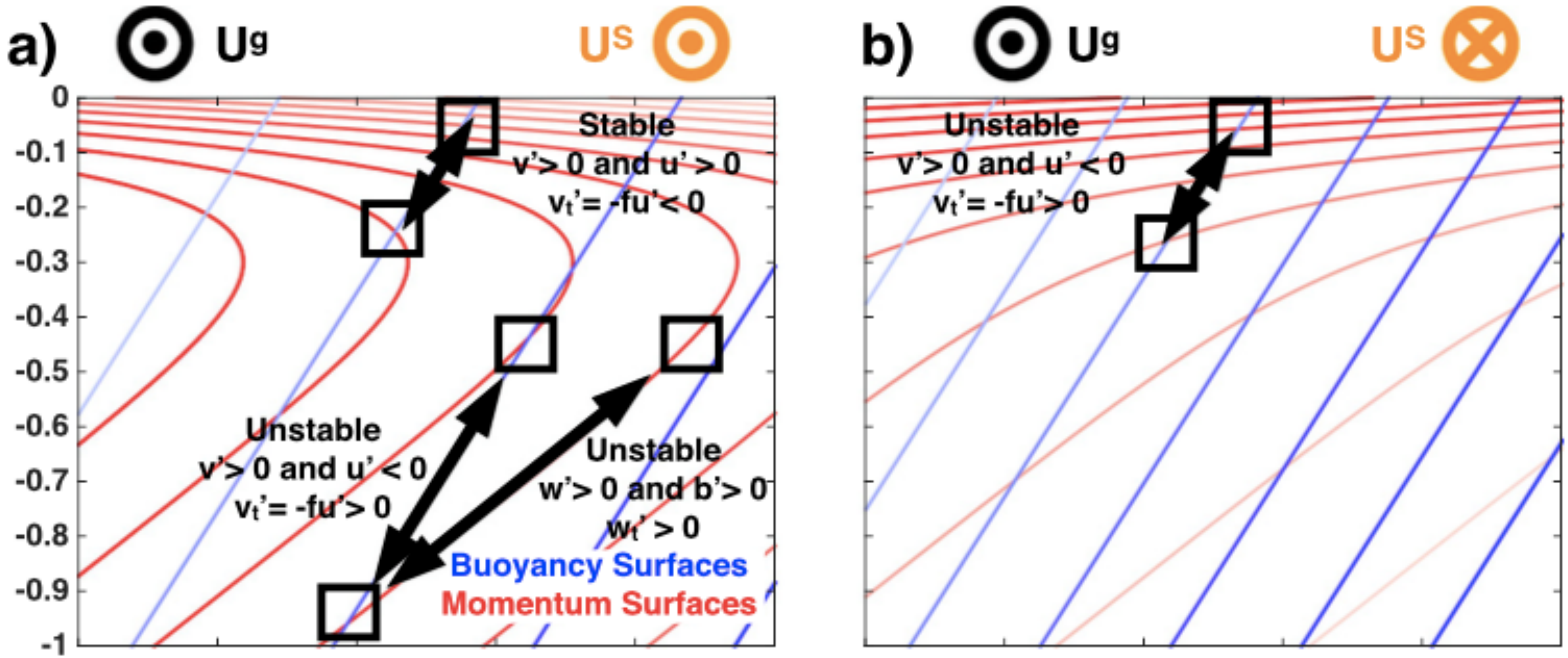

FIG. 1. A schematic of the (a) downfront and (b) upfront Stokes drift scenarios. The blue lines show isopycnals, with darker blue indicating denser water. The red lines show surfaces of constant downfront absolute Eulerian momentum, with darker red indicating greater momentum. The perturbation equations are written from the perspective of the lower of the two parcels. A change of all signs would be from the perspective of the upper parcel and have the same stability. For example, in (b) the lower parcel moves to the right ($v' > 0$) along an isopycnal and brings with it lower downfront momentum than its surroundings ($u' < 0$). This exerts an acceleration in the cross-front v' direction due to the Coriolis force that further enhances the initial perturbation ($v' > 0$). In both cases, $\mathrm{Ri} = 0.5$. Lines of constant buoyancy and absolute momentum are only parallel when $\mathrm{Ri} = 1$.

S. Haney, BFK, K. Julien, and A. Webb. Symmetric and geostrophic instabilities in the wave-forced ocean mixed layer. JPO 45:3033-3056, 2015.

Ri < 1 ⇒ SI

fQ<0 ⇒ SI

Numerical Wavy Stability Criterion: Symmetric Instability

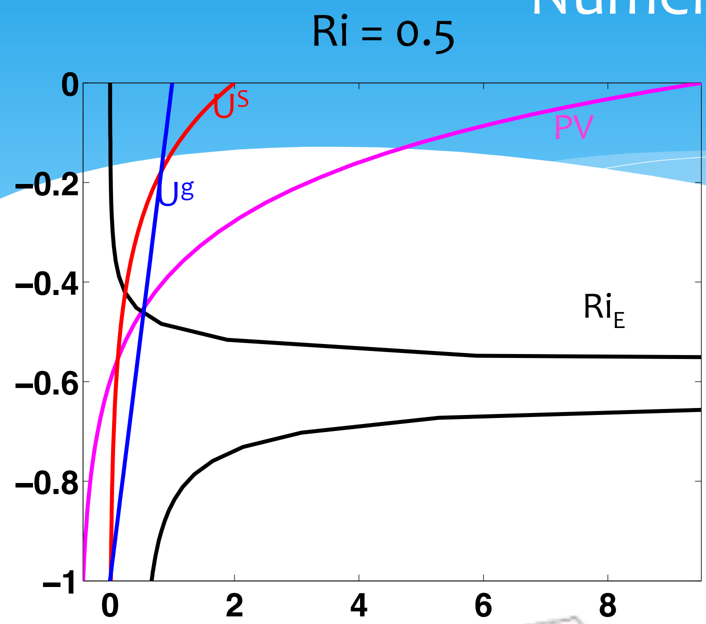

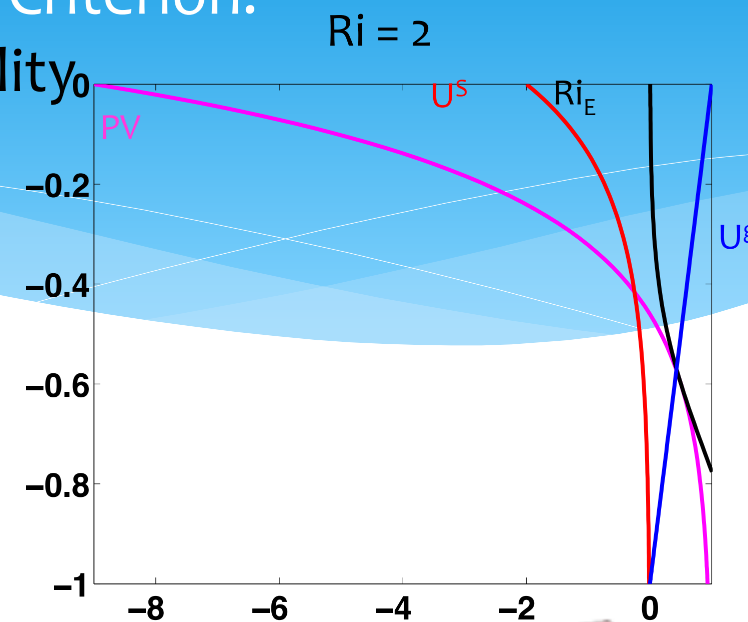

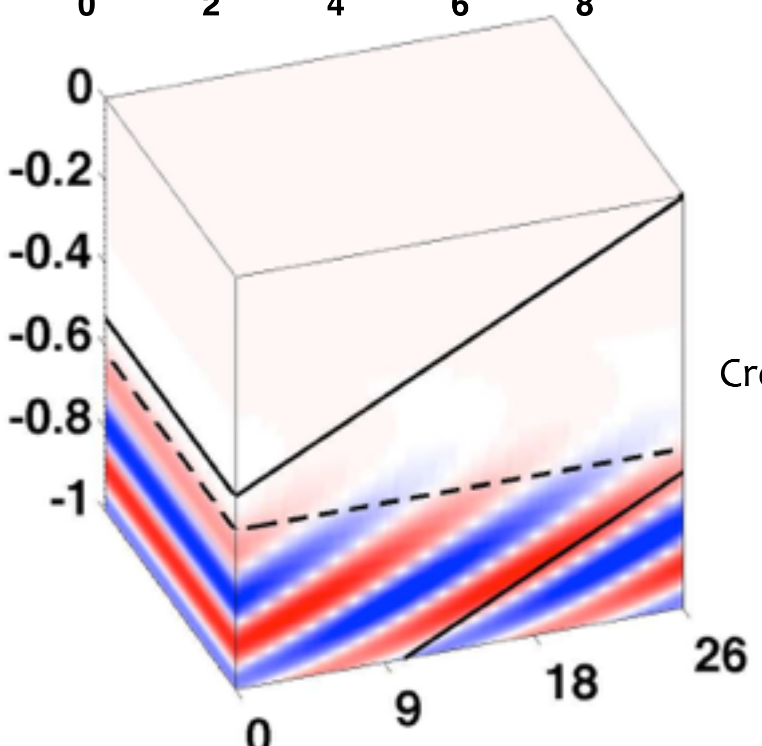

—— Isopycnals

- - PV=0

Cross front velocity for the fastest growing mode

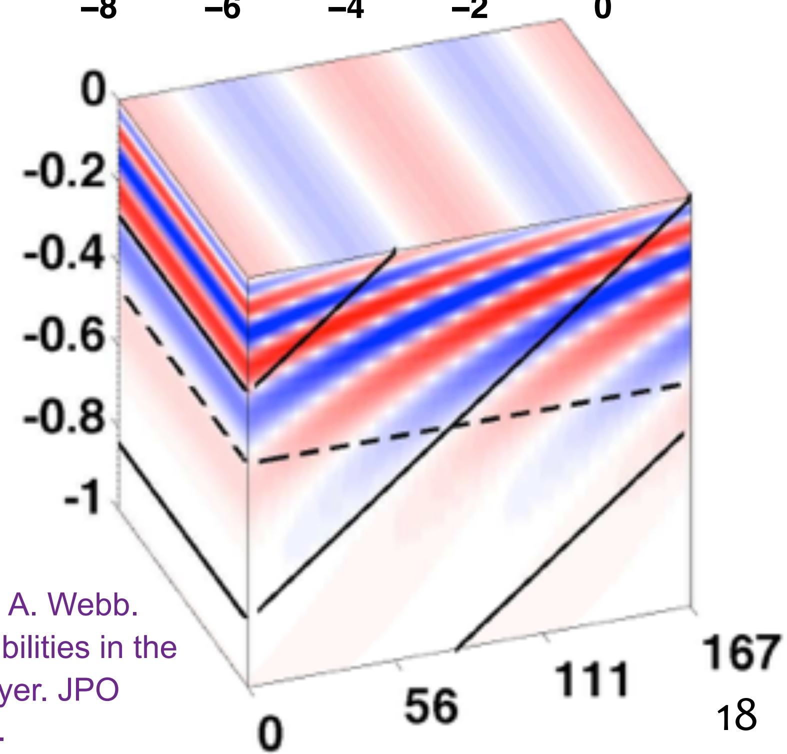

S. Haney, BFK, K. Julien, and A. Webb. Symmetric and geostrophic instabilities in the wave-forced ocean mixed layer. JPO 45:3033-3056, 2015.

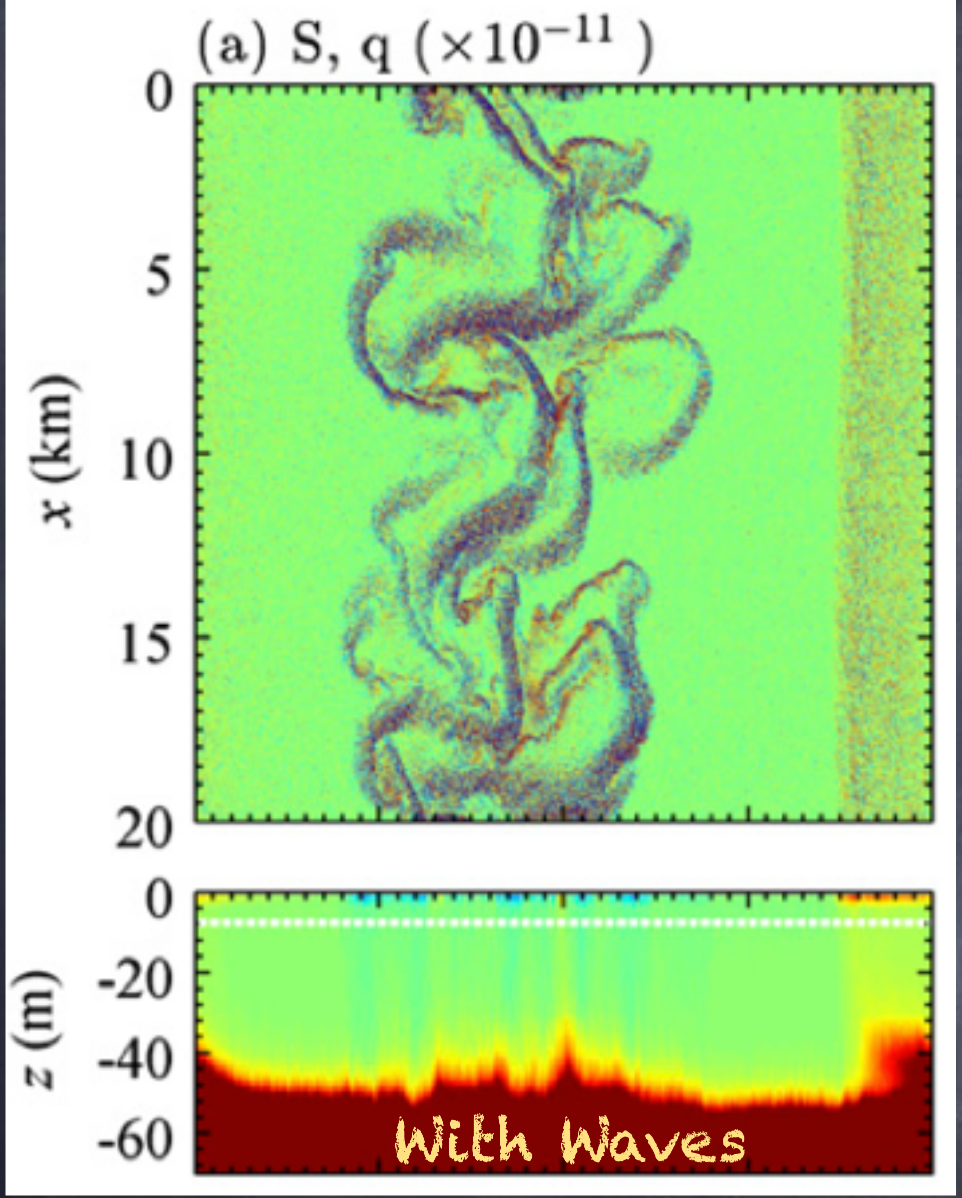

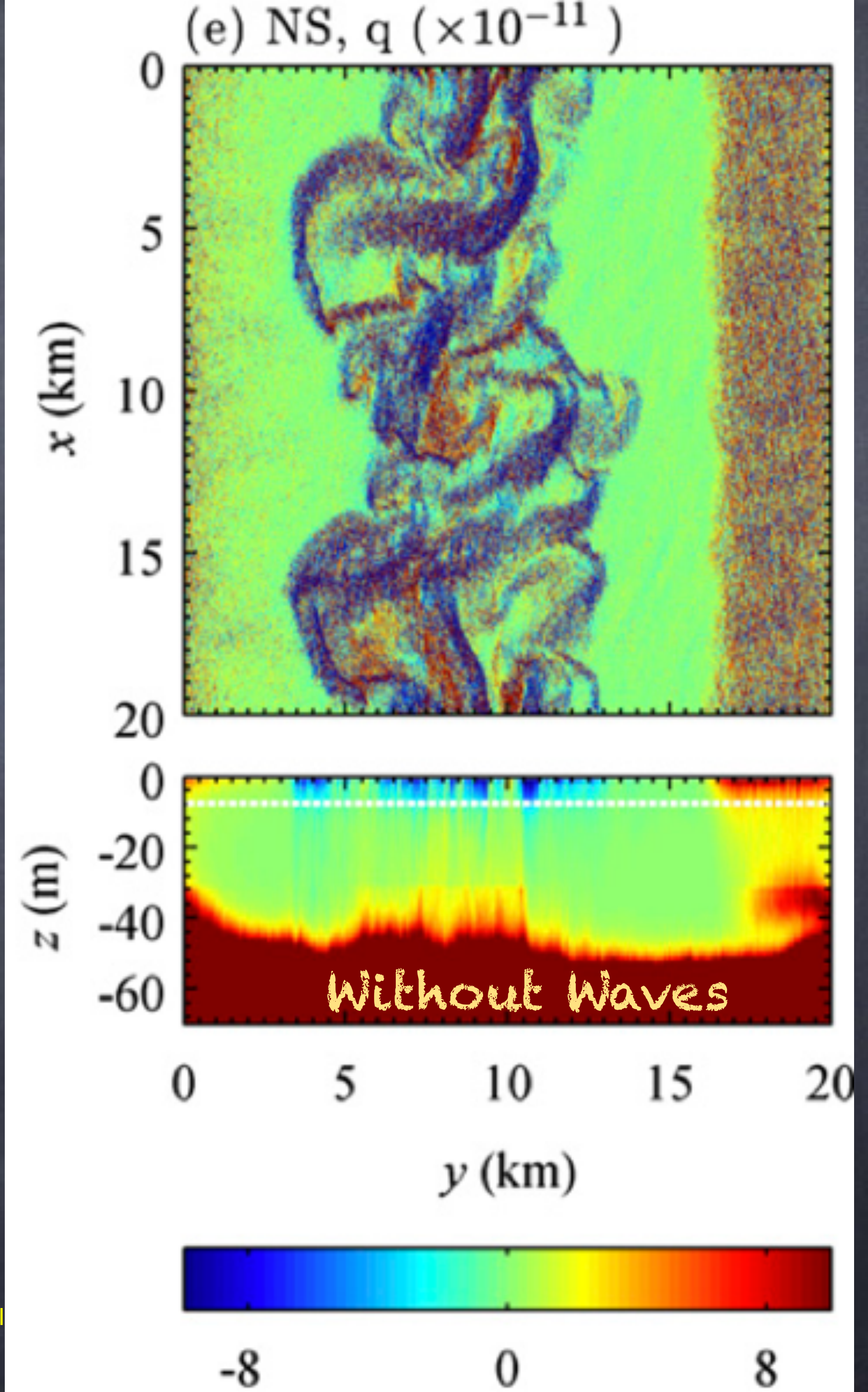

So, if fQ<0 indicates likely regions of symmetric instability—Surface Waves STRONGLY affect SI!

P. E. Hamlington, L. P. Van Roekel, BFK, K. Julien, and G. P. Chini. Langmuir-submesoscale interactions: Descriptive analysis of multiscale frontal spin-down simulations. Journal of Physical Oceanography, 44(9):2249-2272, September 2014

Stokes force directly affects larger scales?

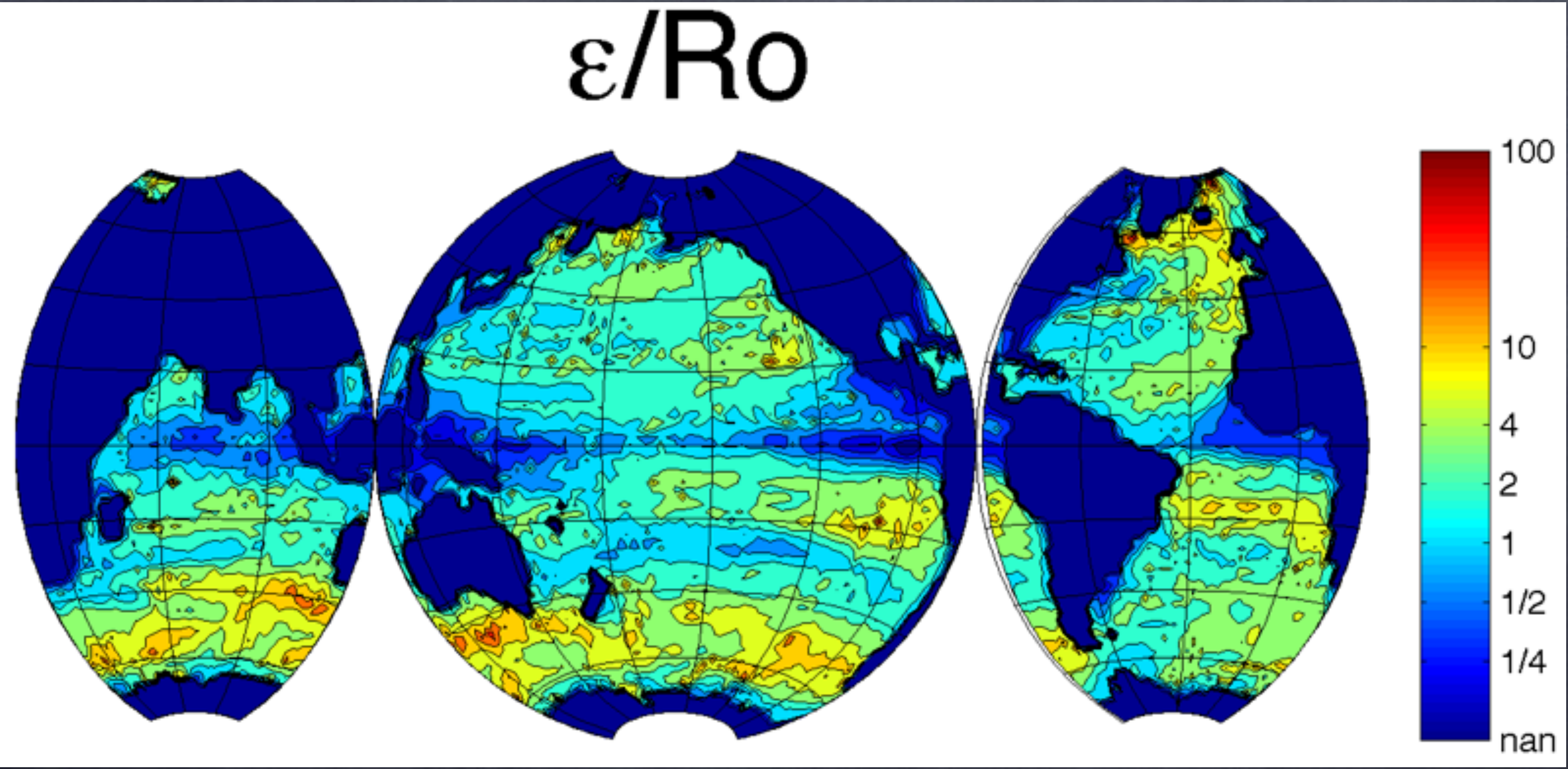

$$\frac{\varepsilon}{Ro} = \frac{V_s}{fL}\frac{H}{H_s}\frac{fL}{V} = \frac{V_s}{V}\frac{H}{H_s}$$

$$\varepsilon = \frac{V^s H}{fLH_s}$$

$$Ro = \frac{U}{fL}$$

J. C. McWilliams and BFK. Oceanic wave-balanced surface fronts and filaments. Journal of Fluid Mechanics, 730:464-490, 2013.

Are Fronts and Filaments different with Stokes shear force?

$$\frac{\alpha^2}{Ri}\left[w_{,t} + v_j^L w_{,j} + \frac{M_{Ro}}{RoRi} w w_{,z}\right] = -\pi_{,z} + b - \varepsilon v_j^L v_{j,z}^s + \frac{\alpha^2}{ReRi} w_{,jj}$$

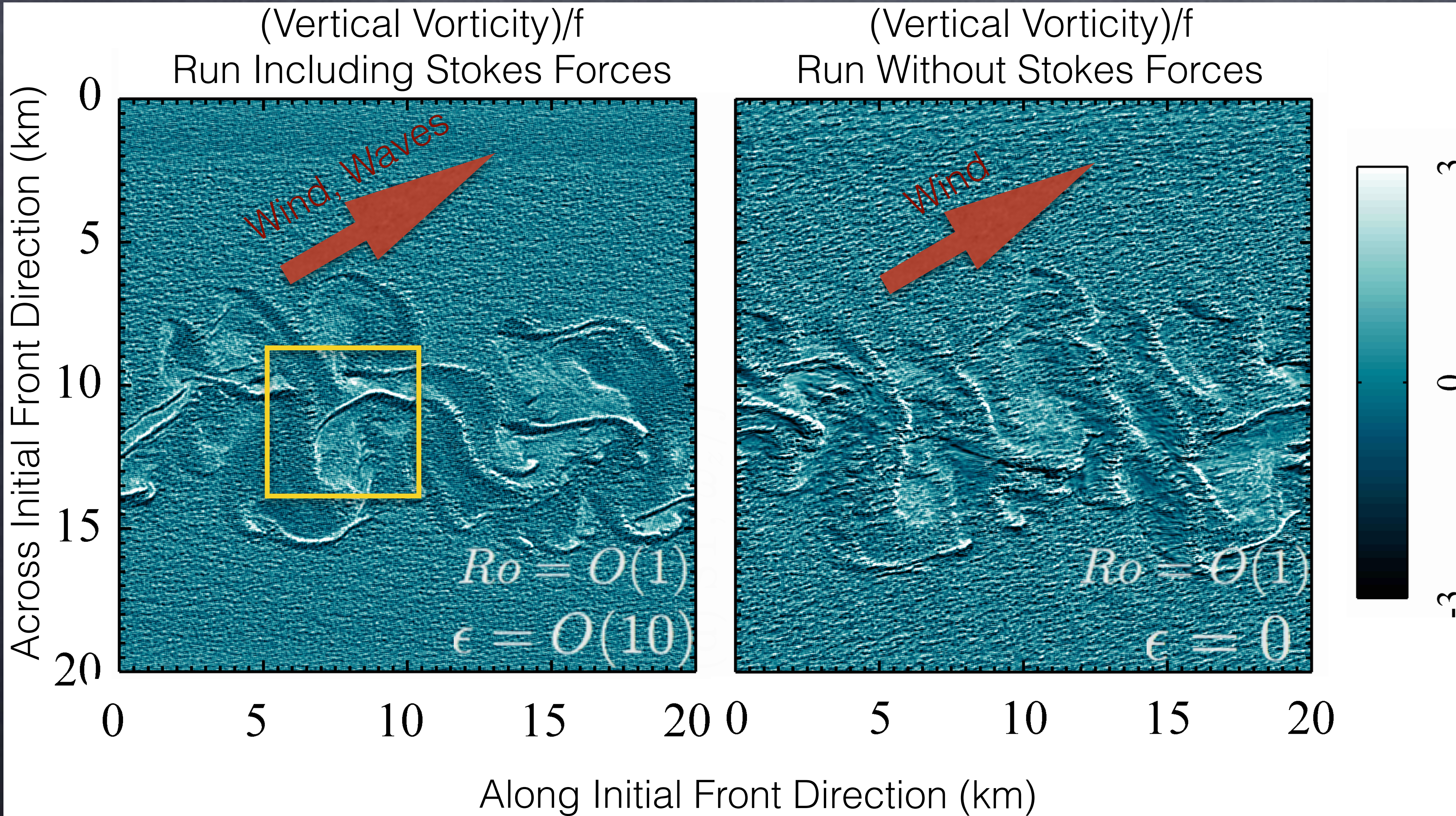

N. Suzuki, BFK, P. E. Hamlington, and L. P. Van Roekel. Surface waves affect frontogenesis. JGR-Oceans, December 2015. Submitted.

J. C. McWilliams and BFK. Oceanic wave-balanced surface fronts and filaments. Journal of Fluid Mechanics, 730:464-490, 2013.

P. E. Hamlington, L. P. Van Roekel, B. Fox-Kemper, K. Julien, and G. P. Chini. Langmuir-submesoscale interactions: Descriptive analysis of multiscale frontal spin-down simulations. Journal of Physical Oceanography, 44(9):2249-2272, September 2014

Are Fronts and Filaments different with Stokes shear force?

$$\frac{\alpha^2}{Ri}\left[w_{,t} + v_j^L w_{,j} + \frac{M_{Ro}}{RoRi} w w_{,z}\right] = -\pi_{,z} + b - \varepsilon v_j^L v_{j,z}^s + \frac{\alpha^2}{ReRi} w_{,jj}$$

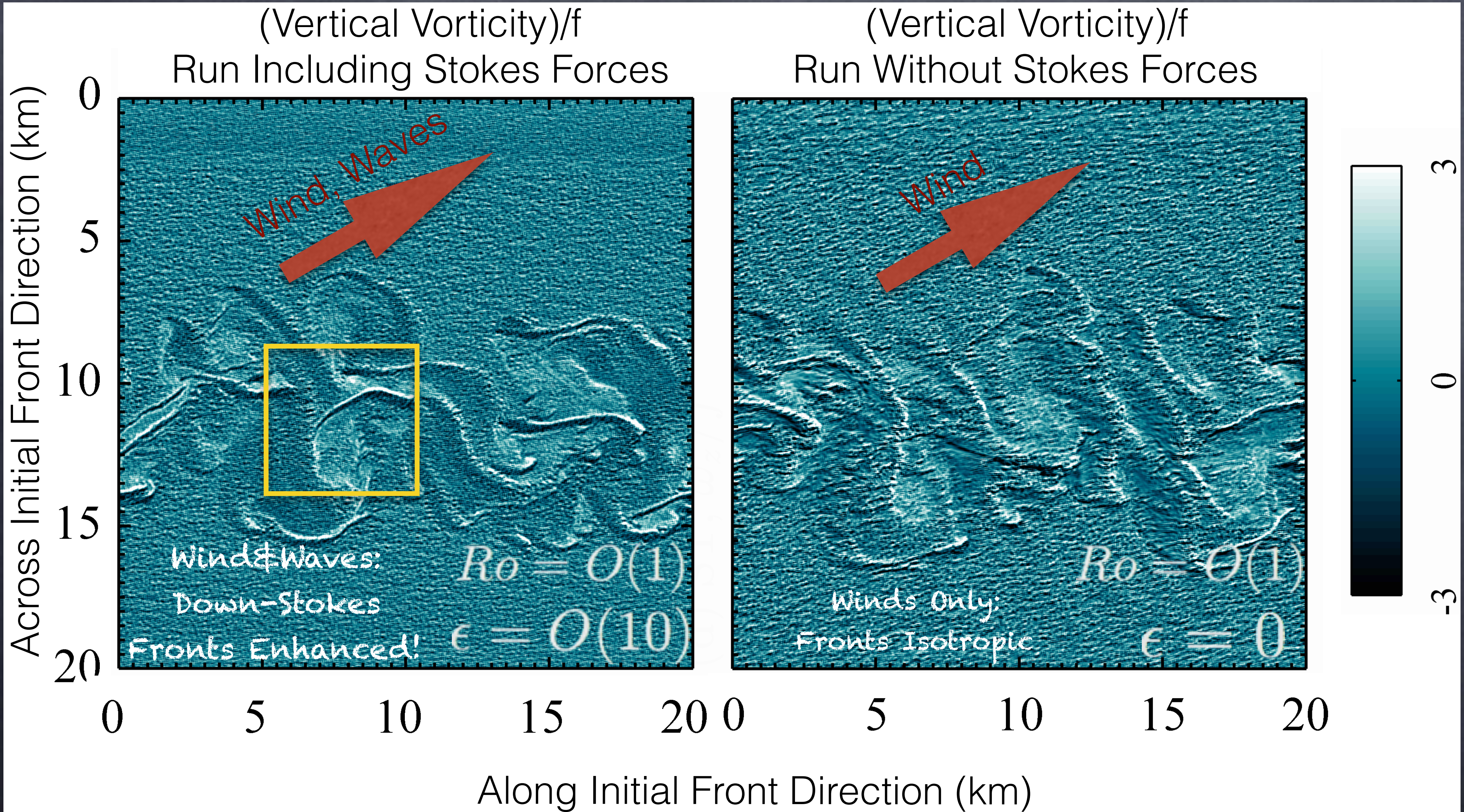

N. Suzuki, BFK, P. E. Hamlington, and L. P. Van Roekel. Surface waves affect frontogenesis. JGR-Oceans, December 2015. Submitted.

J. C. McWilliams and BFK. Oceanic wave-balanced surface fronts and filaments. Journal of Fluid Mechanics, 730:464-490, 2013.

P. E. Hamlington, L. P. Van Roekel, B. Fox-Kemper, K. Julien, and G. P. Chini. Langmuir-submesoscale interactions: Descriptive analysis of multiscale frontal spin-down simulations. Journal of Physical Oceanography, 44(9):2249-2272, September 2014

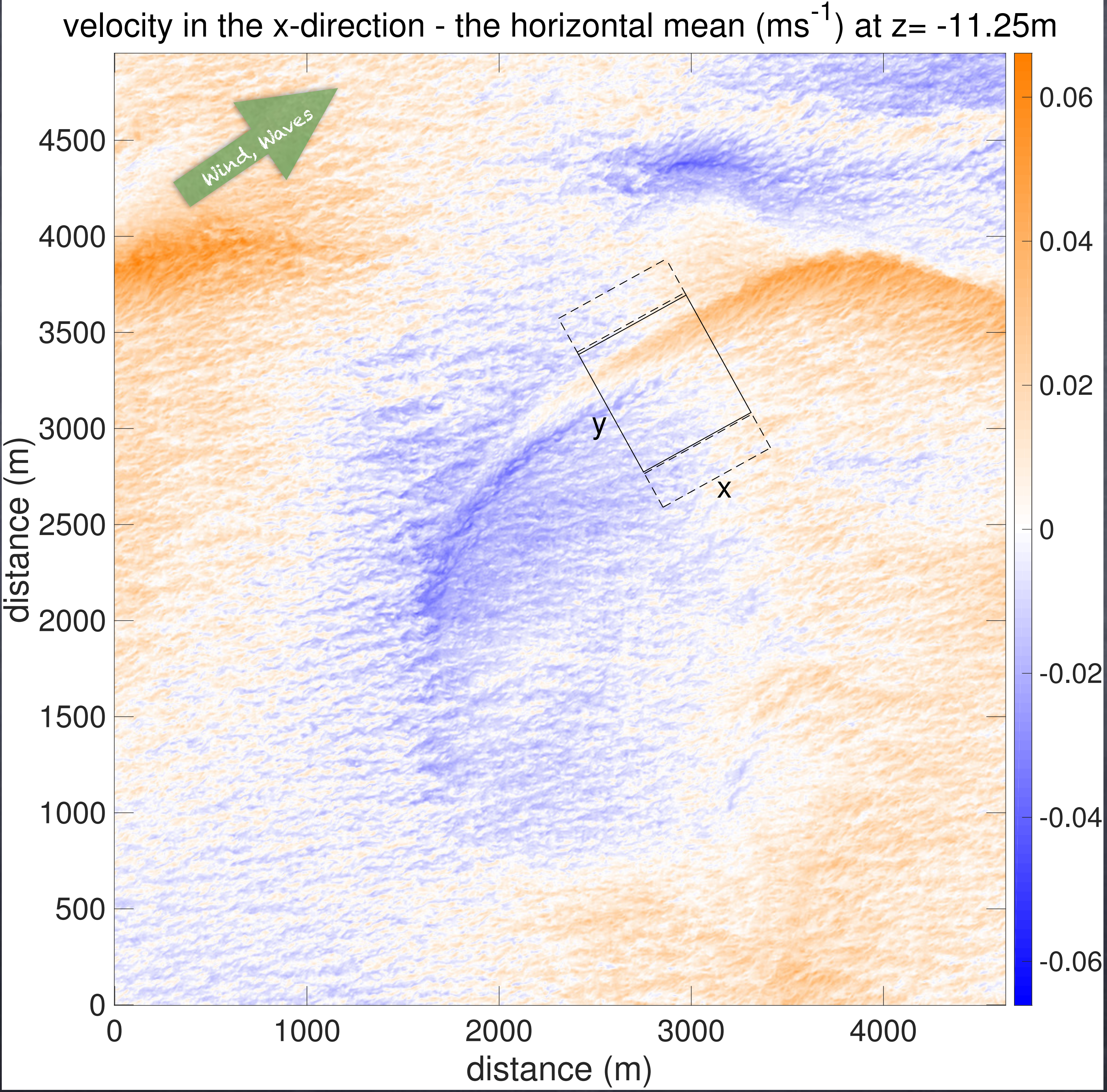

N. Suzuki, BFK, P. E. Hamlington, and L. P. Van Roekel. Surface waves affect frontogenesis. JGR-Oceans, December 2015. Submitted.

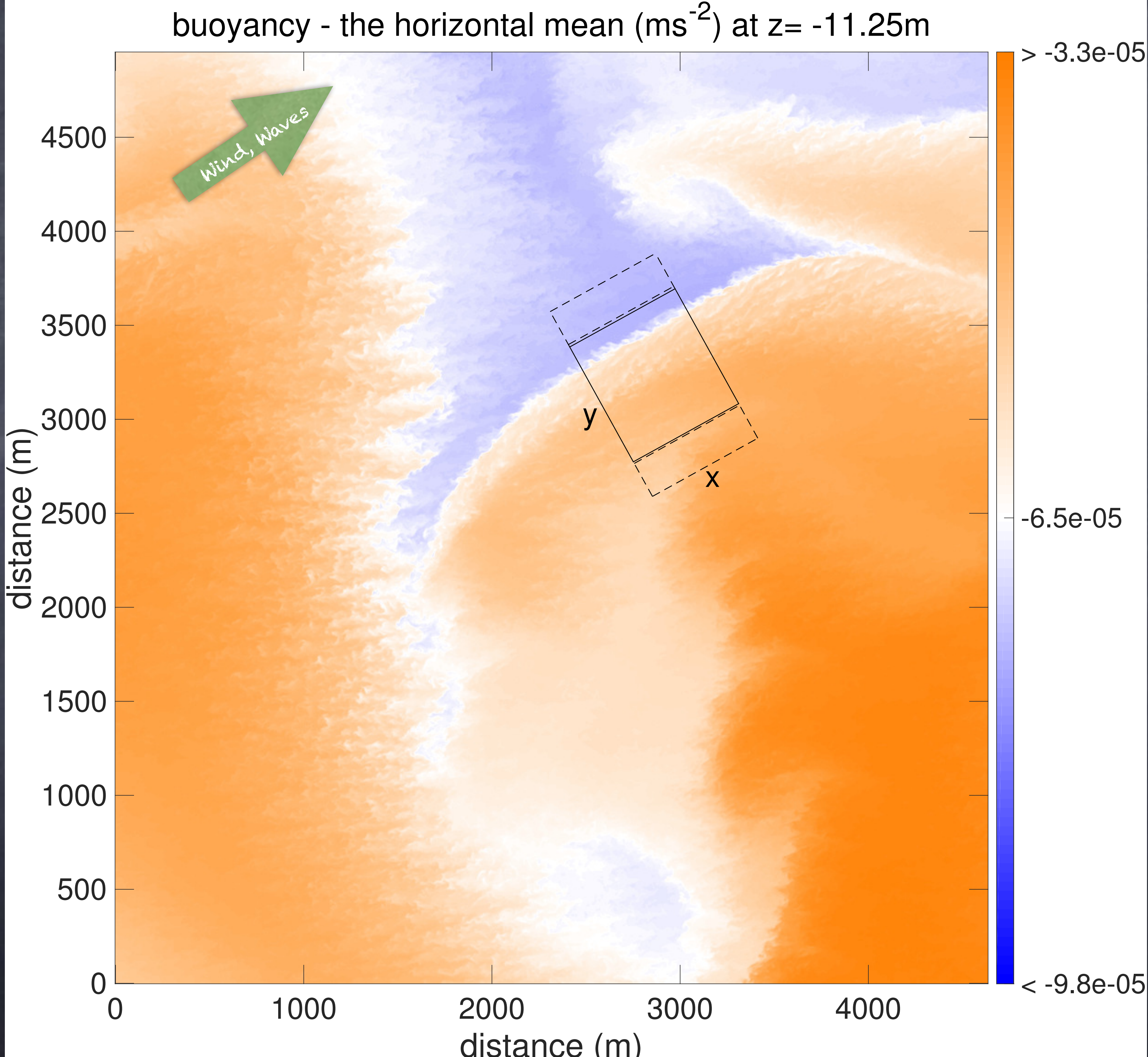

N. Suzuki, BFK, P. E. Hamlington, and L. P. Van Roekel. Surface waves affect frontogenesis. JGR-Oceans, December 2015. Submitted.

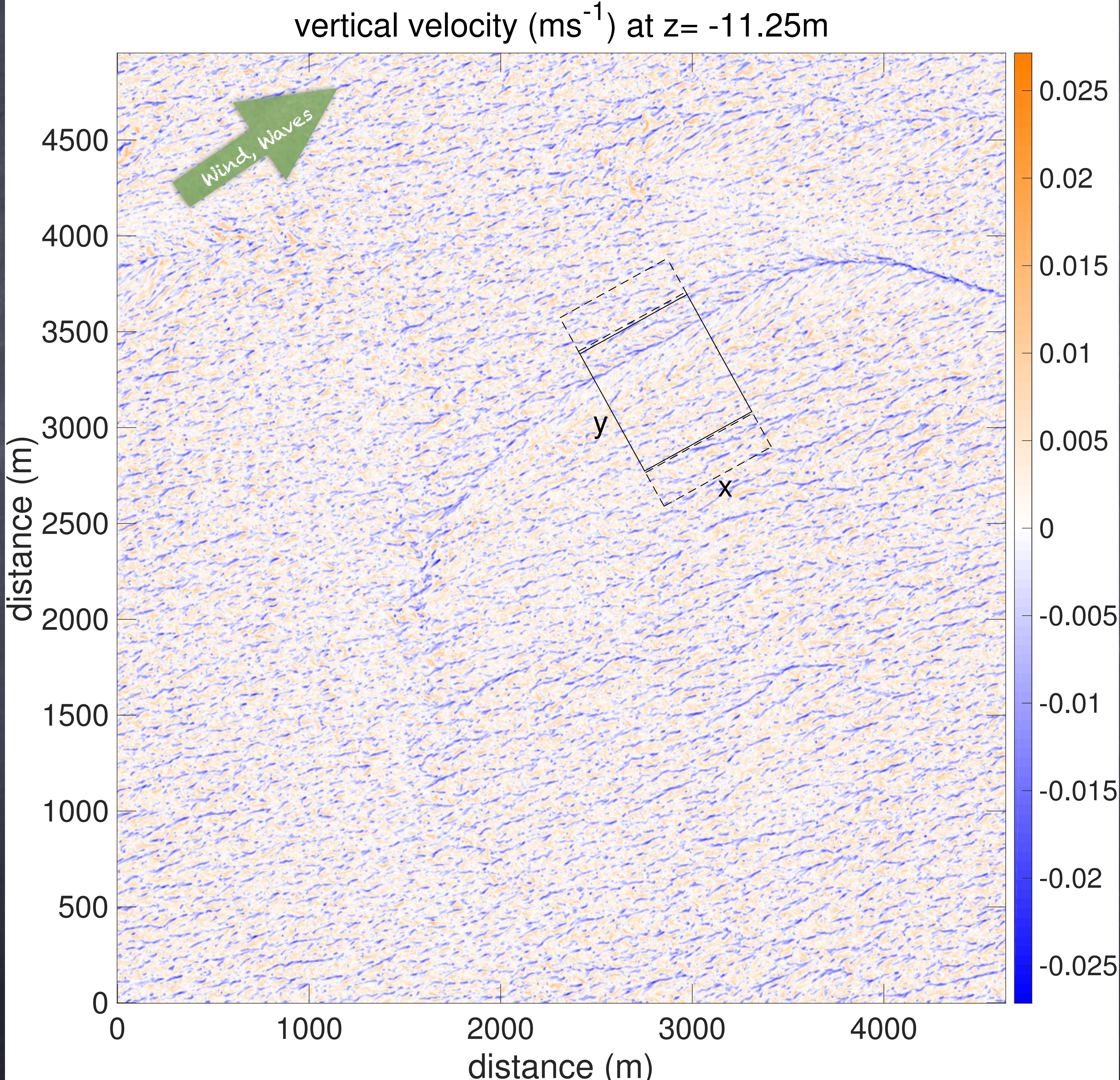

N. Suzuki, BFK, P. E. Hamlington, and L. P. Van Roekel. Surface waves affect frontogenesis. JGR-Oceans, December 2015. Submitted.

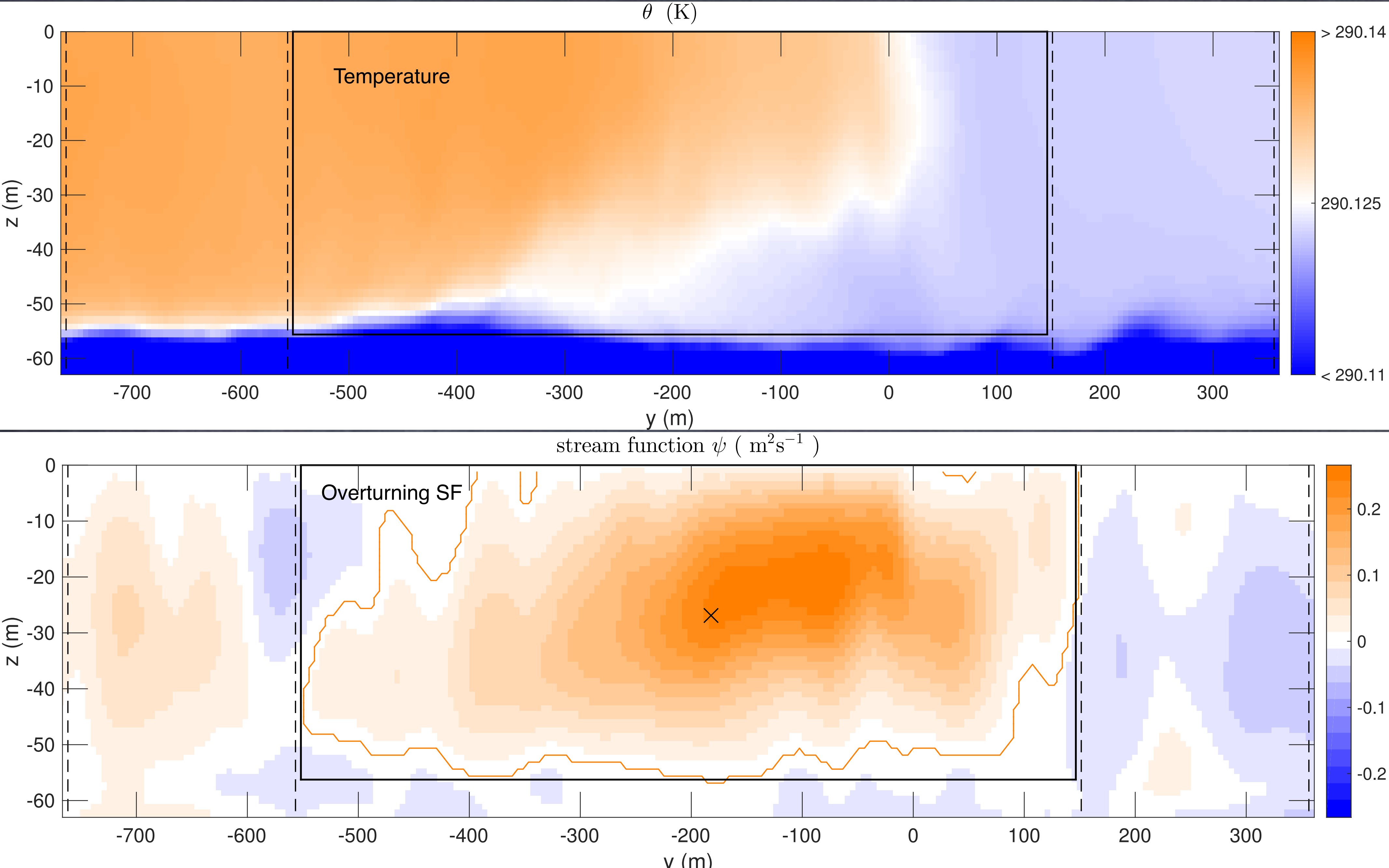

N. Suzuki, BFK, P. E. Hamlington, and L. P. Van Roekel. Surface waves affect frontogenesis. JGR-Oceans, December 2015. Submitted.

Stokes Shear Force in Budgets for Overturning

- 2nd Largest Source in Ang. Momentum (26% of buoyancy)
- 3rd Largest Source in Overturning KE (24% of buoyancy)
- 2nd Largest Source of Overturning Vorticity (44% of buoyancy)

$$\frac{\alpha^2}{Ri}\left[w_{,t} + v_j^L w_{,j} + \frac{M_{Ro}}{RoRi} w w_{,z}\right] = -\pi_{,z} + b - \varepsilon v_j^L v_{j,z}^s + \frac{\alpha^2}{ReRi} w_{,jj}$$

N. Suzuki, BFK, P. E. Hamlington, and L. P. Van Roekel. Surface waves affect frontogenesis. JGR-Oceans, December 2015. Submitted.

Stokes Shear Force Affects Fronts and Filaments

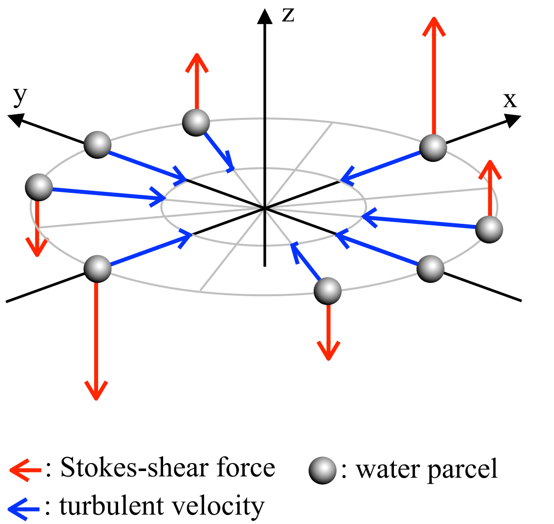

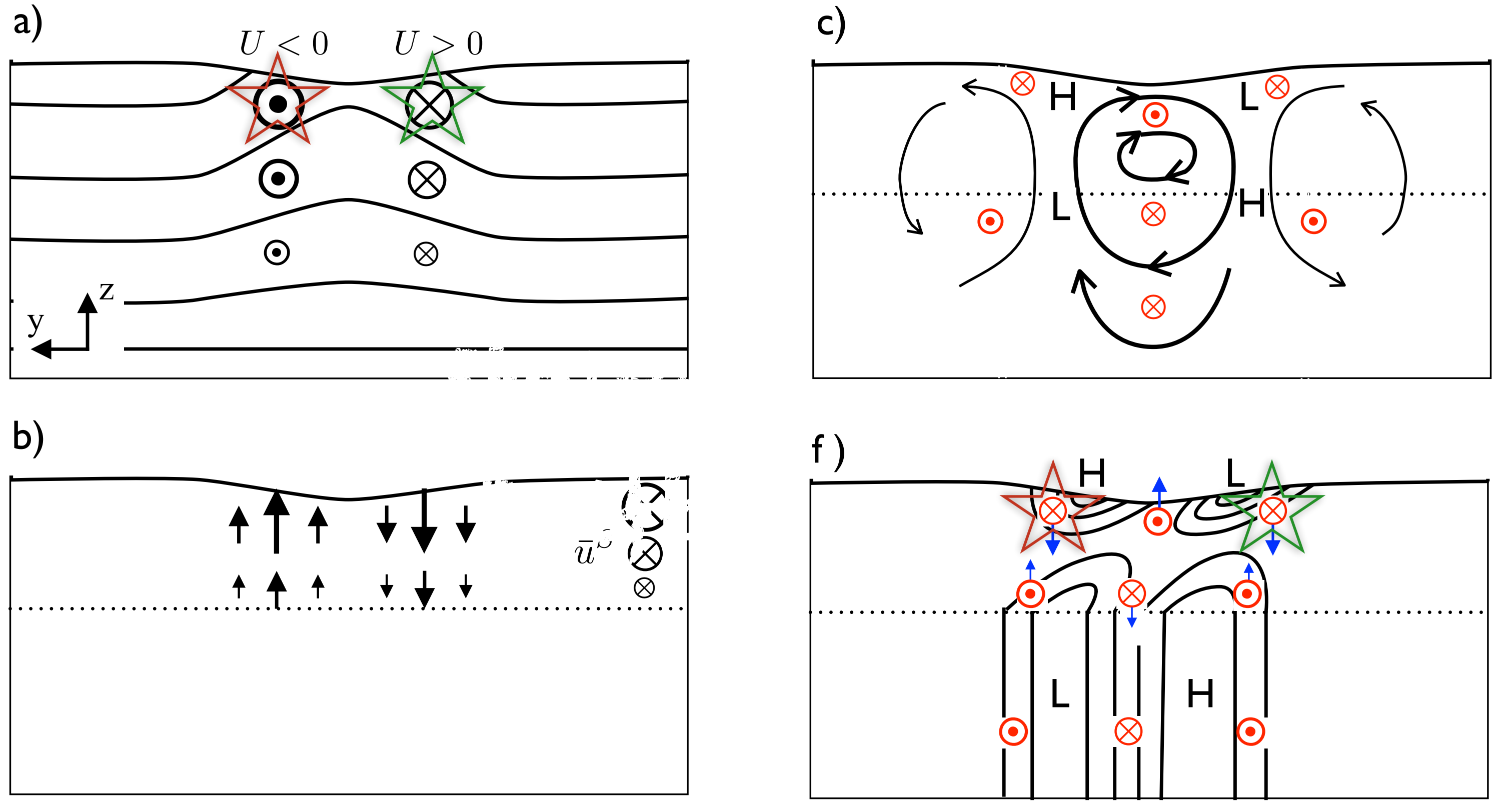

J. C. McWilliams and BFK. Oceanic wave-balanced surface fronts and filaments. Journal of Fluid Mechanics, 730:464-490, 2013.

N. Suzuki and BFK. Understanding Stokes Forces in the Wave-Averaged Equations, submitted, 2015.

Enhances Fronts for Down-Front Stokes

Opposes Fronts for Up-Front Stokes

$$\frac{\alpha^2}{Ri}\left[w_{,t} + v_j^L w_{,j} + \frac{M_{Ro}}{RoRi} w w_{,z}\right] = -\pi_{,z} + b - \varepsilon v_j^L v^s_{j,z} + \frac{\alpha^2}{ReRi} w_{,jj}$$

Can it be observed?
CARTHE LASER (next week)

Can it be observed?

Can it be observed?

Can it be observed?

Can it be observed?

Can it be observed?

Can it be observed?

CARTHE LASER (Feb.)

CARTHE LASER (Feb.)

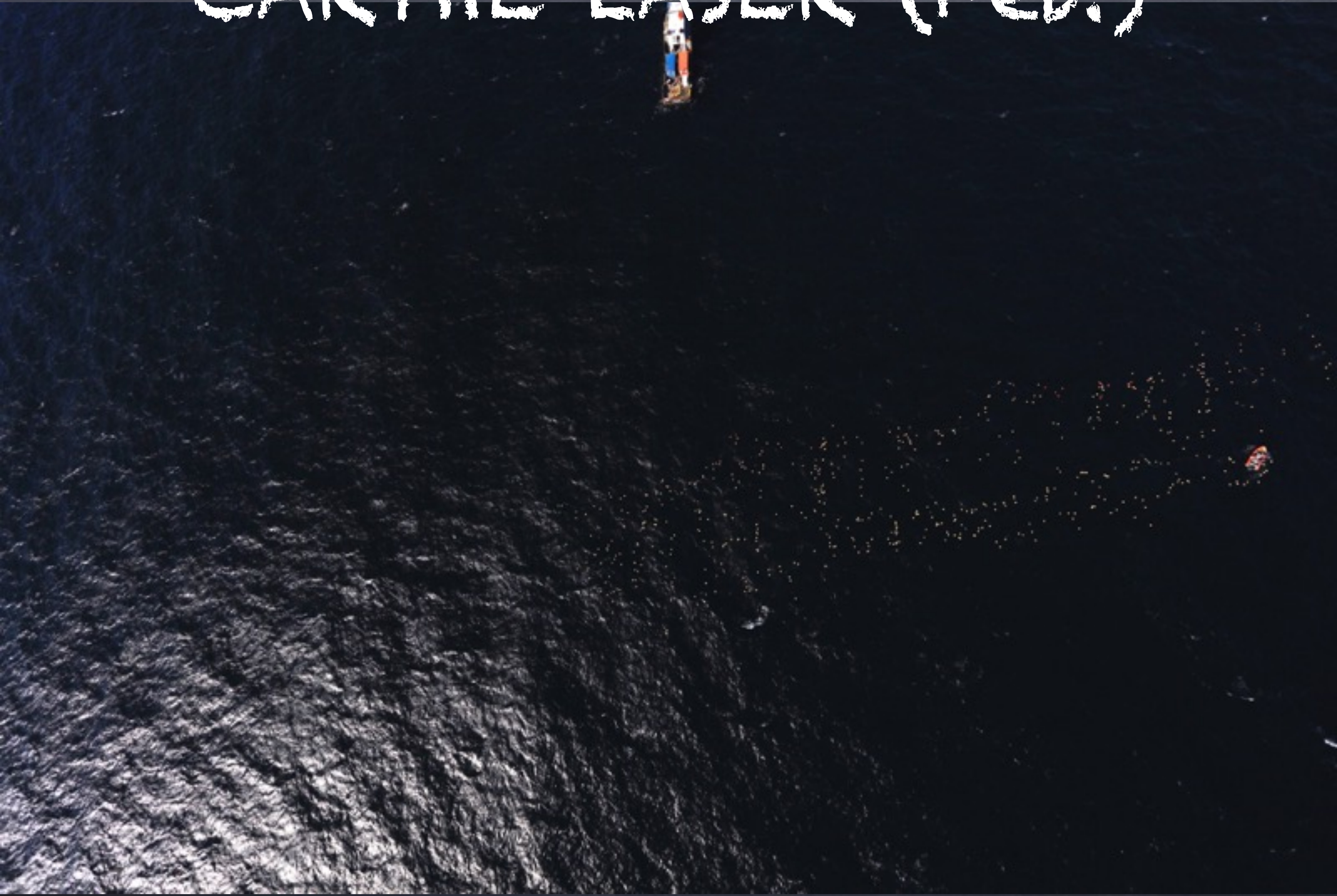

CARTHE LASER (Feb.)

About 45 Min Later.

Conclusions

- In the upper ocean, horizontal scales as big as basins, and as small as meters contribute non-negligibly to the air-sea exchange and climate
- Interesting transition occurs on the Submeso to Langmuir scale boundary, as nonhydro. & ageostrophic effects begin to dominate
- Langmuir mixing scalings consistent with LES & obs., reduce climate model biases in MLD, T, CFCs vs. observations by 5-25%.
- The 25-45% forcing effects of the Stokes Shear force on submesoscale dynamics are under-appreciated.
- All papers at: fox-kemper.com/pubs

How well do we know Stokes Drift? <50% discrepancy

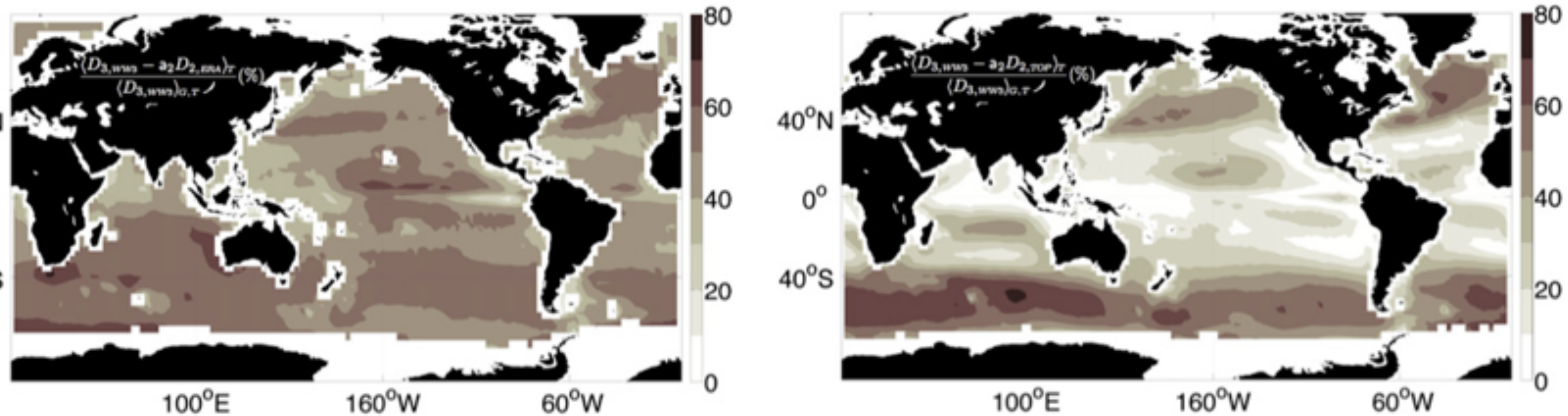

(e) $\langle D_{3,WW3} - a_2 D_{2,ERA} \rangle_T / \langle D_{3,WW3} \rangle_{G,T}$ (%)   (f) $\langle D_{3,WW3} - a_2 D_{2,TOP} \rangle_T / \langle D_{3,WW3} \rangle_{G,T}$ (%)

RMS error in measures of surface Stokes drift,
2 wave models (left), model vs. altimeter (right)

Year 2000 data & models

A. Webb and B. Fox-Kemper. Wave spectral moments and Stokes drift estimation. Ocean Modelling, 40(3-4):273-288, 2011.

Why? Vortex Tilting Mechanism

In CLB: Tilting occurs in direction of $\mathbf{u}_L = \mathbf{v} + \mathbf{v}_s$

Misalignment enhances degree of wave-driven LT

$$\frac{\partial \xi}{\partial t} + \underbrace{(\mathbf{u}_L \cdot \nabla)\xi}_{\text{AD}} = \underbrace{(\omega_a \cdot \nabla)(\mathbf{u}_L \cdot \hat{\mathbf{x}}')}_{\text{TS}} + \underbrace{(\nabla b \times \hat{\mathbf{z}}) \cdot \hat{\mathbf{x}}'}_{\text{BV}} + \text{SGS},$$

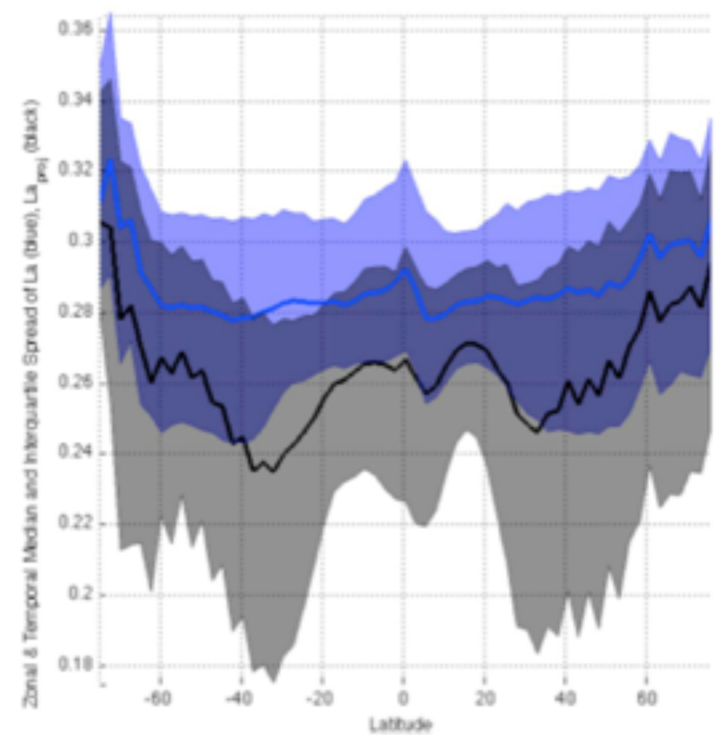

Figure 17. Temporal and zonal median and interquartile range of La_t and La_{proj} for a realistic simulation of 1994–2002 using Wave Watch III.

image: Thorpe, 04

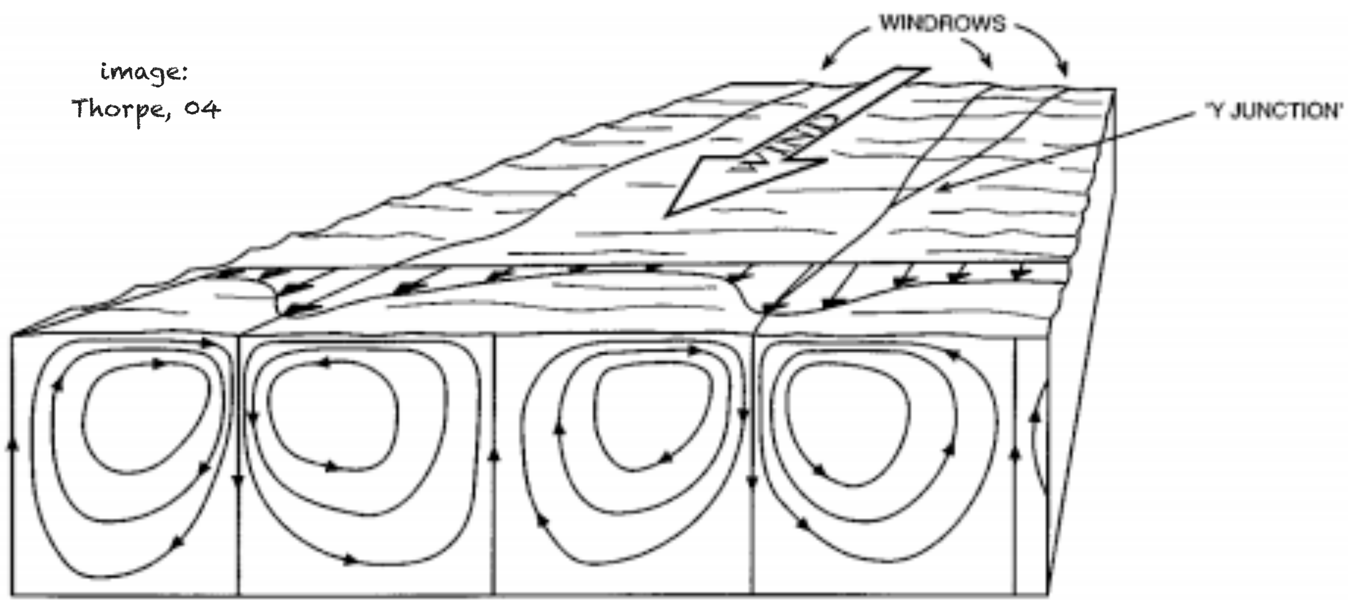

Figure 1 Sketch showing the pattern of mean flow in idealized Langmuir circulation. The windrows may be 2 m to 300 m apart, and the cell form is roughly square (as shown). In practice the flow is turbulent, especially near the water surface, and the windrows (Figure 2) amalgamate and meander in space and time. Bands of bubbles or buoyant algae may form within the downward-going (or downwelling) flow (see Figure 3).

The Ocean Mixed Layer

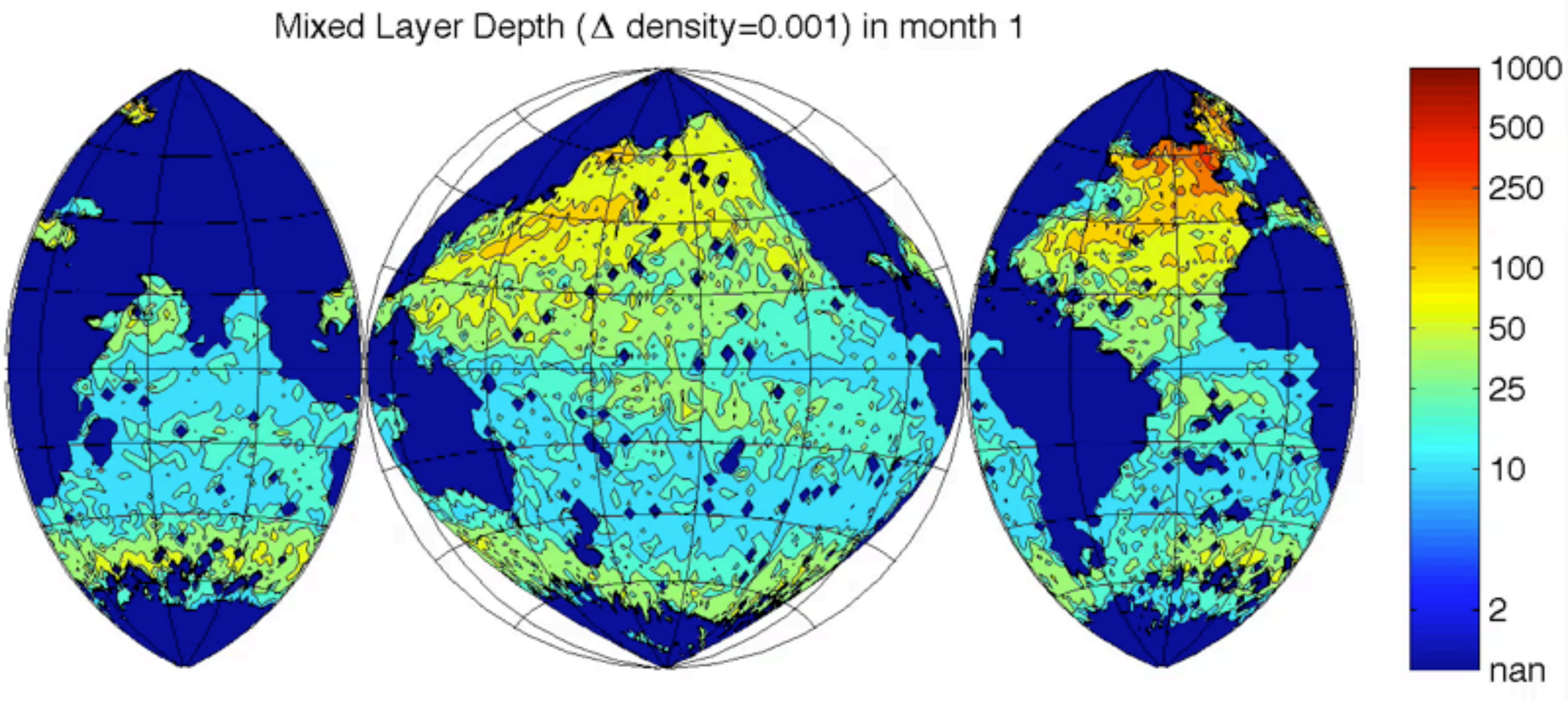

Stommel's Demon: ocean properties at depth set by deepest wintertime mixed layer & its properties

From Argo float data courtesy C. de Boyer-Montegut

The Ocean Mixed Layer

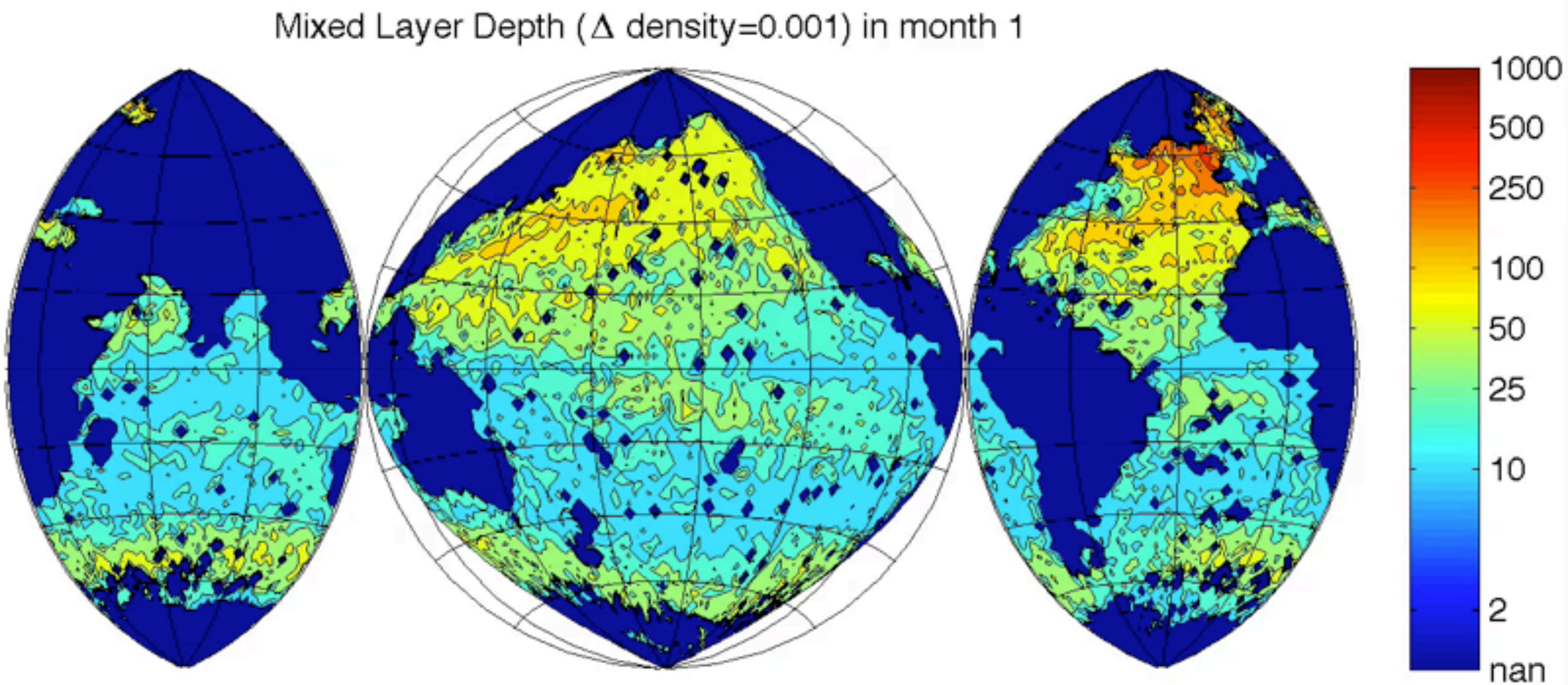

Stommel's Demon: ocean properties at depth set by deepest wintertime mixed layer & its properties

From Argo float data courtesy C. de Boyer-Montegut

The State of the Art:
Observations vs. Mixed Layers in CESM1.2

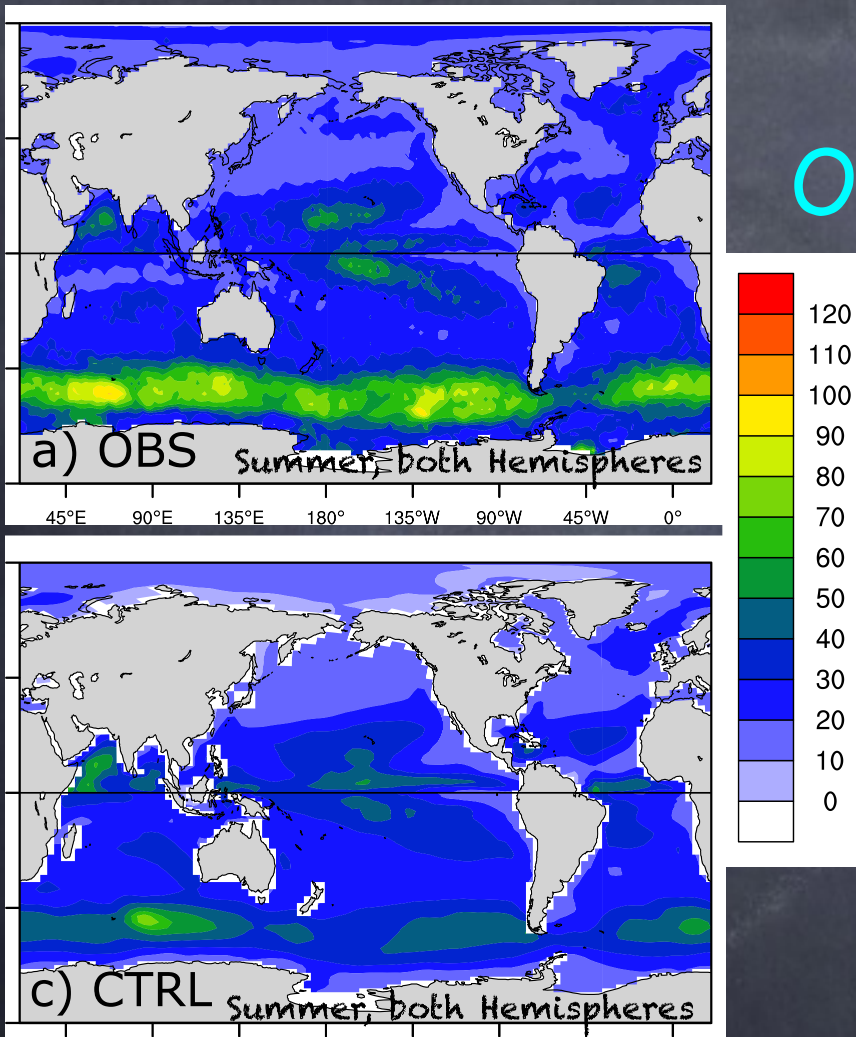

Observed

Climate Model

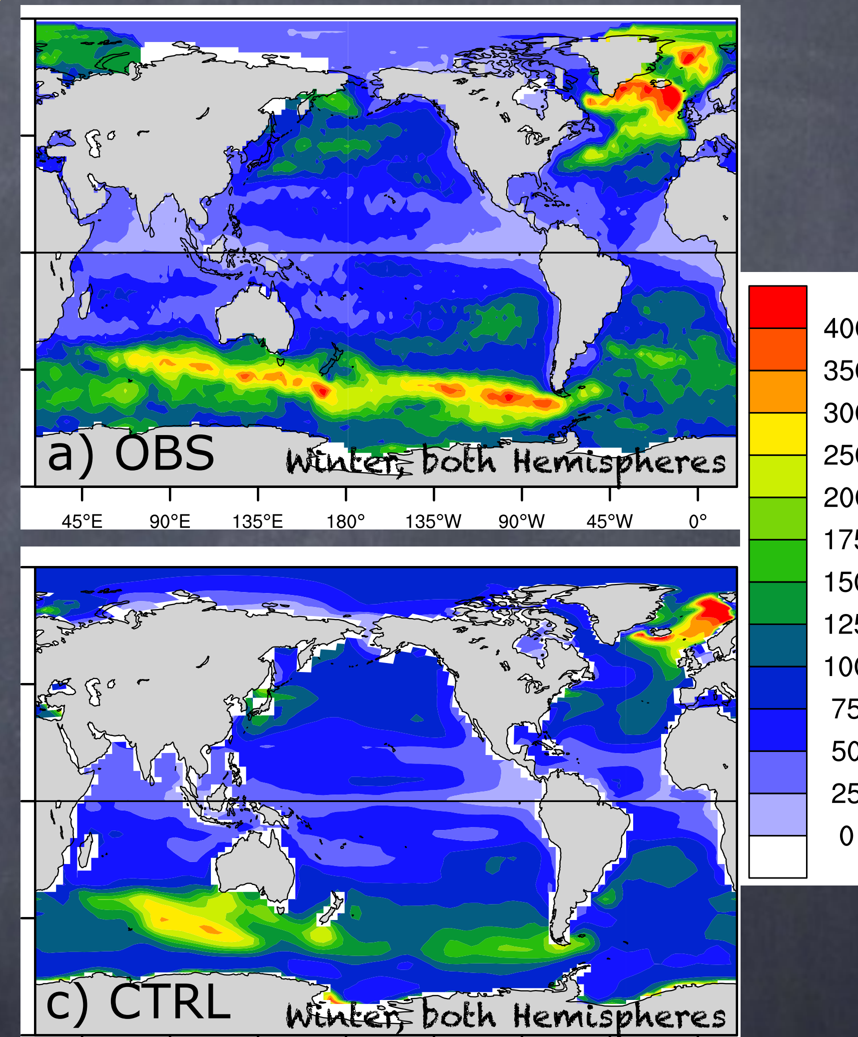

Q. Li, A. Webb, BFK, A. Craig, G. Danabasoglu, W. G. Large, and M. Vertenstein. Langmuir mixing effects on global climate: WAVEWATCH III in CESM. Ocean Modelling, August 2015. in press.

May partly account for large annual cycle errors.

S. C. Bates, BFK, S. R. Jayne, W. G. Large, S. Stevenson, and S. G. Yeager. Mean biases, variability, and trends in air-sea fluxes and SST in the CCSM4.Journal of Climate, 25(22):7781-7801, 2012.

To quantify Langmuir Turb. effects on climate: 3 WAYS

- 1) From OBSERVATIONS, estimate wave effects on key parameters ($\langle w^2 \rangle$, sources of energy) using scalings from Large Eddy Simulations. MODEL INDEPENDENT
- 2) OFFLINE 1d mixing with waves parameterized, mixing into observed Argo profiles, reanalysis winds, waves, cooling. ROBUST TO MODEL ERRORS
- 3) In a climate model, *add in a wave forecast model as a new component in addition to atmosphere, ocean, ice, etc.*, use this to drive parameterizations of wave mixing in ocean component. FEEDBACKS PRESENT

No Retuning! All coefficents from LES

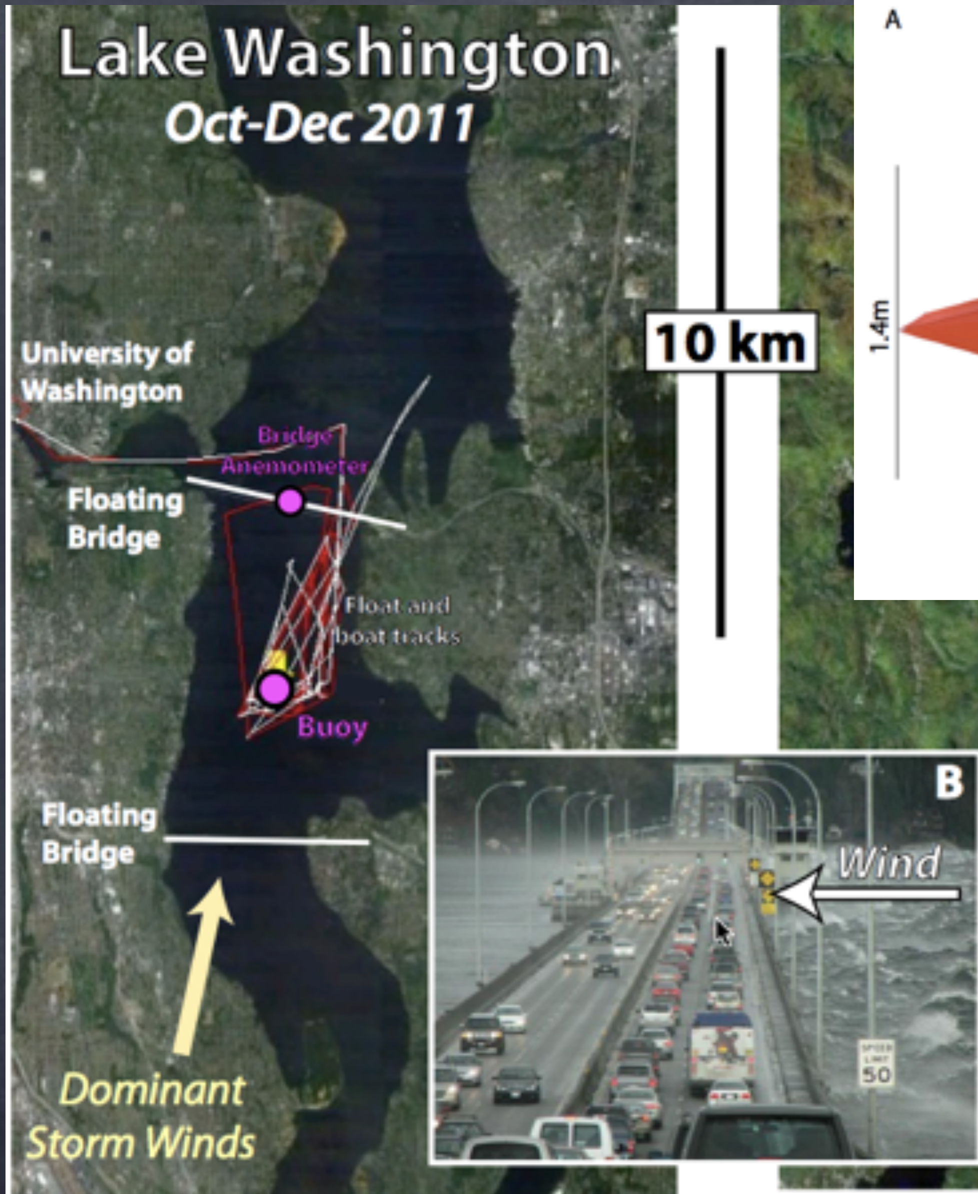

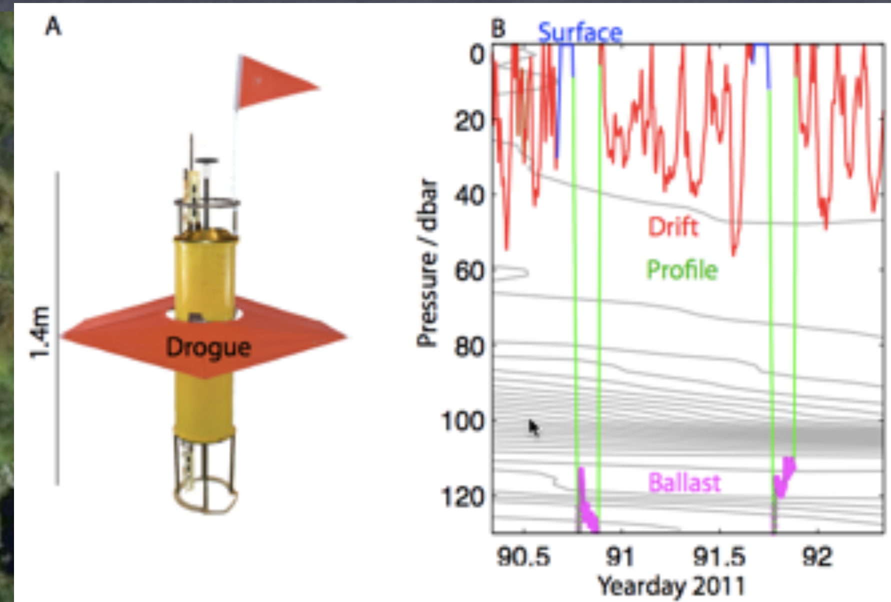

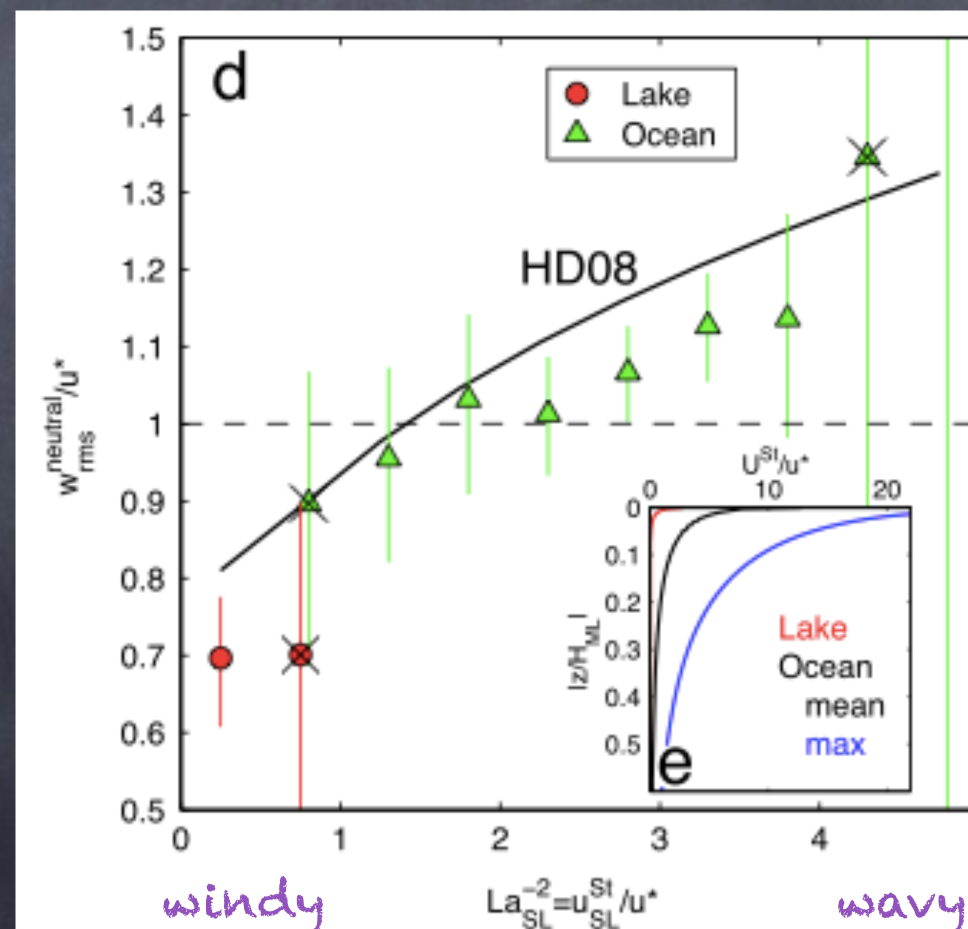

E. A. D'Asaro, J. Thomson, A. Y. Shcherbina, R. R. Harcourt, M. F. Cronin, M. A. Hemer, and BFK. Quantifying upper ocean turbulence driven by surface waves. Geophysical Research Letters, 41(1):102-107, January 2014.

1) Observations obey a particular scaling for <w^2>!

Data + Large Eddy Simulation for scaling laws, Southern Ocean data to determine available mixing energy

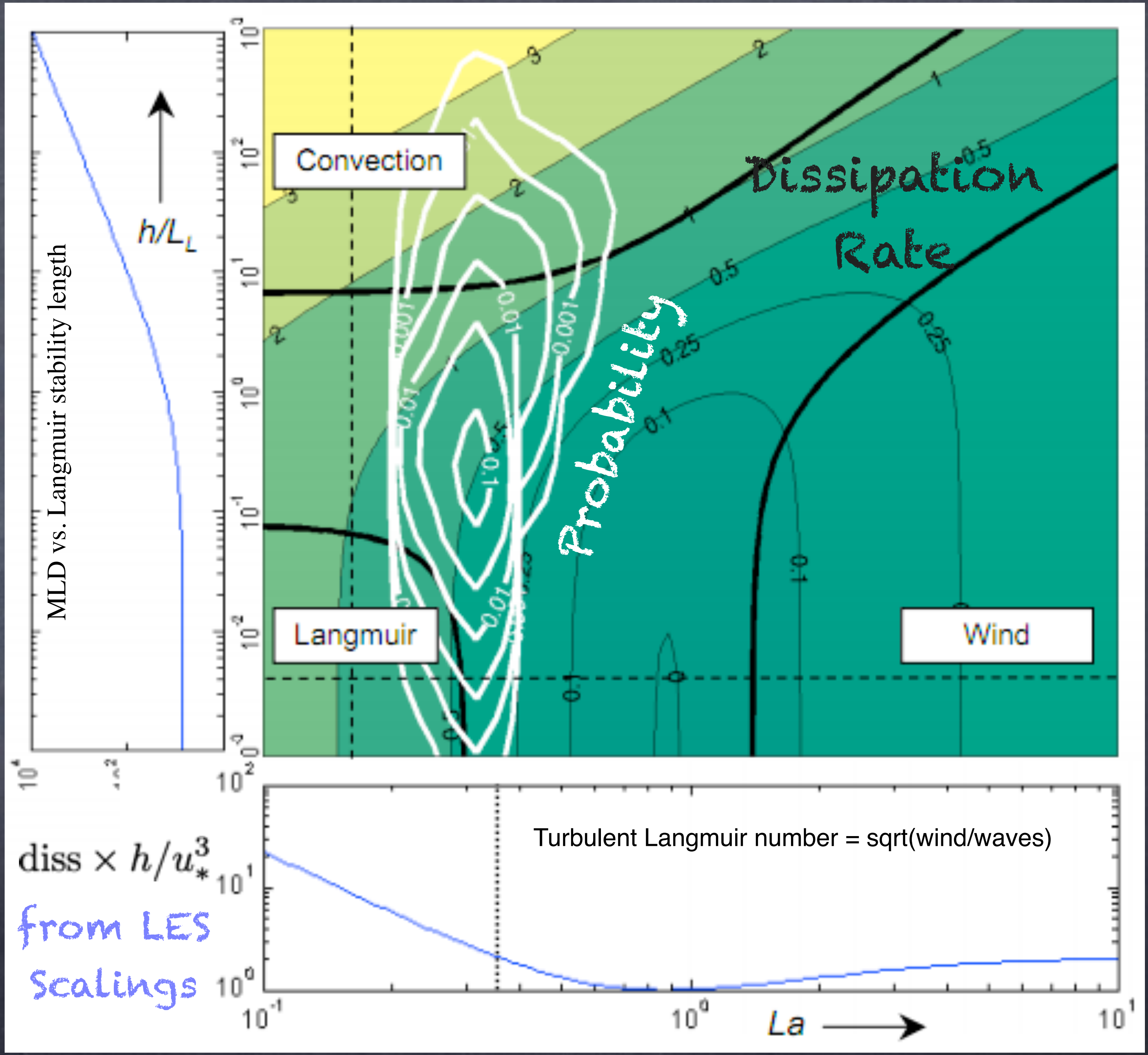

So, waves are likely to drive mixing via Stokes drift (combines with cooling & winds)

S. E. Belcher, A. A. L. M. Grant, K. E. Hanley, BFK, L. Van Roekel, P. P. Sullivan, W. G. Large, A. Brown, A. Hines, D. Calvert, A. Rutgersson, H. Petterson, J. Bidlot, P. A. E. M. Janssen, and J. A. Polton. A global perspective on Langmuir turbulence in the ocean surface boundary layer. Geophysical Research Letters, 39(18):L18605, 9pp, 2012.

Including Stokes-driven Mixing should deepen the Mixed Layer!

E. A. D'Asaro, J. Thomson, A. Y. Shcherbina, R. R. Harcourt, M. F. Cronin, M. A. Hemer, and BFK. Quantifying upper ocean turbulence driven by surface waves. Geophysical Research Letters, 41(1):102-107, January 2014.

As estimated with:
Argo-observed stratification,
modeled waves,
an LES-validated mixing parameterization,
and observed winds, solar, latent, etc.

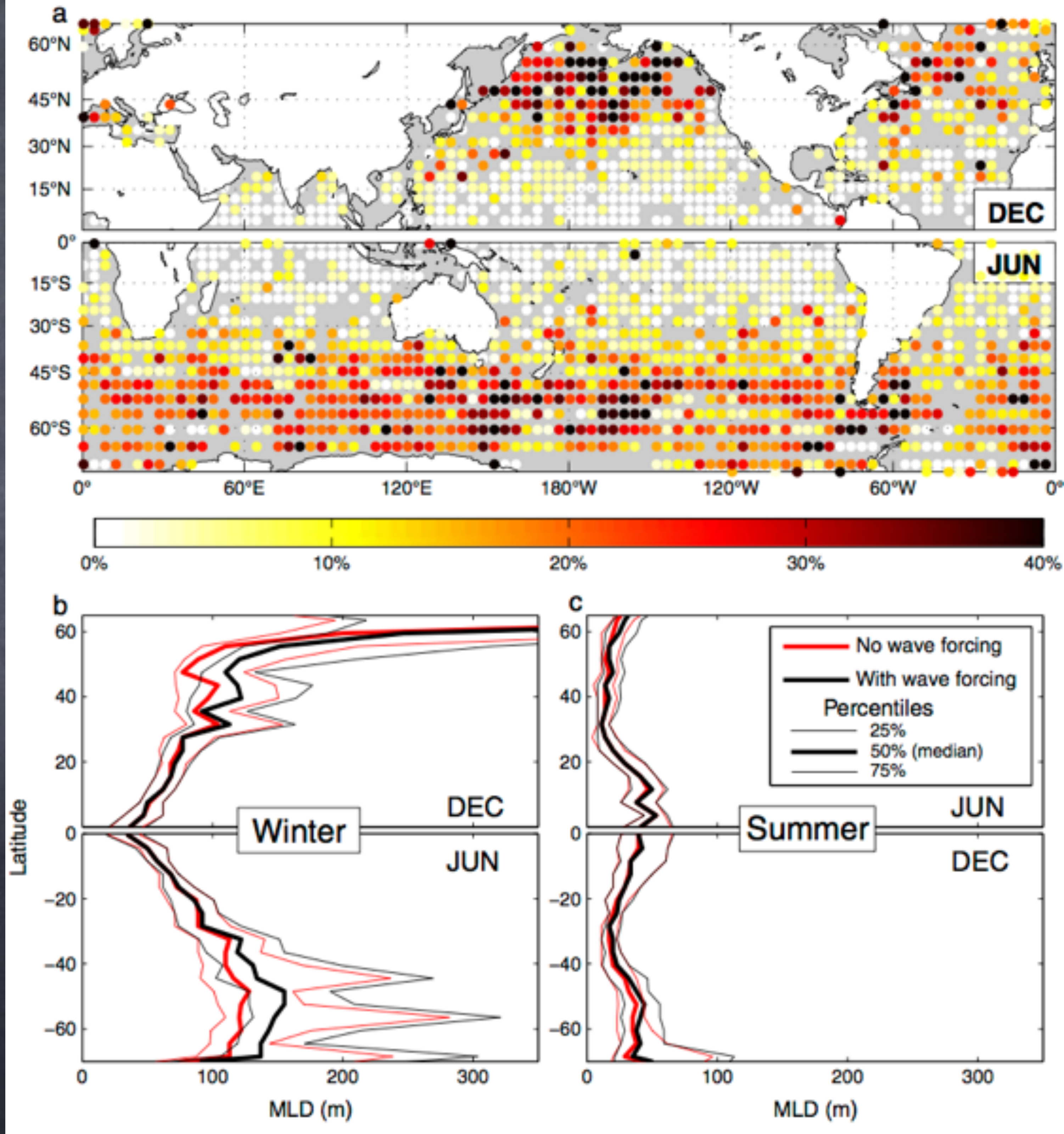

Something that happens often with waves:
Tricky: Misaligned Wind & Waves

A. Webb and BFK. Impacts of wave spreading and multidirectional waves on estimating Stokes drift. Ocean Modelling, 96(1): 49-64, December 2015.

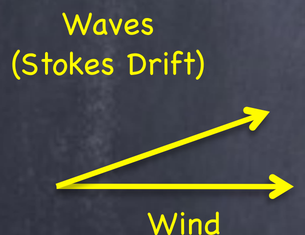

L. P. Van Roekel, BFK, P. P. Sullivan, P. E. Hamlington, and S. R. Haney. The form and orientation of Langmuir cells for misaligned winds and waves. Journal of Geophysical Research-Oceans, 117:C05001, 22pp, May 2012.

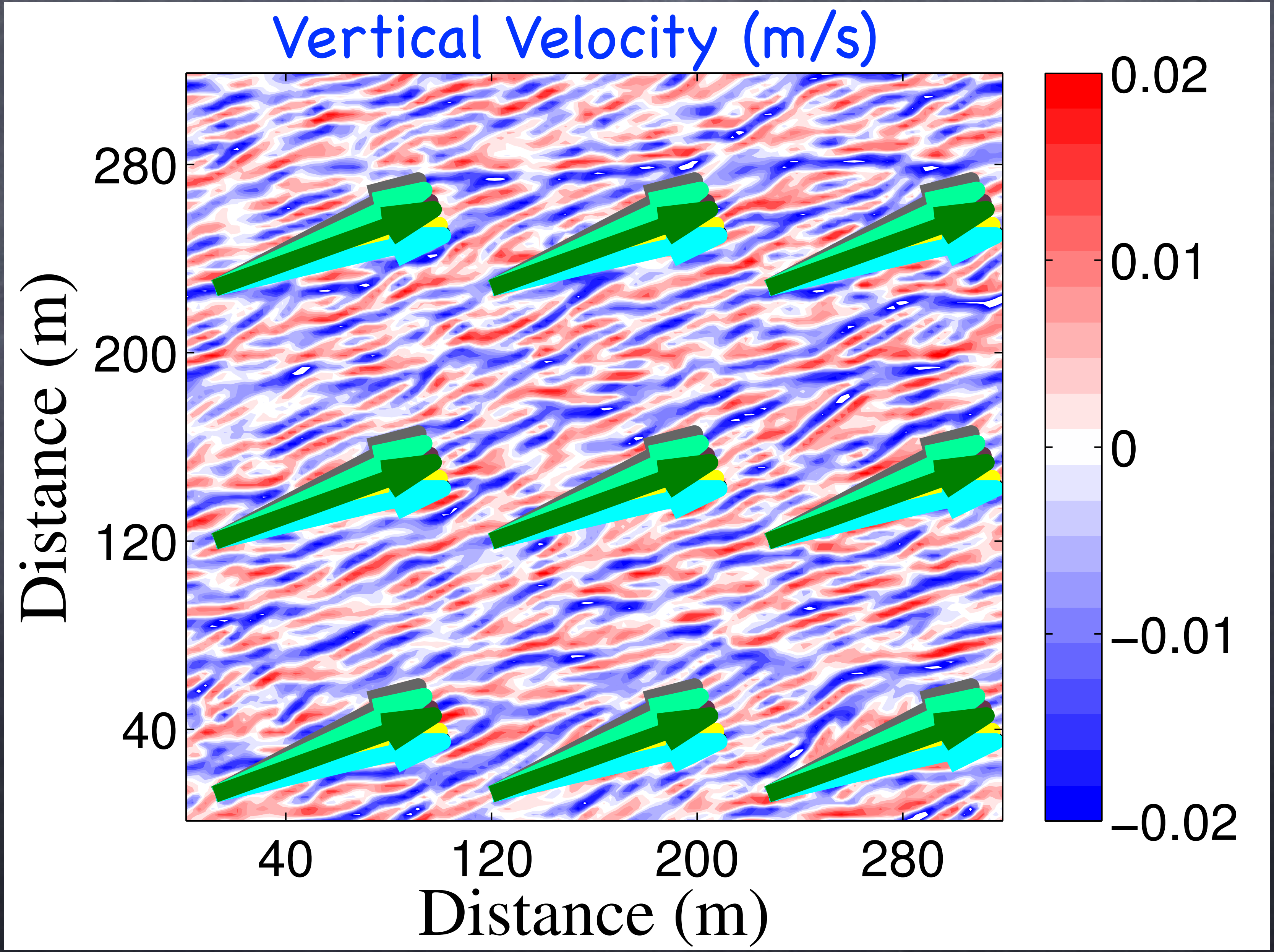

Tricky: Misaligned Wind & Waves

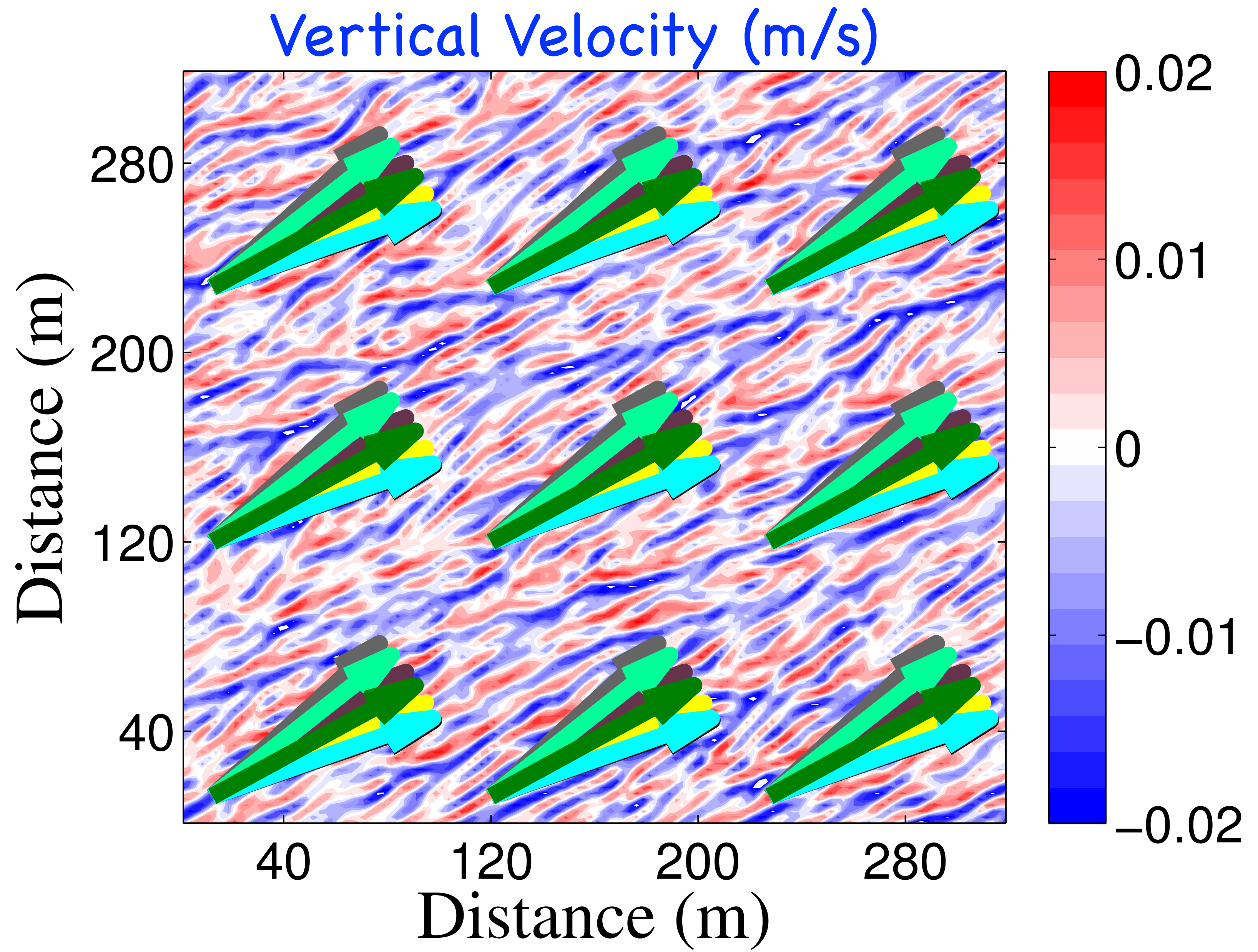

L. P. Van Roekel, BFK, P. P. Sullivan, P. E. Hamlington, and S. R. Haney. The form and orientation of Langmuir cells for misaligned winds and waves. Journal of Geophysical Research-Oceans, 117:C05001, 22pp, May 2012.

Tricky: Misaligned Wind & Waves

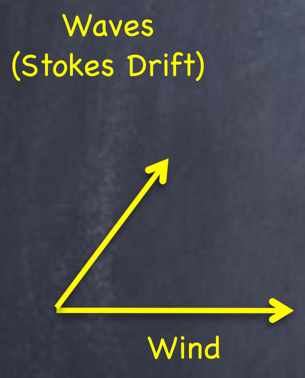

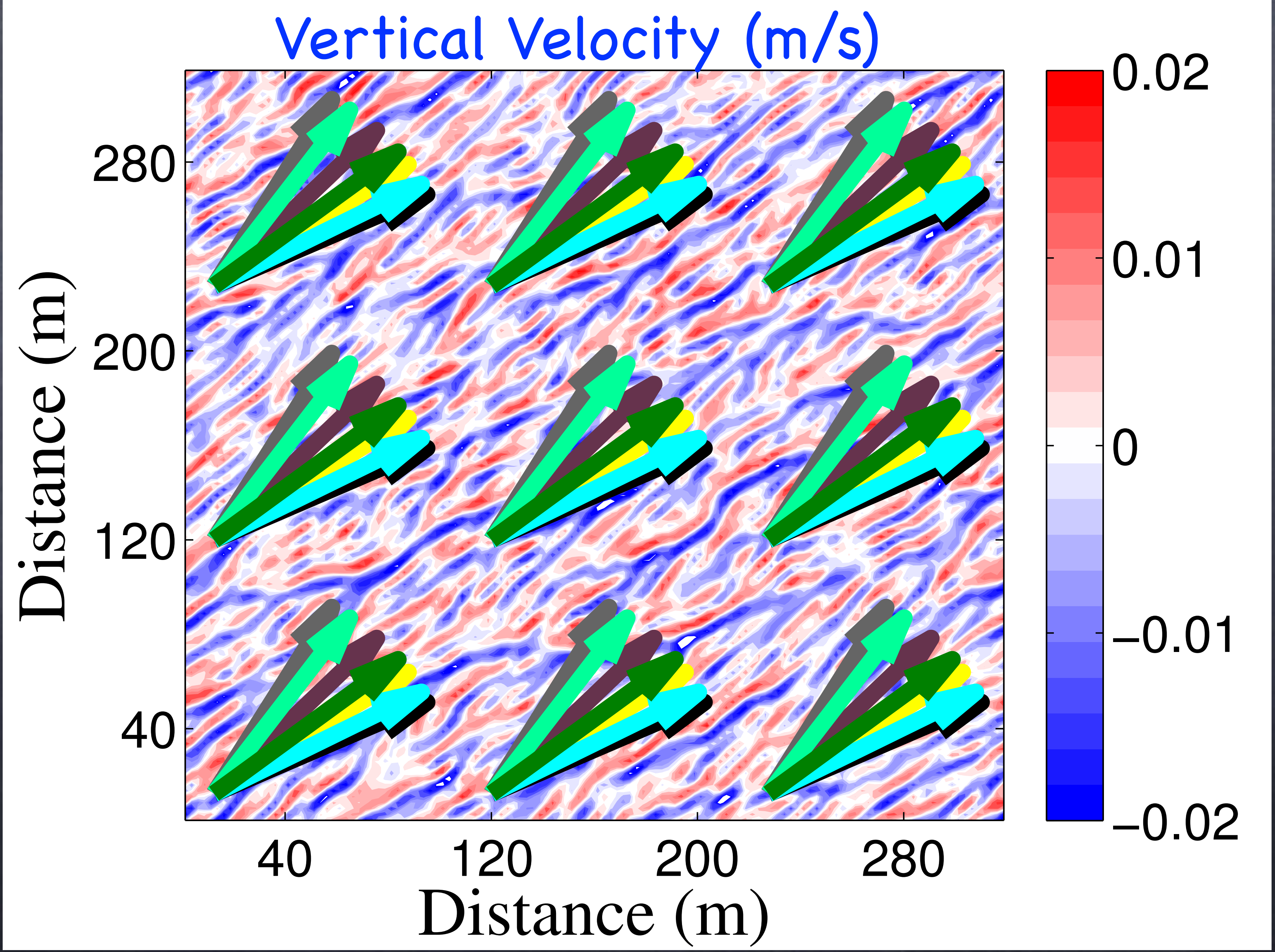

L. P. Van Roekel, BFK, P. P. Sullivan, P. E. Hamlington, and S. R. Haney. The form and orientation of Langmuir cells for misaligned winds and waves. Journal of Geophysical Research-Oceans, 117:C05001, 22pp, May 2012.

Tricky: Misaligned Wind & Waves

L. P. Van Roekel, BFK, P. P. Sullivan, P. E. Hamlington, and S. R. Haney. The form and orientation of Langmuir cells for misaligned winds and waves. Journal of Geophysical Research-Oceans, 117:C05001, 22pp, May 2012.

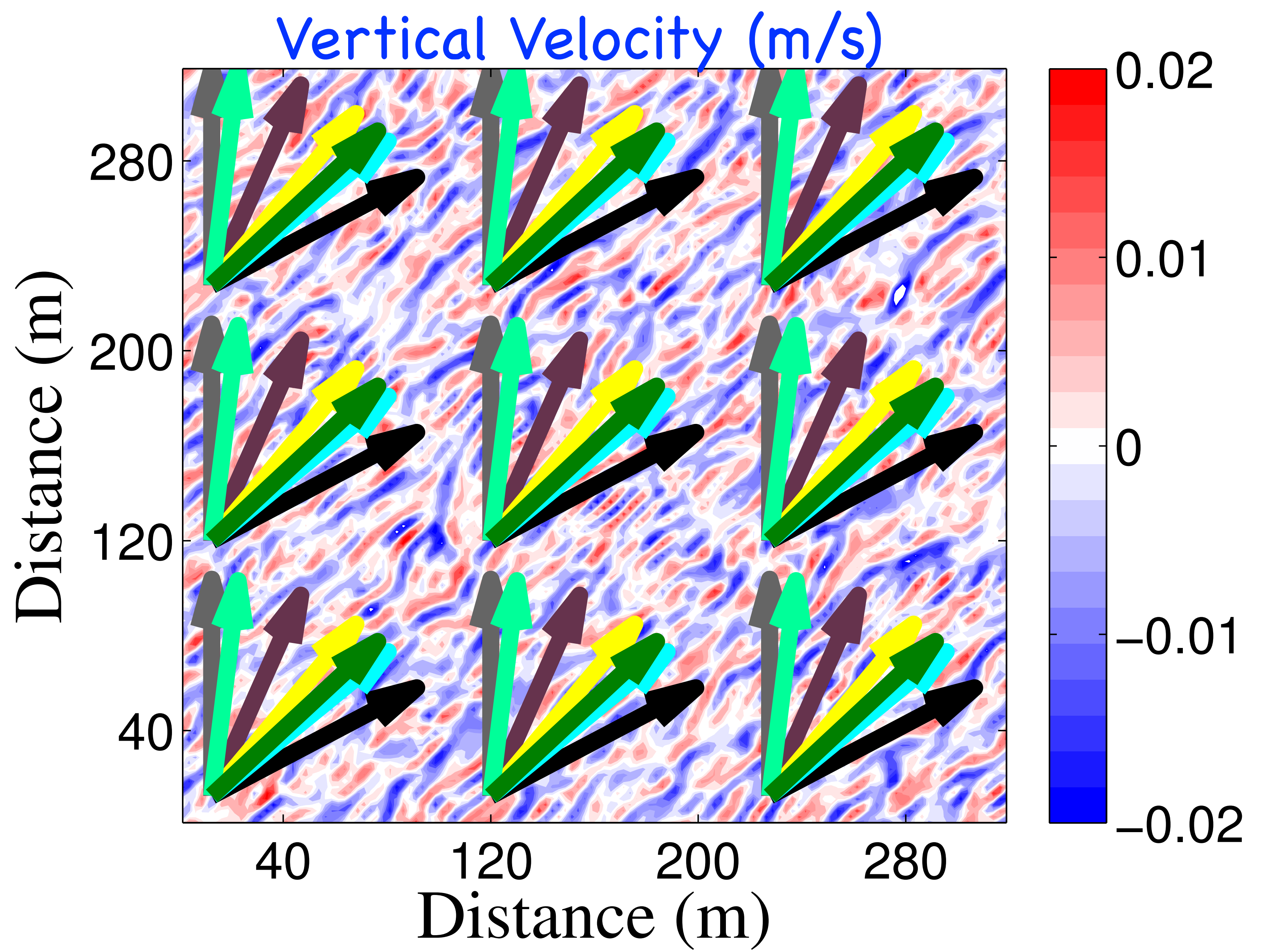

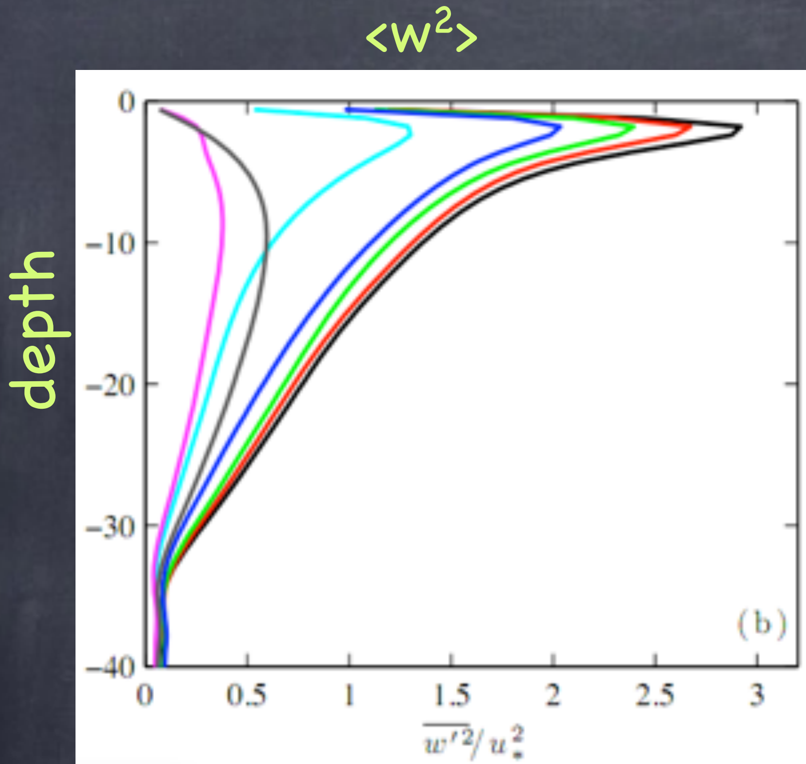

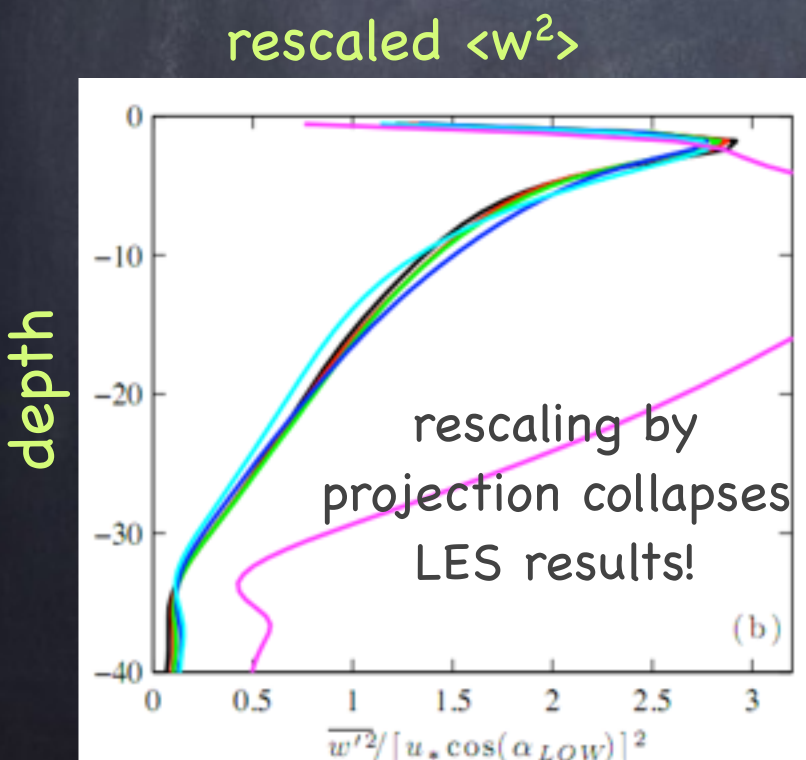

Generalized Turbulent Parameter (Langmuir Number)

Projection of u*, u_s into Langmuir Direction

$$La_{proj}^2 = \frac{|u_*| \cos(\alpha_{LOW})}{|u_s| \cos(\theta_{ww} - \alpha_{LOW})},$$

A scaling for LC strength & direction!

Enough for climate model application

L. P. Van Roekel, BFK, P. P. Sullivan, P. E. Hamlington, and S. R. Haney. The form and orientation of Langmuir cells for misaligned winds and waves. Journal of Geophysical Research-Oceans, 117:C05001, 22pp, 2012.